

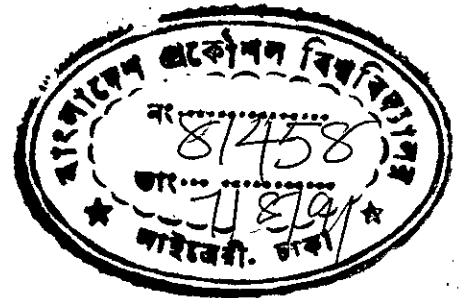
621.011
1990
SYF

STUDY OF THE EFFECTS OF PRESSURE ON NATURAL CONVECTION HEAT
TRANSFER FROM AN INCLINED CYLINDER PLACED IN AN INERT ATMOSPHERE

BY

MD. SYFUL ISLAM.

Thesis submitted to the Department of Mechanical Engineering in
partial fulfilment of the requirements of the degree of
Master of Science
in
Mechanical Engineering



November, 1990.

BANGLADESH UNIVERSITY OF ENGINEERING AND TECHNOLOGY, DHAKA-1000
BANGLADESH



#81458#

Dedicated to

MY PARENTS

CERTIFICATE OF APPROVAL

STUDY OF THE EFFECTS OF PRESSURE ON NATURAL CONVECTION HEAT
TRANSFER FROM AN INCLINED CYLINDER PLACED IN AN INERT ATMOSPHERE..

A Thesis
by
Md. Syful Islam.

Approved as to Style and Contents

Hossain 21.11.90

Dr. Md. Imtiaz Hossain.
Associate Professor,
Department of Mechanical Engineering;
BUET, Dhaka.

Chairman

Rashid

Dr. M.A. Rashid Sarkar.
Assistant Professor,
Department of Mechanical Engineering;
BUET, Dhaka.

Member

S.M. Nazrul Islam

Dr. S.M. Nazrul Islam.
Professor and Head,
Department of Mechanical Engineering;
BUET, Dhaka.

Member

M.A. Razzaq Akhanda

Dr. M.A. Razzaq Akhanda.
Professor,
Department of Mechanical Engineering;
BUET, Dhaka.

Member

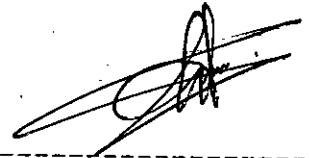
Musharrif Hussain Khan

Professor Musharrif Hussain Khan.
Vice Chancellor, BUET, Dhaka.

Member
(External)

CERTIFICATE OF RESEARCH

This is to certify that the work presented in this thesis is the outcome of the investigations carried out by the candidate under the supervision of Dr.Md. Imtiaz Hossain and co-supervision of Dr.M.A. Rashid Sarkar in the Department of Mechanical Engineering at Bangladesh university of Engineering and Technology, Dhaka.



Candidate

Imtiaz Hossain 21.11.90

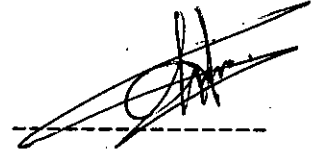
Supervisor

M.A. Rashid Sarkar

Co-Supervisor

DECLARATION OF THE CANDIDATE

It is hereby declared that neither this thesis nor any part thereof has been submitted or is being concurrently submitted anywhere else for the award of any degree or diploma.

A handwritten signature in black ink, consisting of several overlapping loops and strokes, positioned above a horizontal dashed line.

Candidate

ACKNOWLEDGEMENTS

The author hereby expresses his deep gratitude and acknowledges profound indebtedness to his supervisor Dr. Md. Imtiaz Hossain, Associate professor, Department of Mechanical Engineering, BUET, Dhaka and co-supervisor Dr. M. A. Rashid Sarkar, Assistant Professor of the same department, without whose continuous guidance, informal co-operation, invaluable suggestions and constant encouragement it would not be possible for the author to complete this work. The author also expresses his deep gratitude to Dr. S.M. Nazrul Islam, Professor and Head, department of Mechanical Engineering, for his continuous encouragement and permission of use of laboratory facilities even beyond office hours. The author respectfully recalls the encouragements of Dr. M.A. Razzaq Akhanda, Professor of the same department.

The author is highly grateful to Dr. D.K. Das, Professor of the department for his co-operation in the use of instrument facilities from the fluid mechanics laboratory. The author is indebted to Dr. Md. Sadrul Islam, Associate Professor of the department, for his help in the development of computer programs. The author is also grateful to Mr. Durul Huda, Mr. S.K. Selim and Mr. Maniruzzaman, Assistant Professors of the department, for their help in the use of computer softwares.

The author appreciates the co-operation of the university staff who helped the author in fabricating the set up, taking readings during experiments and preparing the thesis.

Finally the author expresses his gratefulness to his family members who sacrificed their times in favor of the thesis.

ABSTRACT

Experimental investigation of natural convection heat transfer at different pressures and inclinations from a heated cylinder to ambient air and argon was carried out. A constant and uniform energy input to the cylinder was maintained. The measurements covered the fluid pressure ranging from 5 to 1700 mm of Hg absolute. The inclinations of the axis of the cylinder with the horizontal were 0° , 30° , 45° , 60° and 90° . The range of Rayleigh number covered was $10^3 \leq Ra_L \leq 1.2 \times 10^8$. The surface temperature of the heated cylinder ranged from 85°C to 155°C .

The investigations revealed that heat transfer coefficient varied logarithmically with pressure. The plots of Nusselt number against Pressure and Nusselt number against Rayleigh number were linear on a log-log graph.

Except at very low pressure, the present results agreed well with some of the available correlations. The maximum differences were within $\pm 12\%$ at atmospheric pressure with McAdams and Nagendra et al equations. Arabi and Salman equation, however, indicated large differences throughout the range of pressure investigated. At low pressures most of the correlations compared exhibited large differences but the equation of Kyte et al did not vary much from the observed results. With one set of argon data the maximum deviation with Kyte et al was about 20%.

From the experimental results a correlation was developed in terms of Nusselt number, Rayleigh number, normalised pressure and inclination of the cylinder. This relationship correlates all of the experimental data of this work within $\pm 10\%$.

CONTENTS

<u>Title</u>	<u>Page</u>
Certificate of Approval	i
Certificate of Research	ii
Declaration of Candidate	iii
Acknowledgements	iv
Abstract	v
Contents	vi
Nomenclature	viii
Chapter 1: INTRODUCTION	
1.1 General	1
1.2 Heat transfer from the Cylindrical Surfaces	3
1.2.1 Horizontal Cylinders	4
1.2.2 Vertical Cylinders	5
1.2.3 Inclined Cylinders	6
1.3 Present work selection	7
1.4 Objective of the Present work	8
Chapter 2: LITERATURE REVIEW	
2.1 General	9
2.2 Variable Fluid Properties	11
2.3 Vertical Surfaces	12
2.4 Horizontal and Inclined Plates	13
2.5 Vertical Cylinders	15
2.6 Horizontal Cylinders	16
2.7 Inclined cylinders	19
2.8 Studies on Natural convection at Pressures other than atmospheric	21
Chapter 3: MATHEMATICAL MODELING OF THE PROBLEM	
3.1 General	25
3.2 Description of the Proble	25
3.3 Similarity Solution	26
3.4 Modification of the similarity equation for the present problem	28

<u>Title</u>	<u>Page</u>
Chapter 4: EXPERIMENTAL SET-UP	
4.1 General	29
4.2 Test specimen	29
4.3 Temperature Measuring Devices	30
4.4 Pressure Measuring and Control Devices	31
4.5 Input Heat Measuring Devices	31
Chapter 5: EXPERIMENTAL MEASUREMENTS AND TEST PROCEDURE	
5.1 Measurement of Temperature	32
5.2 Estimation of Emissivity	32
5.3 Measurement of Pressure	32
5.4 Setting of Inclination	33
5.5 Determination of Heat Transfer coefficient	33
5.5.1 Measurement of Input Power	33
5.5.2 Estimation of Conduction Loss	34
5.5.3 Estimation of Radiation from the Cylinder	34
5.5.4 Estimation of Heat Loss from the Protruded Beads	34
5.5.5 Calculation of Convective Heat Transfer	35
5.5.6 Estimation of Emitting and Convecting Surface Area	35
5.6 Test Procedure	36
5.7 Data Analysis	38
Chapter 6: RESULTS AND DISCUSSIONS	39
Chapter 7: CONCLUSIONS AND RECOMMENDATIONS	
7.1 Conclusions	48
7.2 Recommendations	49
References	50
APPENDICES	
Appendix A: Conduction Correction	55
Appendix B: Emissivity Estimation	57
Appendix C: Computer Program	59
Appendix D: Calibration of thermocouple	67
Appendix E: Correlation Coefficient	69
Figures	71

NOMENCLATURE

<u>Symbol</u>	<u>Meaning</u>	<u>Units</u>
A	Effective heat transfer area	m ²
A'	X-Area of a thermocouple wire	m ²
C	Constant for a given inclination	
c	Specific heat for a viscous fluid	kJ/kg ⁰ K
c _p	Specific heat at constant pressure	kJ/kg ⁰ K
c _v	Specific heat at constant volume	KJ/kg ⁰ K
D	Outside diameter of the cylinder	m
D _i	Inside diameter of the cylinder	m
D _w	Wire diameter	m
Ec	Eckert number, $U_c^2 / (c_p \Delta T)$	dimensionless
Ge	Gebhart number, $g\beta L / c_p$	dimensionless
Gr	Grashof number, $g\beta L^3 \Delta T / \nu^2$	dimensionless
h	Heat transfer coefficient	W/m ² °K
H	Absolute Pressure inside the vessel	mm Hg
k	Thermal conductivity	W/m ⁰ K
k _{cu}	Thermal conductivity of copper	W/m ⁰ K
k _{con}	Thermal conductivity of constantan	W/m ⁰ K
L	Cylinder length	m
m	exponent	
Nu	Nusselt number, hL/k	dimensionless
P	Fluid pressure in the enclosure	N/m ²
P _a	Ambient fluid pressure	N/m ²
Pr	Prandtl number, $\mu c_p / k$	dimensionless
p'	Perimeter	m
q	Heat transfer rate	W
q _{cond}	Heat transfer by conduction	W
q _r	Heat transfer by radiation	W
q _T	Total heat input to the system	W
q _{in}	Actual heat input to the cylinder	W
q _c	Heat transfer by convection	W
q''	Heat flux	W/m ²
q'''	Heat generation rate	W/m ³

<u>Symbol</u>	<u>Meaning</u>	<u>Units</u>
R	Gas constant	KJ/kg ⁰ K
r	Correlation coefficient	dimensionless
Ra	Rayleigh number, $g\beta L^3 \Delta T / (\alpha \nu)$	dimensionless
Re	Reynolds number, $V \rho L / \mu$	dimensionless
t _a	Temperature of ambient fluid	⁰ C
t _o	Temperature of heated surface	⁰ C
T _e	Cylinder surface temperature	⁰ K
T _o	Temperature of any heated surface	⁰ K
T _v	Vessel temperature	⁰ K
T _a	Ambient fluid temperature	⁰ K
ΔT	Temperature difference between the cylinder surface and ambient fluid	⁰ K
u	Velocity component in x-direction	m/s
V	Velocity vector	m/s
v	Volume	m ³
x	Thickness along x-direction	m
Uc	Convection velocity	m/s
Suffix		
x	based on variable dimension x	
L	based on length	
D	based on diameter	
w	wire	
Special Characters		
α	thermal diffusivity, $k / \rho c_p$	m ² /s
β	coefficient of expansion, $1/T_a$	/ ⁰ K
μ	absolute viscosity	kg/(ms)
ν	kinematic viscosity	m ² /s
ε	emissivity	dimensionless
ρ	density	kg/m ³
σ	Stefan -Boltzman constant, $5.77 \cdot 10^{-8}$	W/(m ² K ⁴)
τ	time variable	s
θ	inclination with horizontal	degree

Note: A parameter without any specific dimension indicates length as the characteristic dimension.



CHAPTER 1 INTRODUCTION

1.1 General

The science of 'heat transfer' seeks to explain and predict the process of energy transfer which may take place between material bodies as a result of temperature difference. The physical processes involved in the generation and utilization of heat has great many practical importance. Areas of study range from atmospheric and environmental problems to those in manufacturing systems and space research.

There are three basic processes of thermal energy transport: conduction, convection and radiation. Conduction occurs if a temperature difference exists in a material and is due to the motion of the microscopic particles that comprise the material. The motion of the particles is dependent on local temperature in the material and the energy diffusion is due to differences in motion.

The energy transfer in the last mode, radiation, is in the form of electromagnetic waves. Energy is emitted from a material due to its temperature level, being larger for higher temperature, and is then transmitted to another surface through the intervening space, which may be vacuum or a medium which may absorb, reflect or transmit the radiation depending on the nature and extent of the medium.

In convection, heat transfer processes take place with the motion of the fluid. As a consequence of this fluid motion, the heat transfer rate, as given by conduction is considerably altered.

In the diversity of the studies related to heat transfer, considerable effort has been directed at the convective mode, in which the relative motion of the fluid provides an additional mechanism for the transfer of energy and material. Convection is inevitably coupled with the conductive mechanism, since, though the fluid motion modifies the transport process, the eventual transfer of energy from one fluid element to another in

its neighbourhood is through conduction. Also, at the surface, the process is predominantly conduction due to the relative fluid motion being brought to zero at the surface.

The convection heat transfer is further divided into two basic processes: free convection and forced convection. If the fluid motion arises due to an external agent, such as the externally imposed flow of a fluid stream over a heated object, the process is termed as forced convection.

The fluid flow may be the result of, for instance, a fan, a blower, the wind, or the motion of the heated object itself. Such problems are very frequently encountered in technology where heat transfer to, or from, a body is often due to an imposed flow of a fluid at a temperature different from that of the body. If on the other hand, no such externally induced flow is provided and the flow arises 'naturally' simply due to the effect of a density difference, resulting from a temperature or concentration difference, in a body force field, such as gravitational field, the process is termed as 'natural' or 'free' convection. The density difference gives rise to buoyancy effects due to which the flow is generated. A heated body cooling in ambient air, generates such a flow in the region surrounding it. Similarly, the buoyant flow arising from heat rejection to atmosphere, in bodies of water and many other such heat transfer processes in our natural environment as well as many other technological applications, is included in the area of natural convection.

Flows can be caused by other body forces as well. In a rotating system, for instance, centrifugal and coriolis forces exist as body forces. Flow of cooling air through passages in the rotating blades of gas turbines is an example of flow under the influence of such forces. In the boundary layers which surround missiles flying with high supersonic speed, temperature may be so high that the air may be ionized and therefore the atoms and molecules may carry electrical charges. In this case electric or magnetic forces may arise which as body force will influence the flow.

⁶The main difference between natural and forced convection lies in the very nature of flow generation. In forced

convection, the externally imposed flow is generally known, whereas in natural convection, the flow results from an interaction of the density difference with gravitational or some other fields. As such, the motion that arises is not known at the onset and has to be determined from the considerations of heat and mass transfer processes coupled with flow mechanisms. In general, natural convection velocity levels are much smaller than those encountered in forced convection.

Processes involving natural convection are generally much more complicated than those in forced convection. Special techniques and methods have, therefore, to be devised to study the process with a view to obtain information on the flow and the heat transfer rate. ✓

Natural convection has both upper and lower limits on the heat transfer rates. The upper limit becomes an important consideration for problems in which forced convection is either not possible or not practical. It is also relevant for safety considerations under conditions when the forced convection fails and the system has to depend on natural convection to get rid of the generated heat. This is particularly significant in many electronic devices and systems and in power generation, where such considerations in design are essential to avoid overheating. The lower limit is important for heat losses from appliances like evaporators and plant pipings.

Although literature shows a huge volume of theoretical and experimental works, yet there are many situations for which organized experimental data are not available and sufficient experimental investigations are required to get actual views of heat transfer for these situations.

1.2 Heat transfer from cylinders

The cylindrical configuration is important for many problems, such as heat transfer from pipes, tubes and cables. Due to the relevance of the cylindrical geometry to the heat rejection systems like nuclear reactors, heating elements, pipes conveying hot and cold fluids in energy generation systems, chemical

processing plants, refrigerating and air conditioning plants, manufacturing systems for rods, cables, wires etc., and many other important areas, this configuration has great significance and has been studied by many investigators in detail.

Cylinders can be divided in three classes: wires, small and medium diameter cylinders and large diameter cylinders. For large diameter cylinders, the curvature of the surface is small and the surfaces can be approximated as flat, for which the governing heat transfer equations are simpler and have been widely discussed in literatures.

Free convection flow is caused by temperature differences in a gas or a liquid. Boundary layers are formed on the surface of the solids transmitting heat. Because of the low velocities encountered in natural convection these boundary layers are thicker than those in forced convection.

Since buoyancy plays the major role in natural convection, the orientation of the cylinder with gravity is important when the field is gravitational. Depending on this horizontal, vertical and inclined cylinders are discussed below separately.

1.2.1 Horizontal Cylinders

The manufacture of rolled rods, extrusion of tubes, horizontal pipes carrying hot feed water or steam are the common examples of heat transfer from horizontal tubes. The most simple case of horizontal cylinder is one which is infinitely long and has constant wall temperature. For isothermal cylinders, a number of people have suggested correlations in terms of either Nusselt number and Rayleigh number or Nusselt number, Grashof number and Prandtl number. The constant heat flux and partly adiabatic and partly isothermal situations have also been studied by several investigators. cursory examination of different investigations for horizontal isothermal situations show that they do not agree closely and variations of upto 50% have been reported but the range of Rayleigh numbers compared were different and hence the comparison cannot be considered critical. Heat transfer from horizontal cylinders has been investigated in various fluids like

air, water, silicon oil etc. Experiments for long horizontal wires in air showed that the length to diameter ratio (L/D) effect was not present for L/D ratio greater than perhaps 10^4 . The investigations with finite horizontal wires showed, for the low Grashof number range, the Nusselt number could not be correlated with Rayleigh number in simple terms for fluids of different Prandtl number. However a single Nusselt number correlation was possible if 15% errors were acceptable. Investigation has been carried out for a wide range of Rayleigh numbers that covered both laminar and turbulent regions. Some investigators suggested that the average heat transfer coefficient of a circular tube with diameter D has the same value as the average film heat transfer coefficient for a vertical wall with height $2.5D$. Literatures show that the cylindrical equations on horizontal cylinder are not applicable near the top end due to boundary layer separation or realignment into a plume flow that occurs in this region. The phenomenon is an important one since the mechanism underlying the generation of the wake above the body may considerably affect the local heat transfer rate. This realignment causes a rapid increase in the flow velocity which results in an increased heat transfer rate, despite the accompanying increase in boundary layer thickness.

Almost all investigations in the past have been carried out at atmospheric pressure. A semi-empirical equation has been suggested by one of the studies that converts the heat transfer coefficient of atmospheric pressure to that at high or low pressures by introducing a factor that covers the moderate pressure range. A correlation on the basis of wire data at reduced pressure has been suggested by one of the studies considering the effect of free molecule conduction. The scarcity of the heat transfer data at pressures other than atmospheric pressure requires further investigation.

1.2.2 Vertical Cylinders

The natural convection flow over vertical cylinders is an important case, due to its relevance to many applied problems,

such as those related to flow over tubes as in nuclear reactors and cylindrical heating elements etc.

Analytical and experimental solutions of isothermal vertical cylinders immersed in an infinite fluid have been obtained by different investigators. For Prandtl numbers of 0.72 and 1.0 it has been observed that the results with cylinders are about 5% greater than those with flat plates. Actually for small values of L/D ratio, obviously the results are very close to the flat plate ones. The limiting value of this L/D ratio has been estimated in terms of Grashof number for Prandtl numbers 0.72 and 1.0. Investigations have been carried out with air, water, helium, argon and other fluids in both laminar and turbulent regions.

Experiments with constant heat flux condition show that cylinders have been classified in three groups: short cylinder, long cylinder and wires. Correlations of the similar pattern with different coefficients and exponents have been suggested for these groups of vertical cylinders. The comparison also shows that the constant heat flux condition Nusselt number differs by about 6% with that of isothermal case. For Vertical cylinders, numerical solutions have been obtained for linearly varying surface temperature with the cylinder length using a temperature gradient Grashof number.

For vertical cylinder the data in the literatures other than atmospheric pressure are very limited. Although a correlation has been suggested on the basis of wire data at sub-atmospheric pressure in air, it is not applicable to most practical cases due to its low Rayleigh number range. In order to understand the process more convincingly further studies in the field are required.

1.2.4 Inclined Cylinders

Apart from the horizontal and vertical cylinders and tubes, inclined cylinders and tubes are also used in heat transfer in different plants. Inclined pipes and tubes carrying steam, hot or cold chemicals are common examples of heat transfer from or to inclined cylindrical surfaces. Inclined cylinders have got little

attention of the investigators and have not been studied extensively like horizontal or vertical cylinders. Analytical solutions of such problems are almost absent in the literatures. Although few investigations have been reported for both isothermal and constant heat flux situations in air at atmospheric pressure further investigations are necessary to observe the heat transfer behavior in other fluids at higher and sub-atmospheric pressures.

1.3 Present Work Selection

In the present work attention is directed to the natural convection heat transfer characteristics from an inclined cylinder at different pressures under constant and uniform heat input condition in both air and argon. Although a lot of investigations have been conducted with horizontal and vertical cylinders, little have been carried out with inclined cylinders. Furthermore little attention has been paid to heat transfer behavior at pressures other than atmospheric. In some of the earlier investigations constant heat flux conditions have been studied. With invariant pressure of the ambient fluid the constant input ultimately leads to constant heat flux situation. But this is not true for the present study.

Many industrial and house hold appliances, like refrigerating units, steam and feed water connections in power plants and industrial processes, electrical and electronic equipments employ natural convection from outside surface of cylinders for heating and cooling. These cylindrical surfaces are in different inclinations with horizontal. Since the buoyancy force i.e., gravity plays the major role in natural convection, the orientation of the surfaces with gravity field is of great importance.

The need for basic engineering knowledge of heat transfer at reduced pressure arises due to important developments in the design and availability of vacuum producing equipments and by the increased use of vacuum processes in food, pharmaceutical, metallurgical and other industries. Besides low pressure, high pressure is also employed in many applications like gas turbines and compressors. Therefore a careful investigation of heat transfer rate in these pressure ranges is of vital interest.

Inert gases like helium, argon, neon etc. have many industrial uses. In aerospace applications helium purge is used in pressurising space craft. It is also used as a protective atmosphere in the fabrication of titanium, zirconium and other metals, and the growth of transistor crystals and as a shielding gas for welding. It is also used for leak detection and cryogenic application. Neon has well known applications as a filler gas for display lights. It is also used for high energy research, instrumentation, safe low temperature cryogenics for special applications and in deep sea diving with mixtures of helium. Argon is used in metallurgical processes as a shielding gas in the welding of metals such as aluminum and stainless steel, in decarburizing in the production of stainless steel, in the refining of exotic metals such as zirconium, titanium and many other alloys, as a filler gas for incandescent light bulbs and has multiple use in many other applications.

Due to the numerous applications of the inert gases it is essential to understand their heat transfer behaviour. For the present investigation argon gas has been selected because it is readily available and has a lower cost compared to other inert gases and because of the limited scope of the work.

1.4 Objective of the Present Work

The objectives of the present study are as follows:

- (1) To design an experimental set-up for the determination of average heat transfer coefficient for horizontal, vertical and inclined cylinders.
- (2) To compare the results of the study with other relevant works and correlations available in literatures.
- (3) To determine the dependence of average heat transfer coefficient on pressure.
- (4) To determine the effect of inclination on heat transfer coefficient.
- (5) To determine the dependence of heat transfer coefficient on Rayleigh number.
- (6) To develop a possible correlation in terms of non-dimensional parameters which combines the objectives (3), (4) and (5).

CHAPTER 2

LITERATURE REVIEW

2.1 General

The knowledge of natural convection heat transfer from the cylindrical surface is of great interest to the designers of condenser tubes in different plants, fluid line connections in steam power plants, rod and cable manufacturing and of nuclear reactors. For fluids whose density changes with change of temperature there will be natural convection heat transfer but there exists a limiting situation where the buoyancy will be small compared to viscous and conduction effects. The non-dimensional group that indicates the relative strength of these effects is the Grashof number defined as

$$Gr = (g\beta\Delta T x^3 / \nu)^2 ; \quad \text{-----} \quad (2.1)$$

where, x is the characteristic length dimension of fluid layer, ΔT is the temperature difference across the layer, g is the gravitational acceleration, β is the coefficient of thermal expansion and ν is the kinematic viscosity. When the critical value of the Grashof number for the situation is exceeded (the value depends on the boundary conditions), a disturbance in the fluid will propagate and will result in a steady motion instead of dampening itself. The resulting convective motion has more or less a regular cellular roll pattern. The laminar flow regime has a structure of almost hexagonal cells [1]*. In the interior of these cells flow moves upward, and along the rim of the cell it returns downward.

Schorr and Gebhart [2] investigated the natural convection wake arising from a heated horizontal line source in liquids and air. The three dimensional effects for a wire with a length to diameter ratio of 250 were observed in air and water with Schlieren system. The temperature field in the plume above wires with length to diameter ratios of 250 and 1200 in liquid silicone ($Pr=6.7$) was determined using a 20cm Mach-Zehnder interferometer.

* The number in the parenthesis indicates reference number.

Various wire heating rates were used yielding Grashof numbers, based on vertical distance in the plume, in the range from $4 \cdot 10^3$ to $1.7 \cdot 10^6$. Excellent agreement of the temperature distribution with theory was found for large length to diameter ratio wires at Grashof numbers around 10^5 . A regular natural swaying motion of the plume was observed at high Grashof number, causing temperature fluctuations across the plume width.

Warrington and Powe [3] investigated the natural convection heat transfer between concentrically located isothermal spherical, cylindrical and cubical inner bodies in an isothermal cubical enclosure. They suggested the following correlation

$$Nu_L = 0.1 \cdot Ra_L^{0.317} \quad \text{-----} \quad (2.2)$$

with a maximum deviation of 15%.

Gebhart [4] suggested that the Grashof number range of validity for the laminar boundary layer flow appeared to be approximately 10^4 to 10^9 for vertical plates in air. Beyond this range of Grashof numbers the observed data were higher than that predicted by boundary layer results. In the range of Grashof number smaller than 10^4 it occurred because the boundary layer conception was no longer sufficiently accurate in this range. In such conditions the boundary layer thickness was too large, relative to the size of the object, for the boundary layer approximation to be valid. The deviation at $Gr > 10^9$ occurred because the flow in the convection layers was so vigorous that transition to turbulence occurred. This deviation of the mechanism of transport into regimes characterized by ranges of Grashof number is a general characteristic of natural convection process. Low Grashof number flows have thick boundary layers and the flows are very weak, whereas high Grashof number flows have thin boundary layers, the flows are vigorous and lead to laminar instability and transition.

The laminar flow is an orderly flow, whereas the turbulent one is interwoven and irregular, where individual fluid particles execute fluctuating motions around some mean flow path. Arabi and Khamis [5] claimed that for vertical cylinders critical Rayleigh number was found at $2.7 \cdot 10^9$ but for horizontal cylinder

no such critical value was found and they mentioned that it occurred at infinity.

Bertela, M. [6] studied the compatibility and mutual interaction among Rayleigh number, Grashof number and Eckert number without reference to physical systems. He proposed a new dimensionless group χ , which compactly accounts for the properties of the fluid and temperature difference across the fluid layers. He defined χ as

$$\chi = c_v^3 \Delta T / (g\beta)^2 = Re^6 / (Gr^2 Ec^3) \quad \text{-----} \quad (2.3)$$

2.2 Variable Fluid Properties

Most studies were based upon the assumption that the fluid properties were uniform, except for density. Most fluids, however, had properties which were temperature dependent. Therefore for processes involving large temperature differences the equations had serious limitations. As reported by Gebhart [4], Sparrow and Gregg have shown that for property variations, common to gases, the properties other than β should be evaluated at the following reference temperature t_r for vertical isothermal plates within laminar boundary layer.

$$t_r = t_o - 0.38(t_o - t_a) .$$

Bertela [6] pointed out that viscous dissipation was not always negligible in natural convection. Fand and Brucker [7] obtained a significantly better correlation for heat transfer by natural convection from horizontal isothermal cylinders assuming that Nusselt number was a function of the dimensionless parameter Gebhart number, Ge , that accounted for viscous dissipation. They suggested that following correlation should be used:

$$Nu = 0.4 Pr^{0.0432} Ra^{0.25} + 0.503 Pr^{0.0334} Ra^{0.0816} + 0.958 Ge^{0.122} / (Pr^{0.06} Ra^{0.0511}) \quad \text{-----} \quad (2.4)$$

Karim et al [8] concluded that the confinement of a heated horizontal cylinder by vertical adiabatic walls enhanced the heat transfer from the cylinder. The magnitude of the

relative enhancement decreased with the increase of Rayleigh number for all W/D, where W was the wall spacing. The enhancement of heat transfer from the cylinder decreased with the increase of spacing. They suggested the following equation:

$$Nu = [0.481 + 0.172 \exp(-0.258(W/D))] Ra_D^{0.25} \quad (2.5)$$

2.3 Vertical Surfaces

Warrington and Powe [3] reported that based on Sander's data Lorentz had suggested an equation for vertical surface at uniform temperature given by:

$$Nu_L = 0.548 * Ra_L^{1/4} \quad (2.6)$$

Gebhart [4] gave two correlations for the average convection coefficient for vertical plates of height L or for large diameter vertical cylinders in fluids having Prandtl number around 1.0. The characteristic dimensions used was L.

$$\begin{aligned} Nu_L &= 0.59 * Ra_L^{1/4} ; 10^4 \leq Ra_L \leq 10^8 , \\ Nu_L &= 0.13 * Ra_L^{1/4} ; 10^8 < Ra_L . \end{aligned} \quad (2.7)$$

The fluid properties were evaluated at the film temperature, $(t_o + t_a)/2$.

Holman [9] reported a number of values of constant C and exponent m to determine the average Nusselt number from

$$Nu_L = C * Ra_L^m ;$$

where, C and m were given for the following Rayleigh number range:

C	m	Ra _L range
0.59	1/4	10 ⁴ - 10 ⁹
0.021	2/5	>10 ⁹

Holman also suggested the following correlation using different references

$$Gr_x^* = Gr_x Nu_x = (g\beta q_w x^4)/(k\nu) ; \text{-----} \quad (2.9)$$

where, Gr_x^* was the modified Grashof number and q_w was the wall heat flux.

The local heat transfer coefficient was correlated by the following relation for the laminar range :

$$Nu_x = hx/k = 0.60(Gr_x^* Pr)^{1/5}; 10^5 < Gr_x^* < 10^{11}, \text{-----} \quad (2.10)$$

$$q_w = \text{constant.}$$

For turbulent regions the experiments were correlated as :

$$Nu_x = 0.17*(Gr_x^* Pr)^{1/4}; 2*10^{13} < Gr_x^* Pr < 10^{16}, \text{-----} \quad (2.11)$$

$$q_w = \text{constant.}$$

Properties were evaluated at the film temperature.

For constant heat flux

$$h = 5/4h_{x=L}; q_w = \text{constant.} \text{-----} \quad (2.12)$$

Yang and Yao[10] accounted for the trailing edge effect and gave the following correlation for natural convection along a finite vertical plate.

$$Nu = 0.53Pr^{0.314}Gr^{1/4} + 0.528Pr^{0.129}Gr^{1/28} \text{-----} \quad (2.13)$$

They claimed that the correlation was in good agreement for Prandtl numbers 0.72, 5 and 10 and concluded that, the flow accelerated near the trailing edge due to sudden change in geometry which resulted in the decrease of the flow constraint. The heat flux increased due to this local acceleration. Even though its effect on the total heat flux was small, it modified the local heat flux substantially.

Gryzagoridis[11] suggested that the leading edge of the plate did not influence greatly the average heat transfer rate from vertical plate. Martynenko et al[12] found that the wake effect on the boundary layer at the plate was manifested through the external flow.

2.4 Horizontal and Inclined Plates

For square plates placed horizontally Gebhart[4] suggested the following correlations for heated surface facing upward:

$$\begin{aligned} \text{Nu} &= 0.54\text{Ra}^{1/4} ; 10^5 < \text{Ra} < 10^7, \\ \text{Nu} &= 0.14\text{Ra}^{1/3} ; 10^7 < \text{Ra} < 3 \cdot 10^{10}. \end{aligned} \quad \text{-----} \quad (2.14)$$

The length of the plate was taken as significant dimension.

For heated surface facing downward the following relation was recommended by McAdams [13] :

$$\text{Nu} = 0.27\text{Ra}^{1/4} ; 3 \cdot 10^5 < \text{Ra} < 3 \cdot 10^{10} . \quad \text{-----} \quad (2.15)$$

For inclined surfaces with laminar boundary layer Gebhart [4] showed that the gravitational field in Grashof number was merely modified by the effect of inclination on the tangential body force. Making this change, the vertical surface equations might be used for surfaces where other effects could be neglected.

Fujii and Imura [14] conducted experiments for heated plates in water at various angles of inclination, θ . This θ was considered positive when heated surface faced downward. For constant heat flux the following correlation was suggested :

$$\begin{aligned} \text{Nu}_e &= 0.56(\text{Gr}_e \cdot \text{Pr}_e \cdot \sin\theta)^{1/4} ; \quad \text{-----} \quad (2.16) \\ \text{for } 2^0 < \theta < 90^0 , 10^5 < \text{Gr}_e \cdot \text{Pr}_e \cdot \sin\theta < 10^{11} . \end{aligned}$$

where, properties except β , were evaluated at a temperature T_e defined by

$$T_e = T_o - 0.25(T_o - T_a) , \quad \text{-----} \quad (2.17)$$

and β was evaluated at a temperature of $T_a + 0.25(T_o - T_a)$. For almost horizontal plates $\theta \leq 2^0$, with heated face facing downward the suggested correlation was :

$$\text{Nu}_e = 0.58(\text{Gr}_e \text{Pr}_e)^{1/5} ; 10^6 < \text{Gr}_e \text{Pr}_e < 10^{11} \quad \text{-----} \quad (2.18)$$

For θ between -15 to -75 and $10^5 < \text{Gr}_e \text{Pr}_e \sin\theta < 10^{11}$,

$$\begin{aligned} \text{Nu}_e &= 0.14[(\text{Gr}_e \text{Pr}_e)^{1/3} - (\text{Gr}_c \text{Pr}_e)^{1/3}] \\ &+ 0.56(\text{Gr}_c \text{Pr}_e \sin\theta)^{1/4}, \quad \text{-----} \quad (2.19) \end{aligned}$$

The quantity Gr_c , the critical Grashof number was dependent on θ . They recommended the following values of Gr_c :

θ	Gr_c
-75	$5 \cdot 10^9$
-60	$2 \cdot 10^9$
-30	10^8
-15	10^6

Holman [9] suggested that on constant heat flux surfaces for laminar regime equation 2.10, stated earlier, might be applied for both upward and downward facing heated surfaces if Gr_x^* was replaced by $Gr_x^* \sin\theta$.

Robinson and Liburdy [15] concluded that for horizontal heated disk with a point source at the centre, the outer velocity boundary condition decreased in relative magnitude as the disk Rayleigh number increased. Beyond a Rayleigh number of approximately 10^6 , the outer flow might be ignored in calculating the disk heat transfer rate.

Chen et al [16] on the basis of their analysis on natural convection in laminar boundary layer flow over horizontal, inclined and vertical flat plates for power law variation of surface temperature, $T_w = T_a + a'x^n$ and the power law variation of surface heat flux concluded that for given values of ζ and η where, $\zeta = (Gr_x \cos\theta/5)^{1/5} \tan\theta$, and $\eta = (Gr_x^* \cos\theta/5)^{1/5} \tan\theta$; and Gr_{rx}^* , the modified Grashof number for constant heat flux, $(q'' = g\beta q_{wx} x^4/k)^{1/2}$ and for given values of exponents m and n , the local surface heat flux increased with increasing Prandtl number.

Schulenburg [17] suggested the following correlations for natural convection heat transfer from downward facing horizontal surfaces :

$$Nu/Ra^{1/5} = 0.571 Pr^{1/5} / (1 + 1.156 Pr^{3/5})^{1/3}, \quad \text{-----} \quad (2.20)$$

for an infinite strip with specified surface temperature;

$$Nu/Ra^{*1/6} = 0.643 Pr^{1/6} / (1 + 1.132 Pr^{1/2})^{1/3}, \quad \text{-----} \quad (2.21)$$

for an infinite strip with specified surface heat flux;

where, Ra^* was modified Rayleigh number $= Gr^* Pr = Pr \alpha g \beta_w R'^4 / k \nu^2$ and R' was the half width of the infinite strip.

2.5 Vertical Cylinders

For Prandtl numbers 0.733, 1.0, 10 and 100 Gebhart [4] reported that Millsaps and Pohlhausen developed a correlation of the form:

$$hD/k = 1.058 (Gr')^{1/4} (Pr^2 / (4 + 7Pr))^{1/4}, \quad (2.22)$$

For a surface whose temperature t_o increased linearly with x , i.e., $t_o - t_a = N \cdot x$; Gr' was defined as temperature gradient Grashof number

$$Gr' = g \beta D^4 N / \nu^2 \quad (2.23)$$

In reference [4] Sparrow and Gregg had shown that for Prandtl numbers 0.72 and 1.0 flat plate solution was not in error by more than 5% in heat transfer rate from vertical cylinders of sufficiently large diameter such that

$$D/L \geq 35 / Gr_L^{1/4} \quad (2.24)$$

Arabi and Khamis [5] reported the correlation of Elenbaas for stationary fluid around the vertical cylinder as follows:

$$Nu_D \cdot \exp(-2/Nu_D) = 0.6 (D/L \cdot Ra_D)^{1/4} \quad (2.25)$$

They also quoted the comparison of Ede who had compared the results of different observation with Elenbaas equation and found that the data of water were within 25% and that for gases were within $\pm 20\%$.

Nagendra et al [18] carried out experiments by employing a cylinder of 8 mm diameter and 305 mm length at constant heat flux. They also theoretically studied the effect of diameter on natural convection heat transfer from vertical cylinders and wires. They suggested the following correlation :

$$\begin{aligned} Nu_D &= 0.6 (Ra_D \cdot D/L)^{0.25}, \text{ for } Ra_D \cdot D/L \geq 10^4; \\ &= 1.37 (Ra_D \cdot D/L)^{0.16}, \text{ for } 0.05 \leq Ra_D \cdot D/L \leq 10^4; \\ &= 0.93 (Ra_D \cdot D/L)^{0.05}, \text{ for } Ra_D \cdot D/L \leq 0.05; \end{aligned} \quad (2.26)$$

where, the average temperature difference was used in Rayleigh number calculation. They claimed that the constant heat flux results differed from constant wall temperature ones by less than 5%.

Fujii et al [19], on the basis of the experimental investigation with water, spindle oil and molybdenum oil, suggested the following correlation :

$$(Nu_L)_a \left(\frac{\nu_o}{\nu_a} \right)^{0.21} = (0.017 \pm 0.002) * (Gr_L Pr)_a^{2/3}; \quad \text{-----} \quad (2.27)$$

for $10^{10} \leq (Gr_L Pr)_a$

where, 'a' represented the condition in the ambient fluid. They claimed that the equation was also applicable for air.

Lee et al [20], on the basis of their analysis concluded that for the power-law variation in wall temperature, $T_w = T_a + a' * x^n$, x being the axial coordinate, the local surface heat transfer increased with increasing value of curvature for given values of the exponent n and Pr.

2.6 Horizontal Cylinders

McAdams[13] analyzed experimental data of many investigators to correlate the average natural convection heat transfer for horizontal cylinders. He derived an equation similar to Lorentz's equation, namely

$$Nu = C Ra^m; \quad \text{-----} \quad (2.28)$$

where, the constant C and the exponent m depended on the range of Ra. The fluid properties were evaluated at the mean film temperature.

Kutateladze [21] modified Lorentz formula using the experimental data of many investigators and arrived at the following equation applicable to horizontal cylinders:

$$Nu = K(Pr) (Ra)^{0.25}, \quad 5 * 10^2 \leq Ra \leq 2 * 10^7; \quad \text{-----} \quad (2.29)$$

where, $K(Pr) = 0.54$ for $0.5 \leq Pr \leq 200$ and $K(Pr) = 0.65$ for $Pr > 200$.

Morgan[22] recommended a correlation similar to Lorentz and suggested the values of C and m as follows:

C	m	Ra
0.675	0.058	10^{-4} to 10^{-2}
1.02	0.148	10^{-2} to 10^2
0.85	0.188	10^2 to 10^4
0.48	0.25	10^4 to 10^7
0.125	0.333	10^7 to 10^{11}

Churchill and Chu[23] published the following correlation for natural convection from horizontal cylinders:

$$Nu = 0.36 + 0.518 \{ Ra / [1 + (0.559/Pr)^{9/16}]^{16/9} \}^{0.25} \quad (2.30)$$

They also stated in their paper that the equation provided a good fit and was representative for all Pr and $10^{-6} \leq Ra \leq 10^9$, except for the data of small diameter wires.

Mikheyeva [24], investigated the process of natural convection from horizontal tubes to air, water and oil and recommended the following correlation:

$$Nu_b = 0.51 * Ra_b^{0.25} (Pr_b/Pr_s)^{0.25} ; \quad (2.31)$$

where, the subscripts b and s referred to bulk and surface conditions respectively and the term $(Pr_b/Pr_s)^{0.25}$ was the correction factor intended to account for the influence of property variation with temperature.

Fand et al[25] presented the results of an experimental investigation of natural convection heat transfer from horizontal cylinders to air, water and three silicone oils, with Rayleigh numbers ranging from $2.5 * 10^2$ to $1.8 * 10^7$ and Prandtl number from 0.7 to 3090. On the basis of experimental data three equations were derived. The equations were of the same algebraic form and differed only in the method used to evaluate fluid properties as a function of temperature. The equations are as follows :

$$\begin{aligned} Nu &= 0.474 * Ra^{0.25} Pr^{0.047} ; \\ Nu_j &= 0.478 * Ra_j^{0.25} Pr_j^{0.05} ; \\ Nu_n &= 0.456 (Gr_q Pr_p)^{0.25} Pr_p^{0.057} ; \quad (2.32) \end{aligned}$$

where, the equation without any subscript referred to the mean film temperature. The equation with subscript j used the fluid at the temperature defined by

$$t_j = t_a + j (t_o - t_a) ; \text{ and } j = 0.32, p=q=0.5, n=0.2$$

also n was the surface correction exponent dependent on Grashof number and Prandtl number.

Eckert and Drake [26] suggested the following correlation for vertical wires :

$$Nu_D = 2 / [\ln\{1 + (2/0.4Gr_D^{1/4})\}]. \text{ ----- (2.33)}$$

Socio [27] presented a paper that dealt with the plane problem of laminar natural convection around horizontal cylinders with partly isothermal and partly adiabatic surfaces. The adiabatic surface subtended an angle 2δ at the axis of the cylinder. He suggested a correlation of the type

$$Nu = BRa^m. \text{ ----- (2.34)}$$

For different values of δ , half angle of the adiabatic sector, the following values of B and m were suggested:

δ^0	B	m
0	0.488	0.246
45	0.543	0.239
90 up	0.581	0.241
90 down	0.569	0.236

2.7 Inclined Cylinders

For inclined cylinders data available are very limited. Al-Arabi and Khamis [5] analyzed the works of different investigators like Crane and Eigenson. Crane carried out experiments on heated cylinders of diameter 5 mm to 76 mm and length 0.076 to 3.30 m in air. Eigenson carried out experiments on cylinders in

gases only in the turbulent region. The following equation was suggested:

$$Nu_L = B(Gr_L Pr)^{1/3}; \text{-----} \quad (2.35)$$

where, B was a function of Gr_D .

Arabi and Salman [28] reported that Ferber and Rennat experimented with a 1.829 meter long and 3.175 mm outside diameter cylinder heated by passing an electric current through it to give a constant heat flux at angles from 0° (horizontal) to 90° . The heat transfer coefficient was found to decrease with the increase of inclination. No general correlation of the results was suggested.

Oosthuizen [29] experimented with cylinders of length between 152.4 and 304.8 mm and outside diameter between 19.1 and 25.4 mm at angles of inclination between 0° to 90° . The heat transfer rate was found to decrease with inclination and the results were correlated in terms of $Nu_D / (Gr_D \cos\theta)^{1/4}$ against $(L/D \cot\theta)$.

Al-Arabi and Salman [28] carried out experiments on a cylinder of 38 mm diameter and 950 mm length under constant heat flux condition. The angle of inclination was varied from 0° to 90° . On the basis of their investigation the following conclusions were made :

(1) For the same flux both the local and average heat transfer coefficients decreased with the angle of inclination of the cylinder.

(2) The critical value of $(Gr_x Pr)$ for the end of the laminar region, decreased with the increase of θ .

(3) Local heat transfer coefficient for all angles of inclination could be represented by the equation :

$$Nu_x = 0.545 - 0.387(\cos\theta)^{1.462} (Gr_x Pr)^{1/4 + 1/12(\cos\theta)^{1.75}} \text{----} \quad (2.36)$$

and the average heat transfer coefficient by the equation:

$$Nu_L = 0.60 - 0.488(\cos\theta)^{1.03} (Gr_L Pr)^{1/4 + 1/12(\cos\theta)^{1.75}} \text{----} \quad (2.37)$$

Al-Arabi and Khamis [5] carried out experiments to determine the average and local heat transfer coefficient by natural convection to air from the outside surface of isothermal

cylinders of different diameters (12.75 mm to 51 mm) and lengths (0.3 meter to 2.0 meter) at different inclinations (30^0 to 90^0) in both laminar and turbulent regions. The following conclusions were made:

(1) The average heat transfer coefficient decreased with the increase of diameter.

(2) For the bigger lengths, h_L , average heat transfer coefficient based on L, decreased with θ . For the shorter lengths it increased with θ . In between, a 'limit length' existed at which the heat transfer coefficient was constant irrespective of θ . This was equal to the heat transfer coefficient corresponding to the horizontal cylinder.

(3) For the same cylinder diameter and inclination, the average heat transfer coefficient decreased gradually with the increase of cylinder length and then it became constant indicating the beginning of turbulence.

(4) Based on average heat transfer coefficient the critical transition point from the laminar to the turbulence region was independent of diameter and only decreased with the increase of the inclination.

(5) Based on local heat transfer the critical transition point representing the end of the laminar region was independent of cylinder diameter and depended on inclination only. The critical point representing the beginning of the turbulent region, however, appeared to be constant.

(6) The following correlations were suggested :

$$\begin{aligned}
 Nu_L &= [2.9 - 2.32(\cos\theta)^{0.8}] Gr_D^{-1/12} [Gr_L Pr]^{1/4 + 1/12(\cos\theta)^{1.2}} \\
 &\text{for } 1.08 \cdot 10^4 \leq Gr_D \leq 6.9 \cdot 10^5 \text{ and } 9.88 \cdot 10^7 \leq Gr_L Pr \leq (Gr_L Pr)_{cr}, \\
 Nu_L &= [0.47 + 0.11(\cos\theta)^{0.8}] Gr_D^{-1/12} [Gr_L Pr]^{1/3}, \quad \text{-----} \quad (2.38) \\
 &\text{for } 1.08 \cdot 10^4 \leq Gr_D \leq 6.9 \cdot 10^5 \text{ and } (Gr_L Pr)_{cr} \leq Gr_L Pr \leq 2.95 \cdot 10^{10}. \\
 Nu_x &= [2.3 - 1.72(\cos\theta)^{0.8}] Gr_D^{-1/12} [Gr_x Pr]^{1/4 + 1/12(\cos\theta)^{1.2}} \\
 &\text{for } 1.08 \cdot 10^4 \leq Gr_D \leq 6.9 \cdot 10^5 \text{ and } 1.63 \cdot 10^8 \leq Gr_x Pr \leq (Gr_x Pr)_{cr}. \\
 Nu_x &= [0.42 + 0.16(\cos\theta)^{0.8}] Gr_D^{-1/12} [Gr_x Pr]^{1/3}, \quad \text{-----} \quad (2.39) \\
 &\text{for } 1.08 \cdot 10^4 \leq Gr_D \leq 6.9 \cdot 10^5 \text{ and } (Gr_x Pr)_{cr-1} \leq Gr_x Pr \leq 2.3 \cdot 10^{10}.
 \end{aligned}$$

2.8 Studies on Natural Convection at Pressures other than Atmospheric

Data in this field are also very limited. Kyte et al [30] reported natural convection at reduced pressures. Heat losses at pressures ranging from 0.1 mm to atmospheric pressure were determined for a 0.00306 inch diameter wire in air and for 0.312 and 1.00 inch diameter spheres in helium, air and argon. Surface temperatures of upto 195°C were employed, and subtractions were made for radiation to obtain the net heat transferred by convection.

At low gas pressure the thickness of convective boundary layer and the effect of free molecule conduction was important. These effects were considered for both spheres and horizontal cylinders. This involved two departures from classical practice:

(1) The characteristic length used in the dimensionless Grashof number became the diameter of the solid plus twice the length of mean free path of the gas.

(2) The concept of a conductive film having the same resistance to the heat transfer as that of the convective boundary layer was used instead of the Nusselt number to arrive at a single correlation. On the basis of the investigation the following correlations were suggested for cylinders :

$Ra_{d',m}$ range	Horizontal
10^{-7} to $10^{1.5}$	$q = 2\pi L k_{b,a} (T_b - T_a) / \ln[1 + 7.09 / (Ra_{d',m})^{0.37}]$ $q = \pi D L \lambda_e P \alpha' \sqrt{(273.2/T_b)} (T_w - T_b)$
$10^{1.5}$ to 10^9	$q = 2\pi L k_{b,a} (T_b - T_a) / \ln[1 + 5.01 / (Ra_{d',m})^{0.26}]$ $q = \pi D L \lambda_e P \alpha' \sqrt{(273.2/T_b)} (T_w - T_b)$

----- (2.40)

 Vertical

$$10^{-11}(\text{Ra}_{d',m} D'/Z) \leq 10^{-4.5}$$

$$q = 2\pi L k_{b,a} (T_b - T_a) / \ln[1 + 4.47 / (\text{Ra}_{d',m} D'/Z)^{0.26}]$$

$$q = \pi D L \Lambda_0 P \alpha' \sqrt{(273.2/T_b)} (T_w - T_b)$$

----- (2.41)

where,

T_b = absolute temperature at a distance of λ_b from the solid in degree Kelvin, λ_b being the length of the mean free path of the gas at that temperature.

P = gas pressure in mm of mercury.

α' = accommodation coefficient.

Λ_0 = free molecule conductivity of the gas at 0°C in $(\text{W}/\text{m}^2)(^{\circ}\text{K})(\text{mm Hg.})$

k = thermal conductivity of the gas.

$D' = D + 2\lambda_b$.

Z = length of the heated wire.

suffix,

d',m -- indicated that the dimensionless groups were evaluated using D' as diameter, $(T_b - T_a)$ as the gas temperature difference, $(T_b + T_a)/2$ as the mean temperature at which the gas properties were to be evaluated.

d,m -- indicated that the dimensionless groups were evaluated using D as diameter, $(T_b - T_a)$ as the gas temperature difference, $(T_b + T_a)/2$ as the mean temperature at which the gas properties were to be evaluated.

'w' indicated wall.

'a' indicated ambient gas.

$k_{b,a}$ = thermal conductivity evaluated at a mean temperature of $(T_b + T_a)/2$.

$k_{w,a}$ = thermal conductivity evaluated at a mean temperat-

urature of $(T_w + T_a)/2$.

q = rate of heat loss other than radiation.

They also recommended that, free molecule conduction may be ignored for any gas at atmospheric pressure if the diameter of the solid is 0.001 inch or greater and the solid surface temperature was 200°C or less. In such cases it is required that Ra_{d',m,T_b} and D' be replaced by Ra_{d,m,T_w} and D respectively.

Warner and Arpachi [31] on the basis of their experimental study on turbulent natural convection in air at low pressure along a vertical heated flat plate, suggested the correlation as:

$$Nu = 0.10 Ra^{1/3}, \quad Ra < 10^{12}. \quad \text{-----} \quad (2.42)$$

Hesse and Sparrow [32] on the basis of their experiments at both atmospheric and higher pressures with 0.4 mm diameter platinum wire within a horizontal cylinder of 165 mm diameter and 110 mm length, concluded that the data fell within 10% of the McAdams correlation [13], with a tendency for the data to lie below the correlating line.

Holman [9] suggested that for pressures above and below atmospheric the simplified natural convection equations from the various surfaces to air at atmospheric pressure should be multiplied by the following factor:

$$\begin{aligned} & (P/101.32)^{1/2}, \quad \text{for laminar cases and} \\ & (P/101.32)^{2/3} \quad \text{for turbulent cases ;} \quad \text{-----} \quad (2.43) \end{aligned}$$

where, P was the pressure in KPa.

CHAPTER 3

MATHEMATICAL MODELING OF THE PROBLEM

3.1 General

The fundamental physical processes which occur in natural convection flows are essentially same as those occurring in other flow and diffusion processes. Potential energy, kinetic energy, thermal energy, momentum, viscous and pressure forces aid or oppose fluid motion. It is possible to formulate differential equations which result from the consideration of the conservation of mass (continuity), momentum (Navier-Stokes) and of energy (energy equation).

The set of equations of motion embodying the approximation of Boussinesq are written below for constant transport properties μ , k and c_p , from Gebhart [4]. Two energy equations are given, the first for fluids of invariant density and the second for ideal gases.

$$\nabla \cdot \mathbf{V} = 0$$

$$\rho [\partial \mathbf{V} / \partial \gamma + (\mathbf{V} \cdot \nabla) \mathbf{V}] = g \beta \rho (t - t_a) \mathbf{i} - \nabla p_m + \mu \nabla^2 \mathbf{V}.$$

$$\rho c [\partial t / \partial \gamma + (\mathbf{V} \cdot \nabla) t] = k \nabla^2 t + q'' + \delta (R3).$$

$$\rho c_p [\partial t / \partial \gamma + (\mathbf{V} \cdot \nabla) t] = k \nabla^2 t + q'' + (D p_h / D \gamma) (R4) + D(p_m) (R0) / D \gamma + \mu \delta (R3).$$

where, $R0 = g \beta x / R$, $R1 = \beta \Delta T$, $R3 = O(\text{Pr} R0)$, $R4 = O(\beta T R0 / R1)$ and $\beta = 1/T$ for gases, the magnitude of $R0, R1, R3$ and $R4$ are relatively small.

For one-dimensional upward motion along a vertical surface the dissipation function δ has been represented by the equation

$$\delta = 2(\partial u / \partial x)^2 - (2/3)(\nabla \cdot \mathbf{V})^2.$$

3.2 Description of the Problem

The natural convection heat transfer from a cylinder is a complex problem. It is influenced by physical dimensions of the cylinder, its orientation, the environmental condition and properties of the ambient fluid. The test cylinder of the present inves-

tigation was suspended from the top of a large container (vessel) by copper wires. The L/D ratio of the test cylinder was about 25.5 and it could be set at any desired inclination. The container temperature did not vary considerably. The temperature variation along the axis of the test cylinder could also be ignored for any particular data point although considerable changes of surface temperature of the test cylinder were noticed among different data points. A constant electric energy input to test cylinder was maintained which was converted into heat. This heat was transferred firstly by radiation to the container, secondly by conduction through the thermocouple and holding wires and thirdly by convection to the ambient gas. The conduction losses were small and could be estimated. The amount of heat transfer by radiation could also be calculated directly by using Stefan-Boltzman equation. The net heat transferred by convection, natural convection in the present case, couldn't however be directly quantified as it is dependent on fluid properties, orientation of the convecting surface, ambient fluid pressure etc. So the present problem was to correlate these parameters to obtain the convective heat transfer.

3.3 Similarity Solution

The solution of equations presented in section 3.1 are very complicated, but the parameters upon which the characteristics of the flow and transport depend may be found by the similarity technique.

Considering a vertical surface of height L at a uniform temperature t_0 in an extensive uniform medium at t_a , the coordinate, velocity, pressure and temperature are generalized by L, U_c, U_c^2 and $(t_0 - t_a)$ respectively, where U_c is the convection velocity and can be determined by using Boussinesq approximation. According to this approximation, pressure gradient can be approximated as a pure temperature effect, $\rho_a - \rho = \rho \beta (t - t_a)$ and the density variation in the continuity equation is ignored. Thus

$$U_c = \sqrt{g \beta x (t_0 - t_a)}$$

Neglecting energy generation and considering steady state condition, the equations for a gas in terms of generalized quantities $V, \delta = (t - t_a) / (t_o - t_a)$, p_h (local hydrostatic pressure), p_m (difference between the actual pressure and p_h) and δ become

$$\nabla \cdot V = 0$$

$$(V \cdot \nabla) V = \delta i - \nabla p_m + (\nu / U_c L) \nabla^2 V.$$

$$(U_c L / \nu) (V \cdot \nabla) \delta = (k / c_p \mu) \nabla^2 \delta + (gBL / c_p) (U_c L / \nu) (V \cdot \nabla) \delta + (gBL / c_p) \delta.$$

The boundary conditions are as follows:

$$\text{On the surface : } V=0 \text{ and } \delta=1,$$

$$\text{in the distant medium : } V=0, \delta=0 \text{ and } p_m = 0.$$

Two sets of differential equations are similar if they have constant coefficients. Thus the above generalization of the equations indicates that the temperature distribution $\delta(x, y, z)$ depends only upon Gr, Pr and (gBL / c_p) . Thus the dimensionless parameters that arise in natural convection are

$$U_c L / \nu = (gBL^3 \Delta T / \nu^2)^{1/2} = \sqrt{Gr},$$

$$c_p \mu / k = (\mu / \rho) / (k / \rho c_p) = \nu / \alpha = Pr, \text{ and}$$

$$gBL / c_p, \text{ which is one form of Eckert number, } Ec.$$

The quantity

Gr , the Grashof number is a measure of the vigor of the flow induced by U_c and represents the ratio of buoyant force to viscous force.

Pr , the Prandtl number is the ratio of viscous diffusivity to thermal diffusivity. It affects the temperature gradient of a flow field.

gBL / c_p gives an indication of the relative importance of viscous dissipation.

Therefore the natural convection expressed in nondimensional form as Nusselt number ($= hL / k$) can be written in the form

$$Nu = F(Gr, Pr, gBL / c_p) \text{ ----- (3.1)}$$

3.4 Modification of the Similarity Equations for the Present Problem

To account for pressure variation the normalized pressure P/P_a can be introduced in the Nusselt number equation. Assuming heat transfer to ideal gases, the viscous dissipation function can be modified as

$$gBL/c_p = (g/c_p)(1/T)L = (g/c_p)(R/Pv)L = (gRL/c_p v)(1/P).$$

For the present study the volume v is constant. So the term $(gRL/c_p v)$ is constant. Therefore the last group in the Nusselt number equation (3.1) can be expressed in terms of pressure and it takes the form

$$Nu = F(Gr, Pr, P/P_a). \quad \text{-----} \quad (3.2)$$

For surfaces other than vertical, the inclination θ should be included in the Nusselt number equation. In evaluating convection from an inclined surface, the gravitational acceleration g in the Grashof number equation must be replaced by $g \sin \theta$ [4] for $\theta > 0$ (i.e. except for horizontal surfaces). Therefore the Nusselt number equation can be corrected for inclined surfaces as

$$Nu = F(Gr, Pr, P/P_a, \theta). \quad \text{-----} \quad (3.3)$$

For cylindrical surfaces the analysis is much complicated and is not readily available in the literatures. But as discussed in section 2.5, the vertical cylinders with large diameters can be approximated as vertical flat plates. So instead of deducing separate differential equation the similarity solution of flat plates will be applied to cylindrical surfaces to correlate the non-dimensional parameters on the basis of the experimental data.

CHAPTER 4

EXPERIMENTAL SETUP

4.1 General description

This chapter describes the experimental aspects of the investigation and includes a description of the apparatus used. Figure 21 and 22 show a schematic diagram of the experimental set up and the test cylinder. The apparatus used in the investigation was a 'Radiation and Convective Heat Transfer Equipment', manufactured by Plint and Partners Ltd., England. It consisted of an almost spherical steel vessel, within which the test cylinder was suspended. It was equipped with a voltmeter, an ammeter, a vacuum pump, a high pressure connection line and a mercury manometer.

4.2 Test Specimen

Two test cylinders made of copper were separately tested and they were designated as specimen 1 and specimen 2. The test cylinders with matt black surface finishing could be suspended from the top of the vessel at a predetermined inclination. Specimen 1 was 159 mm long whereas specimen 2 was 161 mm long. Both of them were of 6.35 mm outside diameter and 4.0 mm inside diameter. The test cylinder was heated internally by passing an electric current through a Ni-Chrome wire. The Ni-Chrome wire was passed through porcelain beads which acted as the insulator between the wire and the cylinder. Beads had approximately 3.85 mm outside diameter, about 1.0 mm internal hole and 3.5 mm length. At each end of the cylinder a bead extended outside by about 2 mm. The Ni-Chrome wire was fastened to 0.62 mm diameter copper wires at both ends for holding the test cylinder. The gaps between the beads and the wire and between beads and the ends of the cylinder were filled with asbestos wool so that the wire and the beads did not move axially or radially. This also acted as a safeguard against any electrical short circuiting between the holding wires and the cylinder. Holding wires were 90 to 100 mm

long and were attached at the other end to insulated flexible wires. These flexible wires were suspended freely from the cover plate of the vessel top, and in turn supported the test cylinder. The top cover plate had two screws, the inner side of which were connected to the suspending wires and the other side to electric leads.

4.3 Temperature Measuring devices

The ambient gas temperature (inside the vessel) could be measured directly by a digital thermometer, provided in the radiation and convective heat transfer equipment, using a No. 36SW Chromel-Alumel thermocouple. The difference between this temperature and the outside environment temperature was not much and the outside air movement was also negligible. The vessel size (shown in figure 21) was sufficiently large, about 447 mm in dia. and 465 mm in height, so that the heated fluid rising upward from the test cylinder cooled down to approximately at the bulk fluid temperature as it reached the vessel surface. Since the air outside the vessel was stagnant and both the outside air and inside gas were at equilibrium with the vessel, its temperature might be taken as that of the undisturbed inside ambient fluid. At steady state, the heat generated by the heater, the test cylinder, was equal to the heat that was conducted through the vessel wall to the outside air before appreciable rise in the inside fluid temperature was noticed. To measure the temperature of the test cylinder surface, No. 28SW Copper-Constantan thermocouples were used. The thermocouples were fixed to the surface of the test cylinder by soldering them on equally spaced holes, 1 mm deep and 2 mm in diameter. This is shown in figure 23. Through a hole at the bottom of the vessel the insulated copper leads (24 gage), connected to the thermocouple wires, were brought out side the vessel and were connected to the digital milli-voltmeter (Drone Digital Indicator, Series 60) through a selector switch (Crapico). The digital milli-voltmeter range was -15.99 to 99.99 mV and the accuracy of the instrument was ± 0.001 mV. Five thermocouples were connected to specimen 1 and three to

specimen 2. The thermocouple lead wires were taken out of the vessel through a opening at the bottom and gland packing was used to prevent any leakage (figure 24).

4.4 Pressure Measuring and Control Devices

System pressure (pressure within the vessel) was measured by a Hg manometer provided in the radiation and convective heat transfer equipment. Pressures upto 1000 mm Hg gage could be measured by this manometer. Atmospheric pressure was measured separately by a barometer. To conduct the experiments at high pressure with air a separate air compressor (1/4 hp, 750 rpm) was connected to the high pressure connection line. By using a pressure release valve, a pressure line disconnection valve and a pressure regulator valve, attached to the apparatus, the desired pressure in the vessel could be maintained. Low pressure could be maintained by operating the vacuum pump (1/4 hp, 822 rpm) of the apparatus. With argon, the experiments were carried out by charging the vessel from a high pressure argon cylinder.

4.5 Input Heat Measuring Devices

The total power input to the apparatus could be measured by the voltmeter and the ammeter provided in the apparatus. In addition a calibrated wattmeter was used to monitor the actual energy transferred to the test cylinder.

CHAPTER 5

Experimental Measurement and Test Procedure

5.1 Measurement of Temperature

Thermocouples fitted to the test cylinder surface were connected to the digital milli-voltmeter through a selector switch, as stated in section 4.3. These thermocouples were calibrated in melting ice (0°C) and in boiling water open to atmosphere (100°C) and the graph was extended linearly over the entire range of measurement (50°C to 155°C). Both during calibration and test run, the cold junction temperature of the thermocouple wires was maintained at 0°C . The set-up of calibration is shown in Appendix D. The calibration curve was found to fit reasonably well with the standard millivolt data from the conversion table. The measurements showed that the temperature along the axis of the cylindrical surface did not vary by more than 2.5°C . The mean of the individual local temperatures was therefore taken as the average temperature of the cylindrical surface. This average temperature was used in calculations and determination of heat transfer coefficient. As mentioned in section 4.3, the temperature of the inside ambient fluid was measured directly by the thermocouple fixed with the apparatus and the temperature of the vessel was taken equal to that of the inside ambient fluid.

5.2 Estimation of Emissivity

The cylindrical surface of the test specimens, painted matt black had emissivity of 0.97 for specimen 1 and 0.99 for specimen 2. The procedure of estimating emissivity is shown in Appendix B.

5.3 Measurement of Pressure

Pressures in the enclosed vessel were measured by a U-tube mercury manometer. An error of 2 mm was observed for the

gage pressure reading of ± 750 mm Hg. This might have been due to the nonuniformity of the tube bore. The error did not affect the result much. Atmospheric pressure was measured once or twice during one set of experiment.

5.4 Setting of Inclination

The top cover-plate of the spherical vessel was fastened to the vessel by twelve bolts fixed on it. To set a given inclination of the test cylinder, the cover plate was opened and the supporting flexible wire length was adjusted. For horizontal position, both supporting wires were of the same length. For 30° , 45° and 60° inclinations one supporting wire length was kept fixed and the other wire length was reduced by $L \sin \theta$ from the length of the wire in the horizontal position, whereby neglecting the obliquity, the inclination of the cylinder could be taken as θ . For vertical position, the test cylinder was practically suspended from one supporting wire and the other support was replaced by a sufficiently long wire so that it hung freely.

5.5 Determination of Heat Transfer Coefficient

The electrical energy input to the test cylinder was transferred partly to the enclosed vessel by radiation, partly to the thermocouples and holding wires by conduction and the rest to the ambient fluid by convection. The procedure of estimating each of them are discussed below. Having obtained the convective heat transfer rate, the convective heat transfer coefficient was determined by dividing the convective heat transfer rate by the product of the surface area of the test cylinder and the temperature difference between the test specimen and the undisturbed ambient fluid.

5.5.1 Measurement of Input Power

A constant heat input to the system was maintained. Input voltage and amperage was measured by the voltmeter and

ammeter provided in the apparatus. The test cylinder was heated electrically by a 220/230 V ac supply through a transformer and a rheostat, contained in the apparatus. The voltmeter could read upto 15 volt with an accuracy of 0.1 volt. The range of ammeter was 0 to 1.0 ampere and the minimum value that could be read was 0.01 ampere. To get the power input to the test cylinder a separate wattmeter was used to measure the actual power consumed by it. It was seen that an input factor of 0.95 could be integrated which on multiplication to the input volt-ampere gave the heater energy consumption.

5.5.2 Estimation of Conduction Loss

Since thermocouples were attached to the surface of the test cylinder a portion of energy generated in it was conducted through the thermocouples and holding wires to the ambient fluid. Appendix A contains the outline of the procedure to calculate the conduction losses.

5.5.3 Estimation of Radiation from the Cylinder

A substantial part of the heat input to the cylinder was transferred by radiation to the enclosed vessel. This radiation heat transfer was evaluated by using the Stefan-Boltzman equation. The relevant emissivity value used was obtained as discussed in section 5.2.

5.5.4 Estimation of Heat Loss from the Protruded Beads

As mentioned in section 4.2, the heating Ni-Chrome wire was passed through porcelain beads inside the cylinder and fastened to the holding copper wires at each end. On both ends the beads were extended 2 mm to avoid the electric contact between the cylinder and the wire. Since the end beads contained the ends of the Ni-Chrome wire, a portion of the heat input to the test cylinder was lost through the bead surface. In stead of measuring the actual heat loss from the bead surfaces, an approximation was

made assuming that the amount of heat transferred from the cylinder surface was proportional to the length of the Ni-Chrome wire contained in it. Thus the fraction of the total input lost by the beads was $(4/L+4)$ and the fraction of total generated heat transferred from the surface of the test cylinder was $(L/L+4)$. This factor was coupled with the input factor(0.95), described in section 5.5.1, to give a modified factor of 0.927 which, when multiplied with the input volt-ampere gave the actual heat transferred from the cylinder surface.

5.5.5 Calculation of Convective Heat Transfer

As mentioned in the previous section, the product of volt, ampere and the modified factor yielded the heat transferred from the surface of the test cylinder. Subtractions from this were made for conduction and radiation, as discussed in sections 5.5.2 and 5.5.3, to obtain the heat transferred from the test cylinder by convection.

5.5.6 Estimation of Emitting and Convective Surface Area

The heating Ni-Chrome wire was fastened to the holding copper wire at each end, as mentioned in section 4.2. Heat generated by the Ni-Chrome wire was conducted through the holding wires. The holding wires lay in vertical position irrespective of the orientation of the cylinder and lost heat by conduction, radiation and convection. It was complicated to account for the actual heat lost by the holding wires. Neglecting the radiation the configuration was therefore analysed as an infinite protruded rod. This is shown in Appendix A. The heat lost by the holding wires were then compensated by an equivalent area of the test cylinder to give the same heat loss by convection and radiation. This area was estimated as 4% of the cylinder surface.

5.6 Test Procedure

The experiments were conducted with two cylindrical specimens marked specimen 1 and specimen 2, one after the other. The two fluids used were air and argon. Five orientations of the test cylinder making angles of 0° , 30° , 45° , 60° and 90° with horizontal were tested. A brief description of the procedure is given below:

- (1) From the two ends of the test cylinder holding wires were taken out and connected to flexible wires, the other ends of which were attached to the screws at inside face of the cover plate. For horizontal position of the test cylinder two equal flexible wires (each 160 mm long) were used.
- (2) The cover plate was held horizontal at the corner of a flat table and the test cylinder was allowed to hang freely to see if it lay at the desired configuration without any kink or twisting in the supporting wires.
- (3) The cover plate was set on the vessel and the nuts were tightened. The leads of the heater line were connected to the screws on the cover plate.
- (4) To carry on experiments with air as the fluid, the gas release valve was closed, the gas line disconnecting valve was opened, the compressor delivery line was connected to the high pressure connection line and the compressor was switched on. The gas disconnecting valve was closed when the Hg manometer showed a gage pressure of about 900 mm. The compressor was switched off and the gage reading was recorded.
- (5) The heater switch was turned on, voltmeter and ammeter readings were adjusted and the test cylinder was heated for about two hours. The milli-voltmeter was switched on to see the variation of mV reading at a particular location. The selector switch was turned to see the readings of different thermocouples. The mV readings of the thermocouples were recorded when steady state was reached. This was taken when the mV reading of a thermocouple did not change for at least five consecutive minutes. The voltmeter and ammeter readings were noted for any variation of the original setting. In case of small variation of

the original setting all the relevant readings were taken. In cases where the variations were appreciable the voltmeter and ammeter were readjusted to the original value and the set-up was allowed to attain steady state before taking the readings.

(6) The enclosed vessel temperature was recorded.

(7) The manometer reading was recorded.

(8) To set at a different pressure, some amount of air was let out by opening the gas release valve until the pressure dropped by about 175 mm, for the next reading. Then the gas release valve was closed.

(9) Sufficient time was allowed to attain steady state for the next set of readings and the relevant readings were recorded.

(10) Steps (8) and (9) were repeated until the vessel pressure became nearly atmospheric.

(11) The vacuum pump was switched on and the pump line connecting valve was opened so that the vessel pressure fell below atmosphere. When inside pressure dropped by about 125 mm, the vacuum pump connecting line valve was closed and the pump was turned off.

(12) Step (9) was repeated.

(13) The vacuum pump was switched on again and the valve in the vacuum pump connecting line was opened. As the inside pressure dropped by about 75 mm, the vacuum line valve was closed and then the vacuum pump was switched off.

(14) Step (9) was repeated.

(15) The steps (13) and (9) were repeated until vessel pressure dropped to about 10 mm Hg absolute which was the lowest attainable pressure range for the set-up. This completed a set of experiments with horizontal cylinder in air.

(16) The valves were then opened letting the pressure inside the vessel to be atmospheric. The wires connecting the heater line were disconnected and the cover plate was opened.

(17) To align the cylinder at 30° inclination, one of the supporting flexible wire lengths was kept fixed (160 mm) and the other wire length was reduced by an estimated amount of $L/2$ ($=L\sin 30^{\circ}$). The supporting wires were then connected to the screws at the inside face of the cover plate of the vessel.

(18) Steps (2) through (15) was repeated. Thus another set of

experiment with 30° inclination of the cylinder was completed.

(19) Step (16) was repeated.

(20) Two more sets of experiments one for 45° and another for 60° were completed taking steps similar to (17) and (2) through (15).

(21) For conducting the experiment with vertical position of the test cylinder, one supporting wire length was let loose keeping the other wire length fixed (160mm). Due to self weight the test cylinder hung vertically from the shorter supporting wire (160 mm). Steps (2) through (15) were repeated.

(22) To carry out investigations with argon, the air pressure inside the vessel was reduced to about 10 mm of Hg absolute before charging it with argon. The enclosed vessel was filled with argon upto 800 mm Hg gage. The vessel pressure was again reduced to about 10 mm Hg abs. and then the final charging was made that raised the inside pressure to about 1700 mm abs. The re-charging of argon was necessary to reduce the dilution of argon with air to 0.002%.

(23) The experimental data with argon were recorded taking similar steps as with air.

5.7 Data Analysis

A computer program was developed to calculate theoretical heat transfer coefficients for the configurations tested using the correlations suggested by McAdams [13], Nagendra et al [18], Arabi and Salman [28] and Kyte et al [30] wherever applicable and also for processing the experimental data of the present work to calculate the relevant heat transfer parameters. This is shown in Appendix C.

CHAPTER 6

RESULTS AND DISCUSSIONS

In the present study an experimental investigation of free convection heat transfer from hot cylinders to cold ambient fluid has been carried out. The fluid and the heated test cylinder were contained in a sealed enclosure. Investigations were carried out with two cylinders one after another and the fluids used were air and argon. The range of Rayleigh number covered was 10^3 to 1.2×10^8 and therefore the experiments were carried out in the laminar region only.

The test cylinder and the fluid under consideration was contained in the enclosure and as such the outside environmental fluctuations did not directly affect the inside fluid properties and heat transfer behavior. Although a variation of the outside air temperature could raise or lower the enclosure-temperature slightly and slowly, this has been neglected in determining the fluid properties, because both the enclosure and the test cylinder temperature were brought to steady state before taking measurements.

The data were taken at constant heat input condition, but it did neither mean constant heat flux condition nor constant wall temperature condition. A reduction in ambient fluid pressure was followed by an increase of surface temperature of the test cylinder. The surrounding enclosure temperature change was comparatively small. An increase of cylinder surface temperature with almost constant enclosure temperature lead to an increase of radiation heat transfer and with constant heat input to the system it ultimately lead to a reduction of convective heat transfer i.e., heat flux is decreased.

Investigations were carried out with two specimens to check the reproducibility of the data and to reduce the experimental error. Figures 1 to 5 show the comparison of observed heat transfer coefficients of the two specimens in both air and argon. Figures 1,2,3,4 and 5 are for 0° (horizontal), 30° , 45° , 60° and 90° inclinations of the test cylinder with horizontal respectively. As the two specimens were of same geometry and tested under

similar boundary conditions, it was expected that they should show the same heat transfer behavior. The graphs plotted have confirmed this. The discrepancies of the observed data may be attributed to the experimental error and accuracy of the devices. From these graphs it is seen that for argon data specimen 1 shows higher heat transfer coefficients than specimen 2 and difference is more at low pressures (below 0.5 bar) where variation as high as 10% is observed. For air data the difference between the two specimens occurs at pressures above atmosphere. Here too the variation does not exceed 10%.

At low pressures, the magnitude of the heat transfer coefficient is low. So a small variation in results is reflected as high percentage of error. Another reason for the variations might be due to the error in calibration of the thermocouples. It can be recalled that the thermocouples were calibrated in melting ice and boiling water open to atmosphere and the corresponding graphs were extrapolated over the entire range of experimental data as mentioned in section 5.1. It is possible that the assumption of linear variation of mV with temperature over the entire range of temperature for the copper-constantan thermocouple could have introduced some errors in the results.

Accepting the errors as mentioned, the results of the two specimens might be considered to be reasonably same. From these graphs it is seen that the nature of variation of argon data is similar to air. It is also observed that at any given pressure, the values of the argon data are about 30% lower than that of air. A probable reason might be that the thermal conductivity of argon is lower than that of air.

Figure 6 shows the plot of average heat transfer coefficient obtained by the two specimens in air for different inclinations. It consists of five curves with 0° , 30° , 45° , 60° and 90° inclinations of the test cylinder with horizontal. It reveals that the variations of the observed heat transfer coefficients with pressure are logarithmic. The heat transfer coefficients approach zero values as absolute fluid pressure approaches zero. At low pressures the heat transfer coefficient increases more than that at high pressures for equal increase of pressure.

Although there are some intermixing of the data, the logarithmic curve fitting gives high correlation coefficients (Appendix E), 0.97 to 0.99. At low pressures the density of the gas decreases i.e. the scope of convection decreases which leads to increase of radiation. Although with the decrease of density inter molecular space or mean free path increases linearly, the molecular velocity distribution is logarithmic with pressure. So heat transfer coefficient decreases logarithmically with the decrease of pressure. Figure 7 is also the average plot of heat transfer coefficients obtained from the two specimens with argon. Nature of these curves in the figure is similar to that in figure 6 and the heat transfer coefficient varies with pressure and inclination exactly in the same way as they do in figure 6 for air. Although in the average plot of the two specimens, some data deviate considerably from the curves, the correlation coefficient of the logarithmic curves is high, in no case less than 0.95.

Figure 8 shows the variation of observed heat transfer coefficient with the inclination of the test cylinders in air. It is seen that with the increase of inclination heat transfer coefficient decreases linearly and this rate of decrease is lower at lower pressures. Figure 9 shows the plot of h vs θ for argon data. The curves in this figure are similar to that in figure 8. With the increase of inclination the thickness of the boundary layer on the cylinder surface increases. The pattern of heat transfer from the upper surface of the cylinder is unaffected by the cylinder inclination except at vertical position. On the upper surface, fluid molecules that come in contact with the cylinder is heated and goes upward without interrupting heat transfer from the cylinder surface. From the lower half of the cylinder the fluid particles cannot directly move upward, they have to overcome the cylinder circumference by enveloping it. For the horizontal cylinders the heated fluid rises in the form of a plume and the maximum length that the fluid particles remain in contact with the cylinder circumference while rising from the lower surface is $D/2$, D being the diameter of the test cylinder. For inclined cylinders except the vertical one this length is $D \sec \theta / 2$, i.e. $\theta < 88.8^\circ$, with the constraint that $D \sec \theta / 2$ must be

less than L , where L is the length of the test cylinder. In vertical position (90°), the fluid particles around the test cylinder form an almost semi-paraboloid boundary layer and the extent of distance to which the fluid layers are in contact is the cylinder length L . As the travel of the plume increases, analytically it has been shown in literatures that heat transfer coefficient decreases. That is as the extent to which fluid particles remain in contact with the solid along the direction of flow increases, the thickness of the boundary layer also increases. Inside the boundary layer the bulk fluid cannot come in contact with the heated surface. Moreover for fluid particles inside the thermal boundary layer, the temperature difference between the solid and fluid is lower. As a result lesser amount of heat is transferred to the ambient fluid.

In figure 10, comparison of the graphs of normalised heat transfer coefficient, which is the ratio of observed heat transfer coefficient to theoretical ones obtained by using different correlations, are made at different pressures for the horizontal cylinder in air. The normalised coefficients, obtained by using Arabi and Salman [28] correlation, show that the curve is logarithmic in nature. The values are very high at low pressures and the curves run toward infinity at vacuum. At high pressures the values are almost invariant and the curve tends to be horizontal. From the graphs it is observed that at standard pressure the ordinate value is even greater than 2. This means that the observed heat transfer values are more than double than that predicted by Arabi and Salman equation. This value is quite high, representing that the constant heat flux condition correlation of Arabi and Salman is not applicable to the present case of almost constant heat input condition. The diameter in the present investigation was 6.35 mm whereas Arabi and Salman used a cylinder of 38 mm diameter. Therefore it is either the curvature of the test cylinder or the heat transfer condition that limits the applicability of Arabi and Salman correlation to the present investigations. At high pressure, about 2 bar, the normalised value of heat transfer coefficient is within 1.6-1.8 but at low pressures the increment rate of these values is much higher. The

normalised coefficient values are 2.2-2.5 at 0.5 bar, 2.6-3.1 at 0.25 bar and 4.5-5.0 at about 0.05 bar. The curve drawn by using McAdams [13] equation is also logarithmic in nature. It becomes almost asymptotic at both ends. It is almost parallel to x-axis at high pressures and parallel to y-axis at very low pressures (about 0.01 bar). Since, the McAdams equation shows large variations at low pressures it is not applicable in these regions. Though both the curves using Arabi and Salman equation and McAdams equation have many similarities, the main difference lies in their relative magnitudes. The graph obtained by comparing the observed heat transfer coefficients and McAdams equation shows that the normalised coefficient values are 2.0, 1.1 and 1.0 at pressures of about 0.02, 1 and 2 respectively; whereas that obtained by using Arabi and Salman correlation shows the values of about 7.2, 2.05 and 1.75 at the corresponding pressures. The McAdams equation therefore does not exhibit significant errors except at low pressures (0.5 bar or lower). On the basis of these high values, obtained by comparing observed results with that of Arabi & Salman, a conclusion that the observed data are not correct would be a blunder, since if it would be so the comparison with other correlation like McAdams would also show similar or higher order of variation. The results can be compared with Kyte et al [30] correlation at low pressures only, as their equation is valid for that pressure range only. In figure 10 the graph obtained using Kyte et al correlation is close to unity even at very low pressures and the curve is almost parallel to horizontal axis. This ratifies the accuracy of the data recorded in the present experiments. As discussed in section 2.8, Kyte et al suggested two simultaneous equations for different Rayleigh number ranges. The temperature at a distance λ_b , the mean free path length, from the solid surface, designated as T_b , was assumed and each of the two equations were solved simultaneously. Both the equations give the convective heat transfer rate, q . When for a particular assumed value of T_b , q given by two equations become equal the iteration is completed and the estimation of q is considered correct. They also suggested that heat transfer rate can be calculated using one correlations when free molecule

conduction can be neglected. They suggested correlation for both horizontal and vertical cylinders, but their range of Rayleigh number did not cover Rayleigh number of the experiments with vertical cylinders in the present investigations. For the horizontal cylinders in the present investigations the difference of the cylinder surface temperature and the temperature T_b , based on the observed heat transfer rate was seen to be very small (order of 10^{-9} °K) for an approximate total input of 6 Watt. It happened so because the mean free path length was of negligible dimension compared to cylinder diameter. In the experiments of Kyte et al a thin wire (0.00306 inch in diameter) was used, and the mean free path length was not relatively negligible. Therefore although the present investigations do not explicitly and completely accord to the conditions in order to neglect the effect of free molecule conduction, the fact that T_b did not vary significantly from the surface temperature ultimately lead to the situation for which free molecule conduction can be neglected. For present investigations the heat transfer coefficient derived using Kyte et al equation is compared in the form of a ratio. The normalised heat transfer coefficient which is the ratio of observed heat transfer coefficient to that obtained using Kyte et al equation is plotted against normalised pressure in figure 10. Figure 11 is similar to figure 10 but drawn with the data of argon.

Figure 12 shows the comparison of the normalised heat transfer coefficient obtained by Arabi & Salman [28] and Nagendra et al [18] correlations using normalized pressure as the independent variable i.e., varied along horizontal axis, for vertical cylinder in air. The curve drawn by using Arabi and Salman equation shows that, even at atmospheric pressure, the normalised heat transfer coefficients have values within 1.5-1.6 and the normalised coefficients are very high at low pressures. The high values of the normalised coefficient indicate that the observed heat transfer coefficient values are much higher than the heat transfer values predicted by Arabi and Salman correlation. The normalised coefficient of 1.5-1.6 indicate that the observed values are 50-60% higher. Therefore it can be concluded that the

observed results are not in agreement with that predicted by reference [28]. The curve drawn by using Nagendra et al [18] equation shows that at high pressures the values of the normalized heat transfer coefficient do not change significantly with the change of pressure and they decrease rapidly with the fall of pressure. The normalised coefficient values are within 0.85-1.1 for a pressure range of 0.5 to 2.25 bar. At about 0.25 bar the normalised coefficient is reduced to within 0.77-0.84, and at about 0.01 bar it is further reduced to 0.5-0.6. The closeness of the normalised heat transfer coefficient to unity indicates good agreement of observed results with theoretical ones. Therefore except at low pressures the observed and predicted values are in good agreement. Figure 13 is a plot similar to figure 12 with the data of argon. From figures 12 and 13 it is observed that for the same pressure Arabi and Salman equation gives lower values of heat transfer coefficient while Nagendra et al correlation gives higher values of heat transfer coefficient than the observed heat transfer coefficient. Therefore a conclusion that the observed data are much higher than they should be, just by comparing them with reference [28] would be erroneous. The figures show that the curves drawn using Arabi and Salman and Nagendra et al correlations show opposite characteristic at low pressures. The normalised heat transfer coefficient given by Arabi & Salman shows very high values and tends to go to infinity upward, at vacuum, but that given by Nagendra et al equation show low values and tend to zero at vacuum. At pressures above atmosphere both the curves are almost parallel to horizontal axis, i.e., with the increase of pressure, normalised heat transfer coefficient does not change significantly. Although both the curves are logarithmic in nature there remains a considerable difference in their numerical values over the entire pressure range. At pressures of about 0.01, 0.05, 1 and 2 bars the normalised coefficients using Arabi and Salman correlation are around 2.9, 1.7, 1.55 and 1.45; and those obtained from Nagendra et al equation are around 0.65, 0.85, 0.9 and 1.0 respectively. Like figure 12, the logarithmic fitting of the curves in figure 13 shows high correlation coefficient for

both the curves and their values are not less than 0.94 for any of the graphs.

Figure 14 shows the plot of normalised heat transfer coefficient against normalised pressure for different inclinations of the test cylinder in air using Arabi and Salman [28] equation. The figure consists of five curves for five orientations of the test cylinder. The inclinations are 0° (horizontal), 30° , 45° , 60° and 90° . The curves are similar and logarithmic in nature. They become almost parallel to horizontal axis at high pressures and run upward toward infinity at very low pressures. The curve with 0° inclination has values considerably higher than other positions of the test cylinder over the entire range of pressure investigated. The normalised heat transfer coefficient decreases with the increase of inclination. The highest and lowest values occur corresponding to the horizontal and vertical positions of the test cylinder. But at pressures above atmosphere, except for the 0° curve, the curves lie on one another and cannot be distinguished sharply. The curves with 45° and 60° inclinations are very close to each other. All the curves show very high values at low pressures. Even at atmospheric pressure the ordinate lies between 1.6-2.1. It may be noted that the curves for $\theta=30^{\circ}$, 45° and 60° lie between the curves obtained for $\theta=0^{\circ}$ and 90° . The curves with 0° and 90° inclinations were also shown in figures 10 and 12 respectively, where they were compared with the results of other investigators. But because of the unavailability of data in literature the high normalised coefficient values for $\theta=30^{\circ}$, 45° and 60° presented by the curves in figure 14 could not be compared with any other correlations. Figure 15 is similar to figure 14 with argon data.

Figure 16 shows the log-log plot of Nusselt number for air data given by figure 6, versus normalised pressure. There are five curves in the figures corresponding to five inclinations of the test cylinder. Like the heat transfer coefficient as in figure 6, the Nusselt number also decreases with the increase of inclination and increases with the increase of pressure. Despite the deviation of the data, the linear curve fitting for the log-log plots gives the correlation coefficient of 0.96 or better.

Figure 17 is similar to figure 16 but with the data of argon.

Figure 18 shows the average plot of observed Nusselt number versus Rayleigh number for both air and argon for different inclinations of the test cylinder. From the graphs it is seen that the merging of air and argon data in non-dimensional form is random. It is observed that the Nusselt number increases logarithmically with Rayleigh number. Figure 19 is the log-log plot of Nusselt number versus Rayleigh number. The fitting of the curves are seen to be linear. The curves show high correlation coefficient, not less than 0.98.

Since pressure was considered to be a pertinent variable in natural convection, it was felt necessary to incorporate it with Rayleigh number. Accordingly a group formed by multiplication of Rayleigh number with normalised pressure raised to the n th power was considered. Various values of n like $1/2, 1, 2$ etc. were checked for their fitting and the best result was obtained for $n=1$.

Figure 20 is the log-log plot of Nusselt number versus the product of Rayleigh number and normalised pressure with linear curve fitting. The curves show correlation coefficient of the order of 0.99. The correlation proposed in this thesis has been derived from this plot.

CHAPTER 7

CONCLUSIONS AND RECOMMENDATIONS

7.1 Conclusions:

The important conclusions as a consequence of the present investigations are enumerated below:

- (1) The natural convection heat transfer coefficient, h , was found to be dependent not only on fluid properties associated, but was also influenced considerably by environmental pressure (P/P_a) and orientation (θ) of the cylinder.
- (2) The natural convection heat transfer coefficient increased logarithmically with the increase of pressure.
- (3) The natural convective heat transfer coefficient was seen to be lower for argon than that for air at any given inclination of the cylinder and ambient fluid pressure.
- (4) The heat transfer coefficient was found to decrease linearly with the increase of inclination and so maximum and minimum values occurred for horizontal and vertical positions of the cylinder respectively.
- (5) The observed heat transfer coefficients were within 12% of McAdams and Nagendra et al equations at atmospheric pressure and fitted well within 0.5-1.5 bar. Arabi and Salman correlation showed similar nature of the curve as McAdams but the values of the normalised heat transfer coefficient showed large differences throughout the range of investigation. The correlations of McAdams, Nagendra et al and Arabi and Salman showed large differences at low pressures. The correlation of Kyte et al showed good agreement (within 10%) even at very low pressure (0.05 bar).
- (6) The plot of Nusselt number (Nu), with normalised pressure was seen to be linear on a log-log plot over the entire pressure range for both air and argon.
- (7) The plot of Nusselt number (Nu) with Rayleigh number (Ra) could be represented by a linear curve fitting in the log-log plot with high correlation coefficient.

(8) The plot of Nusselt number (Nu) with the product of Rayleigh number (Ra) and normalised pressure (P/P_a) could also be represented by a linear curve fitting on a log-log graph over the entire range of investigation .

(9) The Nusselt number (Nu) can be correlated with Rayleigh number (Ra), normalised pressure (P/P_a) and inclination (θ) by the empirical equation:

$$Nu = C(Ra * P/P_a)^m$$

where, C and m are functions of θ .

Their values should be determined by the following relations:

$$C = 10.292 - 0.0484\theta$$

$$m = 0.1382 + 0.0499\cos\theta - 0.1405\cos^2\theta + 0.0808\cos^3\theta$$

for $0.65 \leq Pr \leq 0.72$, $0.01 \leq P/P_a \leq 2.3$, $3 \cdot 10^4 \leq Ra \leq 1.2 \cdot 10^8$, and $0 \leq \theta \leq 90$.

7.2 Recommendations :

(1) The variation of Nusselt number for other fluids specially those with better transport properties like Helium can be carried out to organize a general correlation.

(2) Investigations can be carried out with other geometries and dimensions of the heat transfer element (like wires, different L/D ratio etc.).

(3) Investigations may also be carried out by determining experimentally the velocity and temperature field using methods like interferometric technique and Laser Doppler anemometry (LDA).

(4) By controlling the heat input, the investigation can also be carried out with constant wall temperature.

REFERENCES

1. Kabir, Humayan: An Experimental Investigation of Natural Convection Heat Transfer from a hot corrugated Plate to a Flat cold Plate, M.Sc. Thesis, BUET, Dhaka, 1988.
2. Schorr, A.W. and Gebhart, B.: An Experimental Investigation of the Natural Convection Wakes above a Line Heat Source, Int. Journal of Heat and Mass Transfer, vol.13, pp.557-571, 1970.
3. Warrington, Jr. R.O. and Powe, R.E.: The Transfer of Heat by Natural Convection between Bodies and their Enclosures, Int. Journal of Heat and Mass Transfer, vol.28, pp.319-330, 1985.
4. Gebhart, B., Heat Transfer, 3rd. ed., McGraw-hill, N.Y., 1971.
5. Al-Arabi, M. and Khamis, M., Natural Convection from Inclined Cylinders, Int. Journal of Heat and Mass Transfer, vol.25, No.1, pp.3-15, 1982.
6. Bertela, M.: Compatibility and Mutual Interaction among the Dimensionless Groups present in the Navier-Stokes and Energy Equations, Int. Journal of Heat and Mass Transfer, vol.23, pp. 1243-1250, 1980.
7. Fand, R.M. and Brucker, J.: A correlation for Heat transfer by Natural Convection from Horizontal Cylinders that accounts for Viscous Dissipation, Int. Journal of Heat and Mass Transfer, vol.26, No.5, pp.709-720, 1983.
8. Karim, F., Farouk, B. and Namen, I.: Natural Convection Heat Transfer from a Horizontal Cylinder between Vertical Confining Adiabatic Walls, ASME, Journal of Heat Transfer, pp.291-298, vol.108, 1986.
9. Holman, J.P., Heat Transfer, Metric ed. McGraw-hill, N.Y. 1989.
10. Yang, R. and Yao, L.S.: Natural Convection Along a Finite Vertical Plate, Trans. ASME, Journal of Heat Transfer, vol.109, pp. 413-418, 1987.
11. Gryzagoridis, J.: Natural Convection from a vertical Flat Plate in the Low Grashof number Range, Int. Journal of Heat and Mass Transfer, vol.14, pp.162-165, 1971.

12. Mortynenko, O.G., Berezovskiy, A.A. and Sokovishin, Yu.A. : Laminar Free Convection from a Vertical Plate, Int. Journal of Heat and Mass Transfer, vol. 27, pp. 869-881, 1984.
13. McAdams, W.H., Heat Transmission, 3rd. ed. McGraw-hill, N.Y. 1954.
14. Fujii, T. and Imura, H.: Natural Convection from a Plate with arbitrary inclination, Int. Journal of Heat and Mass Transfer, vol. 15, pp. 755-767, 1972.
15. Robinson, S.B. and Liburdy, J.A.: Prediction of the Natural Convection Heat Transfer from a Horizontal Heated Disk, Trans. ASME, Journal of Heat Transfer, vol. 109, pp. 906-911, 1987.
16. Chen, T.S., Tien, H.C. and Armaly, B.F.: Natural Convection on Horizontal, Inclined and Vertical Plates with Variable Surface Temperature or Heat Flux, Int. Journal of Heat and Mass Transfer, vol. 29, pp. 1465-1478, 1986.
17. Schulenburg, T.: Natural Convection Heat Transfer Below Downward Facing Horizontal Surfaces, Int. Journal of Heat and Mass Transfer, vol. 28, pp. 467-477, 1985.
18. Nagendra, H.R., Tirunarayan, M.A. and Ramachandran, A.: Laminar Free Convection from Vertical Cylinders with Uniform Heat Flux, Trans. ASME, Journal of Heat Transfer, pp. 191-194, Feb., 1970.
19. Fuzjii, T., Takeuchi, M., Fuzjii, M., Suzaki, K. and Vehera, H.: Experiments on Natural Convection Heat Transfer from the outer surface of Vertical Cylinder to Liquid, Int. Journal of Heat and Mass Transfer, vol. 13, pp. 753-787, 1970.
20. Lee, H.R., Chen, T.S. and Armaly, B.F.: Natural Convection Along Slender Vertical Cylinders with Variable Surface Temperature, ASME Journal of Heat Transfer, vol. 110, pp. 103-108, 1988.
21. Kutateledge, S.S., Fundamentals of Heat Transfer, Academic Press, N.Y., 1963.
22. Morgan, V.T.: The Overall Convective Heat Transfer from Smooth Cylinders, Adv. Heat Transfer, pp. 199-209, 1975.
23. Churchill, S.W. and Chu, H.S.: Correlating Equations for

- Laminar and Turbulent Free convection from a Horizontal Cylinder, Int.Journal of Heat and Mass Transfer, vol.11, pp.1049-1053,1975..
24. Mikheyava,M.,Fundamentals of Heat Transfer,Peace,Moscow,1968.
 25. Fand,R.M.,Moris,E.W. and Lum,M.: Natural Convection Heat Transfer from Horizontal Cylinders to Air,Water and Silicone oils for Rayleigh numbers between $3*10^2$ and $2*10^7$,Int. Journal of Heat and Mass Transfer,vol.20,pp.1173-1184,1977.
 26. Eckert,E.R.G. and Drake,R.M.Jr., Heat and Mass Transfer, McGraw-hill,1959.
 27. Socio,L.M.: Laminar Free Convection Around Horizontal Circular Cylinders,Int.journal of Heat and Mass Transfer,vol.26, No.11. pp.1669-1677,1983.
 28. Al-Arabi,M. and Salman,Y.K.: Laminar Natural Convection from an Inclined Cylinder,Int.Journal of Heat and Mass Transfer, vol. 23,pp.45-51,1980.
 29. Oosthuizen,P.H.: Experimental Study of Free convection Heat Transfer from Inclined Cylinders,Journal of Heat Transfer, vol.98, pp.672-674.1976.
 30. Kyte,J.R.,Madden,A.J. and Piert,E.I.: Natural Convection Heat Transfer at Reduced Pressure,Chemical Engineering Progress, vol. 49,pp.653-662,1953.
 31. Warner,C.Y. and Arpachi,V.S.: An EXperimental -Investigation of Turbulent Natural Convection in Air at Low Pressure along a Vertical Heated Flat Plate,Int.Journal of Heat and Mass Transfer, vol.11,pp.397-403,1968.
 32. Hesse,G. and Sparrow,E.M.: Low Rayleigh number Natural Convection Heat Transfer from High Temperature Horizontal Wires to Gases,Int.Journal of Heat and Mass Transfer,vol.17, pp.796-798, 1974.
 33. Jaluria,Y.: On the Introduction of Disturbances in a Natural Convection Flow,Int.Journal of Heat and Mass Transfer,vol. 19, pp. 1057-1063,1976.

34. Hieber, C.A. and Nash, E.J.: Natural Convection above a Line Heat Source: Higher order Effects and Stability, Int. Journal of Heat and Mass Transfer, vol. 18, pp. 1473-1479, 1975.
35. Oosthuizen, P.H. and Donaldson, E.: Free convection Heat Transfer from Vertical Cones, Trans. ASME, Ser. C, Journal of Heat Transfer, vol. 94, pp. 330-333, 1972.
36. Vliet, G.C. and Lin, C.K.: An Experimental Study of Turbulent Natural Convection Boundary Layers, Trans. ASME, Ser. C, Journal of Heat Transfer, vol. 91, pp. 517-531, 1969.
37. Vliet, G.C.: Natural Convection Heat Transfer on Constant Heat Flux Inclined Surfaces, Trans. ASME, Ser. C, Journal of Heat Transfer, vol. 91, pp. 511-516, 1969.
38. Kothandaraman, C.P. and Subramanyan, S., Heat and Mass Transfer Data Book, 3rd. ed. Eastern, Ltd., New Delhi.
39. Jaluria, Y.: Natural Convection Heat and Mass Transfer, Pergamon Press, 1980.
40. Incropera, F.P.: Convection Heat Transfer in Electronic Equipment cooling, ASME, Journal of Heat Transfer, vol. 110, pp. 1097-1111, 1988.
41. Grief, R.: Natural Circulation Loops, ASME, Journal of Heat Transfer, vol. 110, pp. 1243-1258, 1988.
42. Jakob, M., Heat Transfer, vol. 1, John Willey and Sons, Inc. 1949.
43. Kreith, F., Heat Transfer, 3rd. ed. 1966.
44. Doolittle, J.S.: Mechanical Engineering Laboratory, McGraw-hill, 1957.
45. Yao, L.S.: Natural Convection Effects in the Continuous Casting of a Horizontal Cylinder, Int. Journal of Heat and Mass Transfer, vol. 27, pp. 697-704, 1984.
46. Bermister, L.C., Convective Heat Transfer, John Willey and sons, Inc. 1983.
47. Farouk, B. and Gucher, S.I.: Natural Convection from Horizontal Cylinders in Interacting Flow Fields, Int. Journal of Heat and Mass Transfer, vol. 26, pp. 231-244, 1984.

48. Aziz, A. and Benzie, J.Y.: Application of Perturbation Techniques to Heat Transfer Problems with Variable Thermal Properties, Int. Journal of Heat And Mass Transfer, vol. 19, pp. 271-276, 1976.
49. Austien, G.T., Shereve's Chemical Process Industries, 5th ed. McGraw-Hill Book CO., 1985.
50. Ambrocious, E.E., Mechanical Engineering Laboratory Practice; The Ronald Press CO., New York, 1956.
51. Neter, J. and Wasserman, W., Applied Linear Statistical Models; Richard D. Irwin Inc., Illinois, 1974.

APPENDIX A

A.1 Calculation of Conduction Loss for Thermocouples

As mentioned in section 4.2, 5 thermocouples were connected to specimen 1 and 3 to specimen 2. To estimate heat loss through them, radiation loss from these wires was neglected and they were considered to be pin type fins of infinite length. Heat conducted to these thermocouples at the root on the surface of the test cylinder was totally lost by them by convection to the ambient fluid. A brief calculation procedure is shown below.

$$D_w = \text{diameter of either a copper or a constantan wire} = 0.27 \times 10^{-3} \text{ m}$$

$$A' = (\pi/4) D_w^2 = 5.7255 \times 10^{-8} \text{ m}^2$$

$$k_{\text{cu}} = 386 \text{ W/m}^0\text{C}, \quad k_{\text{con}} = 26 \text{ W/m}^0\text{C}$$

$$p' = \pi D_w = 8.4823 \times 10^{-4} \text{ m}$$

Heat loss through a set of thermocouple

= Heat loss by a copper wire + Heat loss by a constantan wire

$$\begin{aligned} q_{\text{cond}} &= (\sqrt{p'A'k_{\text{cu}}h} + \sqrt{p'A'k_{\text{con}}h}) \Delta T \\ &= \sqrt{p'A'} (\sqrt{k_{\text{cu}}} + \sqrt{k_{\text{con}}}) \sqrt{h} \Delta T \\ &= 6.97 \times 10^{-6} (\sqrt{386} + \sqrt{26}) \sqrt{h} \Delta T \\ &= 1.7245 \times 10^{-4} \sqrt{h} \Delta T \end{aligned} \quad \text{-----} \quad (1)$$

Value of h was assumed to be 15 W/m²C.

So heat loss for each thermocouple

$$\begin{aligned} q_{\text{cond}} &= 1.7245 \times 10^{-4} \sqrt{15} \Delta T \\ &= 6.679 \times 10^{-4} \Delta T \text{ Watt} \end{aligned} \quad \text{-----} \quad (2)$$

For specimen 1

$$\begin{aligned} q_{\text{cond}} &= 5 \times 6.679 \times 10^{-4} \Delta T \\ &= 3.3 \times 10^{-3} \Delta T \end{aligned} \quad \text{-----} \quad (3)$$

and for specimen 2

$$\begin{aligned} q_{\text{cond}} &= 3 \times 6.679 \times 10^{-4} \Delta T \\ &= 2.0 \times 10^{-3} \Delta T \end{aligned} \quad \text{-----} \quad (4)$$

Therefore equations (3) and (4) give the heat loss by conduction through the thermocouples from specimens 1 and 2 respectively.

A.2 Calculation of Conduction loss for holding wires

As mentioned in section 5.5.6, the holding wires could also be considered as infinite protruded rods and the radiation from them could be neglected. Heat loss by these wires could be compensated by an equivalent increase of the surface area of the test cylinder to give the same heat loss by convection and radiation. A brief calculation procedure is shown below:

$$D_w = 0.62 \times 10^{-3} \text{ m}$$

$$P' = \pi D_w = 1.948 \times 10^{-3} \text{ m}$$

$$A' = (\pi/4) D_w^2 = 3.019 \times 10^{-7} \text{ m}^2$$

$$k_{cu} = 386 \text{ W/mC}$$

$$h = 12 \text{ W/m}^2\text{C (assumed)}$$

$$q_{cond} = 2 \sqrt{P' A' k_{cu} h \Delta T}$$

$$= 2 \sqrt{1.948 \times 10^{-3} * 3.019 \times 10^{-7} * 386 * 12 \Delta T}$$

$$= 3.3 \times 10^{-3} \text{ T Watt}$$

Since ΔT varied with pressure, an average value of ΔT could be taken for the estimation of this conduction loss. This assumption was a reasonable one since at low pressure ΔT increased but h decreased and the product ($\sqrt{h \Delta T}$) did not change significantly.

In the present calculations ΔT was taken as 70C. So the q_{cond} became

$$q_{cond} = 3.3 \times 10^{-3} * 70 = 0.231 \text{ Watt.}$$

Total power input, q_T was maintained at 6.0 Watt and hence,

$$q_{cond}/q_T = 0.231/6.0 = 0.0385 \approx 0.04$$

Therefore instead of calculating conduction loss through the holding wires the test cylinder surface area could be increased by 4%. This would give the same heat loss by convection and radiation.

APPENDIX B

Emissivity Estimation

In order to determine the emissivity of the test cylinders with matt black surfaces, a test run was made for each, from atmospheric pressure to the lowest attainable pressure which was about 10 mm Hg absolute for the present apparatus. The manufacturer of the apparatus recommended that the temperature difference between the test cylinder and the undisturbed ambient fluid (vessel) varied linearly with the fourth root of the absolute pressure inside the vessel. Figures B-1 and B-2 shows the variation of ΔT i.e., $(T_e - T_v)$ with $H^{1/4}$, where H is the absolute pressure inside the vessel in mm Hg, for specimen 1 and specimen 2 with constant heat input of 6.00 and 5.96 Watt respectively.

In the figures, the linear curves have been extrapolated to reach the absolute zero pressure i.e., vacuum line. The corresponding ordinate represented the temperature difference between the test cylinder and the vessel if the pressure inside the vessel would be reduced to zero. Thus $(T_e - T_v)$ at vacuum can be read from the graph. From figures B-1 and B-2 this value is seen to be approximately 130.5°C and 131.8°C . From observation it was seen that the vessel temperature T_v did not vary much, the variation was less than 2°C , the average temperature corresponding to the three lowest pressure data was taken as the vessel temperature at vacuum and calculations corresponding to vacuum condition were performed. The relevant data and calculation are shown in table B-1 in the next page. In the table 'CA' and 'fac' represent the cylinder surface area and the factor that accounts for the bead loss and Wattmeter correction.

Table B-1

Parameter	Specimen 2	Specimen 1
$(T_e - T_v)$ °K	131.8	130.5
T_v °K	303.1	306.5
T_e °K	434.9	437.0
q_T Watt	5.96	6.00
L mm	161	159
D mm	6.35	6.35
Di mm	4	4
q_{cond} Watt	$2.0 \times 10^{-3} * T = 0.2636$	$3.3 \times 10^{-3} * T = 0.4307$
$CA = \pi DL + \pi/4(D^2 - Di^2)$ mm ²	3230.91	3191.01
$A = CA * 1.04$ m ²	3.360×10^{-3}	3.319×10^{-3}
$fac = 0.95 * L / (L + 4)$	0.927	0.927
$q_{in} = q_T * fac$ Watt	5.5247	5.562
$q_r = q_{in} - q_{cond}$	5.2611	5.1313
$\epsilon = q_r / [A \sigma (T_e^4 - T_v^4)]$	0.99	0.97

Therefore the emissivity for specimen 1 was 0.97 and that for specimen 2 was 0.99.

APPENDIX C

COMPUTER PROGRAM

```

INTEGER T,PM,SP,FL
PARAMETER (T=12,N=5)
DOUBLE PRECISION MU,Z,Z1,GL(T),GD(T),RAD(T),RAL(T),NUL(T),NUD(T),
+NUS(T),Z2,Z3,NUOL(T),NUOD(T),RLP(T),RDP(T),O1(T),O2(T),MU1,GD1,RD1
DIMENSION PM(T),P(T),TEK(T),TVK(T),HTH1(T),SIH(T),QC(T),QCM(T)
REAL SI(T),SIV(T),HOB(T),HTH(T),HTS(T),Y1(T),Y2(T),Y3(T),Y4(T)
REAL L,M,K,K1,QT(T),TV(T),V(T),AI(T),SUM(T),MV(T,N),B5(T),B6(T)
REAL MVB(N),MVRF(N),TM(T,N),P1(T),B(T),B1(T),B2(T),B3(T),B4(T)
REAL QM(T),HK(T)
OPEN(UNIT=1,FILE='IN',STATUS='OLD')
OPEN(UNIT=3,FILE='OUT',STATUS='NEW')
c FL,SP,INC,PM,TB,TRF,MVB,MVRF,MV AND TV indicate fluid,specimen no.,
+inclination,absolute pressure in mm.Hg,upper reference temperature
+,lower reference temperature,MV at upper reference temperature,MV
+at lower reference temperature,milli volt reading of the element
+thermocouple and vessel temperature respectively.
READ (1,*) FL,SP,INC
READ (1,*) (PM(I),I=1,T)
READ(1,*)TB,TRF,(MVB(J),J=1,N),(MVRF(J),J=1,N)
READ (1,*) ( V(I), I=1,T)
READ (1,*) (AI(I), I=1,T)
READ (1,*)((MV(I,J),I=1,T),J=1,N)
READ (1,*) (TV(I),I=1,T)
c Converting MV readings into temperatures and calculating input power
DO 29 I=1,T
    SUM(I)=0.0
    DO 30 J=1,N
        YY= MVB(J)- MVRF(J)
        TM(I,J)=TRF+(TB-TRF)*(MV(I,J)-MVRF(J))/YY
30    SUM(I)=SUM(I)+TM(I,J)
        XTM=SUM(I)/N
c TEK is average specimen temperature and TVK is vessel temperature.
TEK(I)=XTM+273
C Vessel temperature correction 20 C.
TVK(I)=TV(I)+2+273
QT(I)=V(I)*AI(I)
29 CONTINUE
G=9.81
SIG=5.77
D=6.35E-03

```

```

BL=4.E-03
PI=3.1416
c -- Emissivity estimation -----
DI=4.E-03
CH=0.95
IF(SP.EQ.8) THEN
L=159E-03
QTO=6.00
DT0=130.5
CC=3.3E-03
TV0=306.5
ELSE
L=161E-03
QTO=5.96
DT0=131.8
TV0=303.1
CC=2.0E-03
ENDIF
RR=0.04
CA=PI*D*L+(PI/4)*(D*D-DI*DI)
A=CA*(1+RR)
FAC=L/(L+BL)*CH
L=A/(PI*D)
QIO=QTO*FAC
QCON0=CC*DT0
QO=QIO-QCON0
TE0=TV0+DT0
TOO=(TE0/100)**4-(TV0/100)**4
EP=QO/(TOO*SIG*A)
c -----
WRITE(3,6) SP
6 FORMAT(/,15X,'Specimen No.='I1)
c ----- Constant and index values for Arabi and Salman equation -----
IF (INC.EQ.0) THEN
M=1./3.
K1=0.158
ENDIF
IF (INC.EQ.30) THEN
M=0.315
K1=0.229
ENDIF
IF (INC.EQ.45) THEN
M=0.295
K1=0.335

```

```

      ENDIF
      IF (INC.EQ.60) THEN
          M=0.275
          K1=0.422
      ENDIF
      IF (INC.EQ.90) THEN
          M=0.25
          K=0.6
      ENDIF
      WRITE(3,7) INC
7      FORMAT(/,5X,'Inclination with horizontal is:',I2)
      FAC=(L-4E-03)*0.95/L
      DO 99 I=1,T
          TF=(TEK(I)+TVK(I))/2.
          DT=TEK(I)-TVK(I)
c      ----- Fluid properties for air -----
          IF(FL.NE.0) GO TO 11
          PR=0.7
          R=29.3*G
          WRITE(3,96)
96      FORMAT('1',/,16X,'Air')
          IF(TF.GE.300.AND.TF.LE.350)THEN
              X=TF-300
              K=(0.03003-0.02624)/50.*X+0.02624
              MU=((2.075-1.8462)/50.*X+1.8462)*1E-05
          ENDIF
          IF(TF.GE.350..AND.TF.LE.400)THEN
              X=TF-350
              K=(0.03365-0.03003)/50.*X+0.03003
              MU=((2.286-2.075)/50.*X+2.075)*1E-05
          ENDIF
c      ----- Fluid properties for argon -----
          IF(FL.EQ.0)GOTO 12
11      PRINT*,'Argon data'
          PR=0.662
          R=21.2*G
          WRITE(3,*)          'Argon'
          IF(TF.GE.273.AND.TF.LE.373)THEN
              X=TF-273
              K=(0.02117-0.016151)/100.*X+0.016151
              MU=((2.75-2.15)/100.*X+2.15)*9.81E-06
          GOTO 132
          ENDIF
12      PRINT*,"Air data'

```



```

c ----- Calculations -----
132      P(I)=PM(I)*13.6*G
          RO =P(I)/(R*TF)
          FID=K/D
          FIL=K/L
          Z1=MU*MU
          Z2=RO**2./Z1
          Z=Z2*DT
          Z3=Z/TVK(I)
          GL(I)=G*L**3.*Z3
          RAL(I)=GL(I)*PR
          GD(I)=(G*D**3.0*RO**2.*DT)/(MU**2.*TVK(I))
          RAD(I)=GD(I)*PR
          O1(I)=LOG(RAL(I))
          O2(I)=LOG(RAD(I))
c ----- Calculation of Heat Transfer by Arabi and Salman equation --
          NUL(I)=K1*RAL(I)**M
          HTH(I)=FIL*NUL(I)
          PRINT*, 'HTH( ', I, ')=' ,HTH(I)
c -----
c      Observed heat transfer value calculation -----
c
          TO=(TEK(I)/100)**4.-(TVK(I)/100)**4.
          QR=A*SIG*EP*TO
          QI=QT(I)*FAC
          QCON=CC*DT
          Q=QI-QCON
          QC(I)=Q-QR
          PRINT*, 'QC( ', I, ')=' ,QC(I)
          HOB(I)=QC(I)/(A*DT)
c ----- Processing observed heat transfer coefficient. -----
          NUOL(I)=HOB(I)/FIL
          NUOD(I)=HOB(I)/FID
          P1(I)=PM(I)/760.
          RLP(I)=P1(I)*RAL(I)
          RDP(I)=P1(I)*RAD(I)
          Y1(I)=LOG(NUOL(I))
          Y3(I)=LOG(RLP(I))
          Y2(I)=LOG(NUOD(I))
          Y4(I)=LOG(RDP(I))
          B1(I)=RAL(I)**0.25
          B2(I)=NUOL(I)/B1(I)
          B3(I)=ALOG(P1(I))

```

```

B(I)=ALOG(B2(I))
B4(I)=RAD(I)**0.25
B5(I)=NUOD(I)/B4(I)
B6(I)=ALOG(B5(I))

```

c SI is the normalized heat transfer coeff. obtained by using Arabi & Salman equation.

```

SI(I)=HOB(I)/HTH(I)
PRINT*, 'HOB( ', I, ')=' , HOB(I)
PRINT*, 'SI( ', I, ')=' , SI(I)

```

C-----

```

IF(INC.NE.0)GOTO 74
NUS(I)=0.525*RAD(I)**0.25
HTS(I)=NUS(I)*FID
SIH(I)=HOB(I)/HTS(I)

```

74 PRINT*, 'ADVANCE'

C-----

```

IF(INC.NE.90)GOTO 44

```

C----- Comparison with Nagandra et al correlation -----

```

Y=RAD(I)*D/L
IF(Y.GE.10E04) NUD(I)=0.6*Y**0.25
IF(Y.LE.10E04.AND.Y.GE.0.05) NUD(I)=1.37*Y**0.16
IF(Y.LE.0.05) NUD(I)=0.93*Y**0.05
HTH1(I)=FID*NUD(I)
SIV(I)=HOB(I)/HTH1(I)

```

C----- Comparison with Kyte et al correlation -----

```

44 PRINT*, 'NUL( ', I, ')=' , NUL(I)
IF(INC.NE.0.AND.INC.NE.90)GOTO 99
IF(P1(I).GE.0.99.AND.P1(I).LE.1.01)GOTO 614
IF(PM(I).GT.760)THEN
QCM(I)=9E-14
GOTO 468
ENDIF
AL=0.90
IF(FL.EQ.0) THEN
VO=163.6
ELSE
VO=92.3
ENDIF
C1=QC(I)/(P1+D*1.+VO*PM(I)*AL)
CO=C1*C1/273.2
C=CO*CO/4.+TEK(I)*CO

```

c TA is fluid temperature at a distance equal to mean free path from the solid
TA=TEK(I)+0.5*CO=SQRT(C)
IF(FL.EQ.0)THEN

81458

```

C ----- XLA is the mean free path length -----
XLA=3.46E-08*TA**1.28/PM(I)
ELSE
XLA=2.29E-08*TA**1.36/PM(I)
ENDIF
D1=D+XLA
AK=PI*D1*L+PI*0.25*(D1**2-DI**2)
TF1=(TA+TVK(I))/2.
DT1=TA-TVK(I)
IF(FL.NE.0)GOTO 652
IF(TF1.GE.300.AND.TF1.LE.350)THEN
X1=TF1-300
K1=(0.03003-0.02624)/50.*X+0.02624
MU1=((2.075-1.8462)/50.*X+1.8462)*1E-05
ENDIF
IF(TF1.GE.350..AND.TF1.LE.400)THEN
X1=TF1-350
K1=(0.03365-0.03003)/50.*X+0.03003
MU1=((2.286-2.075)/50.*X+2.075)*1E-05
ENDIF
652 IF(FL.EQ.0)GOTO 129
IF(TF.GE.273.AND.TF.LE.373)THEN
X1=TF1-273
K1=(0.02117-0.016151)/100.*X+0.016151
MU1=((2.75-2.15)/100.*X+2.15)*9.81E-06
ENDIF
129 PRINT*, '1000'
CZ=MU1*MU1*TVK(I)
GD1=(G*D1**3.*RO**2.*DT1)/CZ
RD1=GD1*PR
C ----- Horizontal low Rayleigh number -----
IF(INC.EQ.0)THEN
IF(RD1.GE.1E-07.AND.RD1.LE.10**1.5)THEN
QCM(I)=2*PI*L*XK1*DT1/LOG(1+7.09/RD1**0.37)
c ----- Horizontal high Rayleigh number -----
ELSE IF(RD1.GT.10**1.5.AND.RAD(I).LE.1E09)THEN
QCM(I)=2*PI*L*XK1*DT1/ LOG(1+5.01/RD1**0.26)
ENDIF
ENDIF
c ----- Vertical -----
IF(INC.EQ.0)GOTO 468
XX=RD1*D1/L
IF(INC.EQ.90.AND.XX.GE.1E-11.AND.XX.LE.10**(-4.5))THEN
QCM(I)=2*PI*L*XK1*DT1/ LOG(1+4.47/XX**0.26)

```

```

ELSE
QCM(I)=9E-14
ENDIF
GOTO 468
C   Free molecule convection neglected -----
c   ----- Horizontal -----
614 IF(INC.EQ.0)THEN
IF(RAD(I).GE.1E-07.AND.RAD(I).LE.10**1.5) THEN
QCM(I)=2*PI*L*K*DT/ LOG(1+7.09/RAD(I)**0.37)
ELSE IF(RAD(I).GT.10**1.5.AND.RAD(I).LE.1E09) THEN
QCM(I)=2*PI*L*K*DT/ LOG(1+5.01/RAD(I)**0.26)
ELSE
QCM(I)=9E-14
ENDIF
ENDIF
c   ----- Vertical -----
IF(INC.EQ.90.AND.Y.GE.1E-11.AND.Y.LE.10**(-4.5))THEN
QCM(I)=2*PI*L*K*DT/ LOG(1+4.47/Y**0.26)
ELSE
QCM(I)=9E-14
ENDIF
C
468 PRINT*, 'QCM(', I, ')=' , QCM(I)
HK(I)=QCM(I)/(AK*DT1)
PRINT*, 'HK(', I, ')=' , HK(I), 'SSS=' , SSS, 'DT1=' , DT1
QM(I)=HOB(I)/HK(I)
99 CONTINUE
C ***** End of do loop *****
IF (INC.EQ.0) THEN
WRITE(3,92)
92 FORMAT(/, 'I', 'PX', 2X, 'PX/PA', 1X, 'SI-K', 2X, 'HOB', 1X, 'HTH-AR', 2X,
+'SI', 2X, 'NUL-AR', 1X, 'RAL.NO.', 2X, 'NUL-O', 1X, 'L-NOL', 1X, 'L-RAL', 1X,
+'L-RAD', 2X, 'B2', 2X, 'L-B2', 2X, 'B5', 2X, 'L-B5', 2X, 'TEK', 2X, 'QC-W', 2X,
+'QC-MP', 2X, 'L-RLPR', 2X, 'HTH-H', 1X, 'SI-H', /)
GO TO 598
ENDIF
-C
IF(INC.EQ.90) THEN
WRITE(3,16)
16 FORMAT(/, 1H1, 'PX', 2X, 'PX/PA', 1X, 'SI-K', 2X, 'HOB', 1X, 'HTH-AR', 2X,
+'SI', 2X, 'NUL-AR', 1X, 'RAL.NO.', 2X, 'NUL-O', 1X, 'L-NOL', 1X, 'L-RAL', 1X,
+'L-RAD', 2X, 'B2', 2X, 'L-B2', 2X, 'B5', 2X, 'L-B5', 2X, 'TEK', 2X, 'QC-W', 2X,
+'QC-MP', 2X, 'L-RLPR', 2X, 'HTH-V', 1X, 'SI-V', /)
GO TO 598

```

ENDIF

C

WRITE(3,41)

41 FORMAT(/,1H1,'PX',2X,'PX/PA',1X,'L-P/PA',1X,'HOB',2X,'HTH-AR',
12X,'SI',2X,'NUL-AR',1X,'RAL.NO.',1X,'NUL-OB',1X,'L-NOL',1X,
2'L-RAL',1X,'L-RAD',2X,'B2',2X,'L-B2',2X,'B5',3X,'L-B5',2X,'TEK',
32X,'TVK',2X,'QT-W',2X,'RL*P/PA',2X,'L-RLPR',/)

C

598 DO 367 I=1,T
IF(INC.EQ.0) GOTO 1000
IF(INC.EQ.90)GOTO 2000
WRITE(3,63) PM(I),P1(I),B3(I),HOB(I),HTH(I),SI(I),NUL(I),RAL(I),NU
+OL(I),Y1(I),O1(I),O2(I),B2(I),B(I),B5(I),B6(I),TEK(I),TVK(I),QT(I)
+,RLP(I),Y3(I)
63 FORMAT(I4,F6.2,3F6.2,F5.2,F7.2,E9.2,F7.2,F5.2,2F6.2,2(F5.2,F6.2),
+2F6.1,F5.2,E9.2,F6.2)
GOTO 317
1000 PRINT*,'0'
WRITE(3,13) PM(I),P1(I),QM(I),HOB(I),HTH(I),SI(I),NUL(I),RAL(I),NU
+OL(I),Y1(I),O1(I),O2(I),B2(I),B(I),B5(I),B6(I),TEK(I),QC(I),QCM(I)
+,Y3(I),HTS(I),SIH(I)
13 FORMAT(I4,F6.2,3F6.2,F5.2,F7.2,E9.2,F7.2,F6.2,2F6.2,2(F5.2,F6.2),
+F6.1,F5.2,F6.2,F7.2,2X,F6.2,F5.2)
GOTO 317
2000 PRINT*,'90'
WRITE(3,23) PM(I),P1(I),QM(I),HOB(I),HTH(I),SI(I),NUL(I),RAL(I),NU
+OL(I),Y1(I),O1(I),O2(I),B2(I),B(I),B5(I),B6(I),TEK(I),QC(I),QCM(I)
+,Y3(I),HTH1(I),SIV(I)
23 FORMAT(I4,F6.2,3F6.2,F6.2,F6.2,E9.2,F7.2,F5.2,2F6.2,2(F5.2,F6.2),
+F6.1,F5.2,F6.2,F7.2,2X,F6.2,F5.2)
317 PRINT*,'OK'
367 CONTINUE
STOP
END

APPENDIX D

CALIBRATION OF THERMOCOUPLES

The hot or measuring junction formed by the copper-constantan (60% copper and 40% nickel) thermocouples were subsequently soldered on the surface of the test cylinder after calibration. The thermocouples were calibrated in 0° and 100°C and the calibration curve was extended upto 155°C . The schematic diagram of thermocouple is shown below.

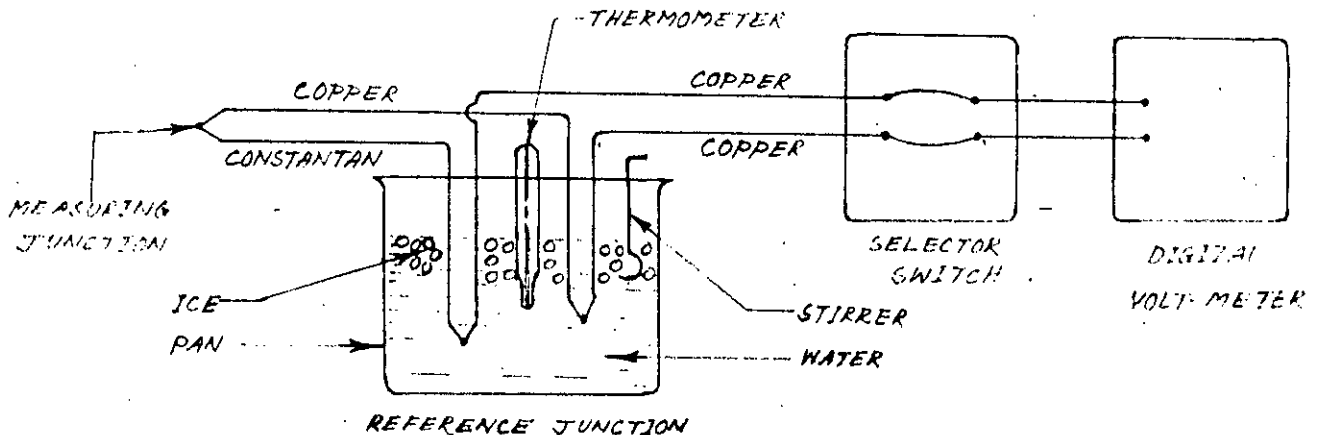


DIAGRAM OF THE THERMOCOUPLE CONNECTION

The reference junction of the thermocouples were maintained at 0°C by placing both the measuring and the reference junctions in a pan containing crushed melting ice, equilibrium with water. The mixture was continuously stirred. A calibrated thermometer was used to check temperature of the mixture. The accuracy of the thermometer was 0.5°C . The bulb of the Hg thermometer and the thermocouple junctions were kept just below the surface of the water. The calibration at 100° was done by putting the cold or reference junction in the melting ice pan as before and placing the measuring junctions in another pan containing boiling water open to atmosphere. A separate thermometer of the same order of accuracy and the measuring junctions were immersed in the boiling water. The thermocouple junctions and the thermometer bulb were kept just below the surface of the water at locations close to each other.

Since the thermocouple wires are expensive, extension copper wires were used for the connection to the selector switch and digital volt-meter. The necessary condition to avoid the effect of introducing the third metal was that the cut junctions be kept at the same temperature and the lengths of both extension wire are same. These copper wires were connected to the digital volt-meter which measured the emf produced by the thermocouples through a selector switch.

APPENDIX E

CORRELATION COEFFICIENT

The analysis is based upon the variance approach regression analysis. Let X and Y be independent and dependent variables respectively and suffix 'i' indicate any variable point. Let bar (-) and hath (^) symbol on a variable indicate the mean and regression line respectively.

Let

$$SSTO = \sum (Y_i - \bar{Y})^2$$

$$SSE = \sum (Y_i - \hat{Y}_i)^2$$

$$SSR = \sum (\hat{Y}_i - \bar{Y})^2 = SSTO - SSE$$

Here SSTO stands for *total sum of squares* of the deviations from the mean. If SSTO=0, all observations are same. The greater the SSTO, the greater is the variation among the Y observations. SSE denotes *error sum of squares*. If SSE=0, all observations fall on the fitted regression line. The larger the SSE, the greater is the variation of Y observations around the regression line. SSR stands for the *regression sum of squares*. If regression line is a horizontal one SSR=0, otherwise SSR is positive. SSR may be considered as a measure of variability of the Y's associated with the regression line. The larger the SSR in relation to SSTO, the greater is the effect of regression relation in accounting for the total variation in the Y observations.

Coefficient of Determination

It is a measure of the 'degree of association' between X and Y; denoted r^2 by the following relation:

$$r^2 = (SSTO - SSE) / SSTO = SSR / SSTO = 1 - SSE / SSTO$$

Since $0 \leq SSE \leq SSTO$, it follows that $0 \leq r^2 \leq 1$.

This r^2 may be interpreted as the proportionate reduction of total variation associated with the use of the independent variable X. Thus, the larger the r^2 , the more is the total variation of Y reduced by introducing the independent variable X.

Coefficient of Correlation

The square root of r^2 :

$$r = \pm \sqrt{r^2}$$

is called the *coefficient of correlation*. A plus or minus sign is attached to this measure according to whether the slope of the fitted regression line is positive or negative. Thus the range of r is: $-1 \leq r \leq 1$.

Whereas r^2 indicates the proportional reduction in the variability of Y attained by the use of information about X , the square root, r , does not have a clear-cut operational interpretation. Nevertheless, there is a tendency to use r instead of r^2 in much applied work in business and economics. It is worth noting that since for any r^2 other than 0 or 1, $r^2 < |r|$, r may give the impression of a closer relationship between X and Y than does the corresponding r^2 . For instance $r^2 = 0.10$ indicates that the total variation in Y is reduced by only 10% when X is introduced, yet $|r| = 0.32$ may give an impression of greater association between X and Y . The graphs in the present investigations were drawn by using 'Cricket Graph' Software, where the correlation coefficient is directly given by the software itself when the data are asked to fit on a selected curve fitting.

Computational Formula for r

A direct computation formula for r , which automatically furnishes the proper sign, is

$$r = \frac{[\sum (X_i - \bar{X})(Y_i - \bar{Y})]}{[\{\sum (X_i - \bar{X})^2 \cdot \sum (Y_i - \bar{Y})^2\}^{1/2}]}$$
$$= \frac{[\sum X_i Y_i - (\sum X_i \sum Y_i)/n]}{[\{\sum X_i^2 - (\sum X_i)^2/n\} \{\sum Y_i^2 - (\sum Y_i)^2/n\}]^{1/2}}$$

A value of r or r^2 close to 1 is taken as an indication that sufficiently precise inferences on Y can be made from the knowledge of X .

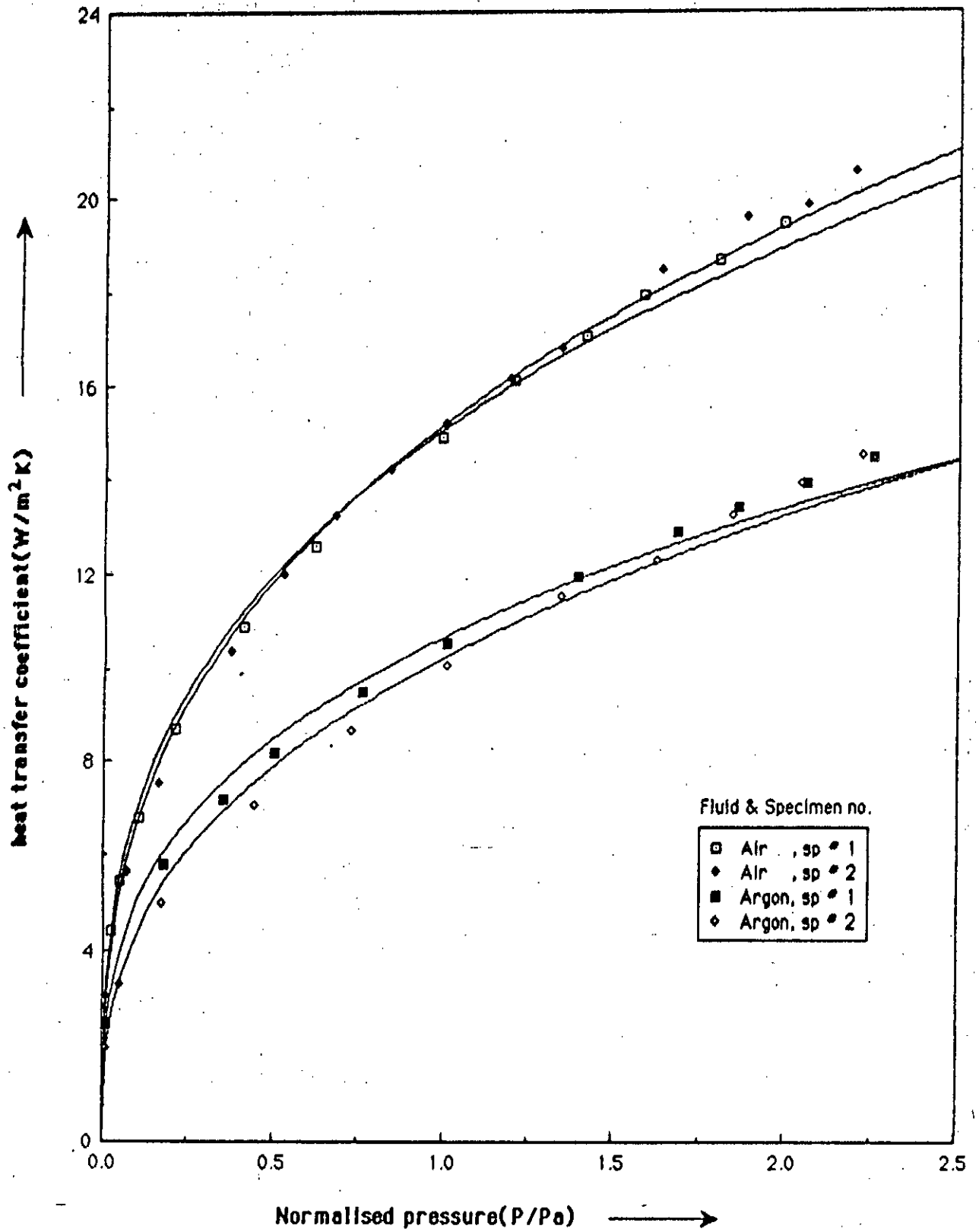


Fig-1. Comparison of heat transfer coefficient obtained from the two specimens in both air and argon for horizontal position of the cylinder.

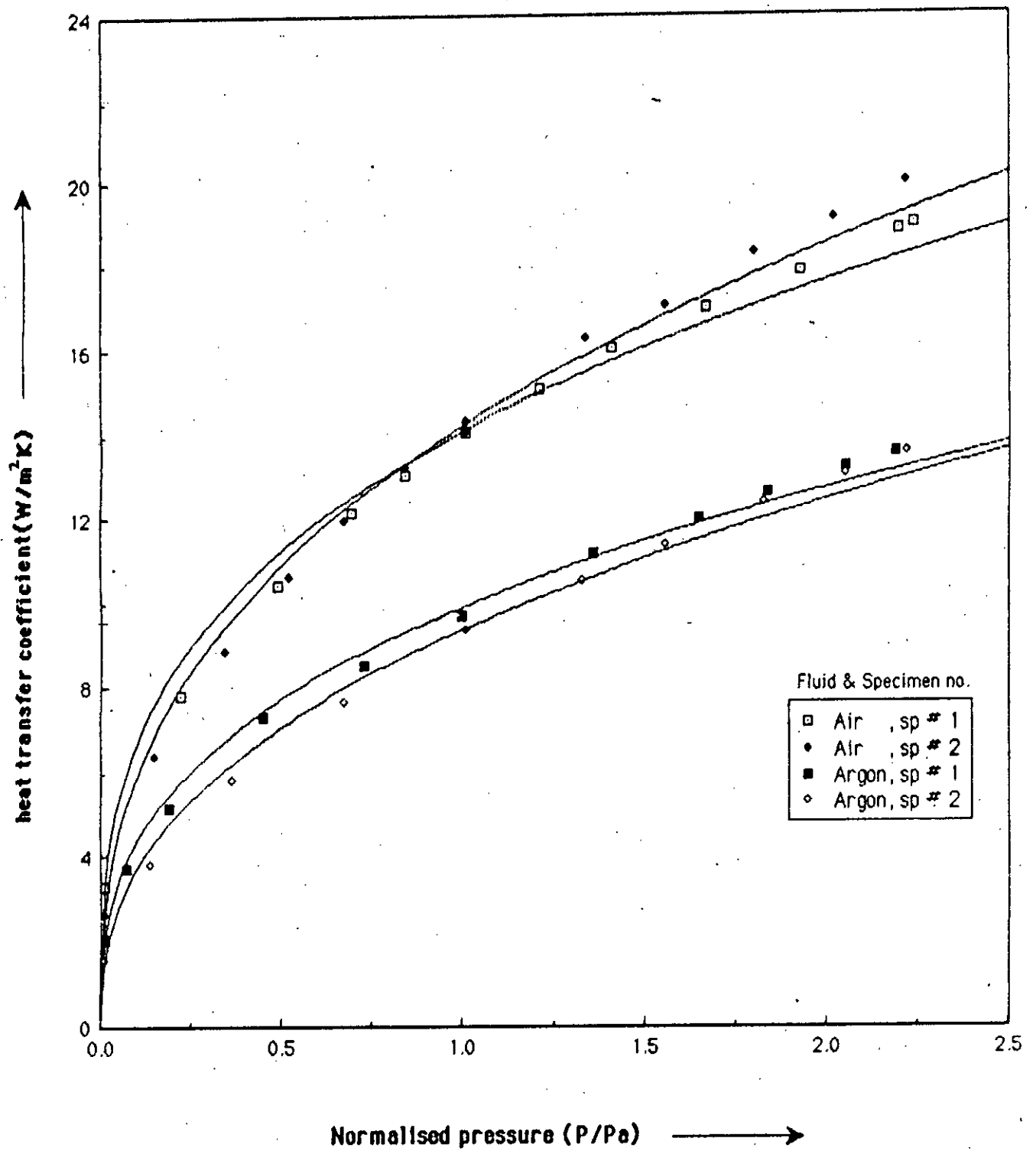


Fig-2. Comparison of heat transfer coefficients obtained from the two specimens in both air and argon for 30 degree inclination of the cylinder with horizontal.

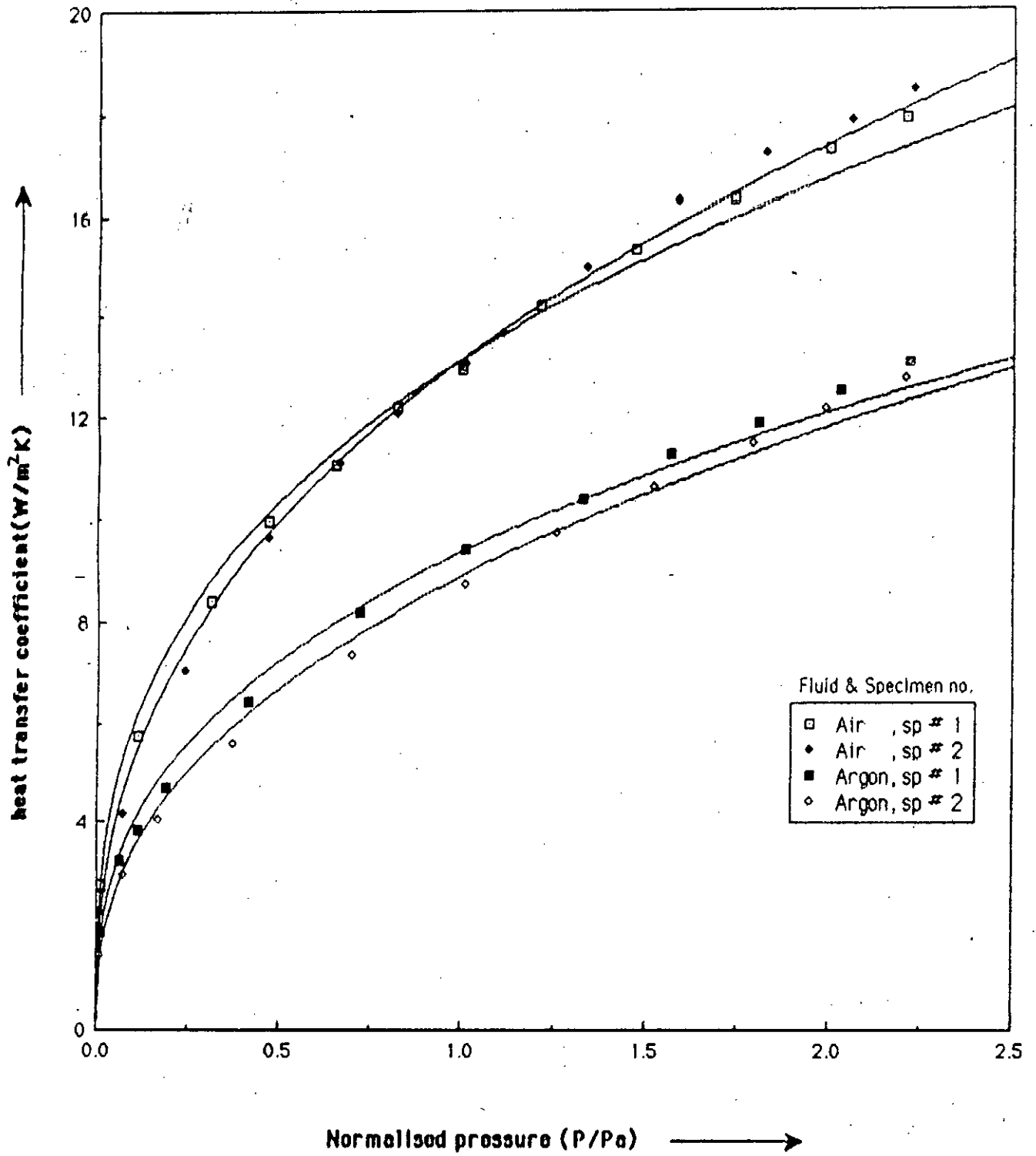


Fig-3. Comparison of heat transfer coefficients obtained from the two specimens in both air and argon for 45 degree inclination of the cylinder with horizontal.

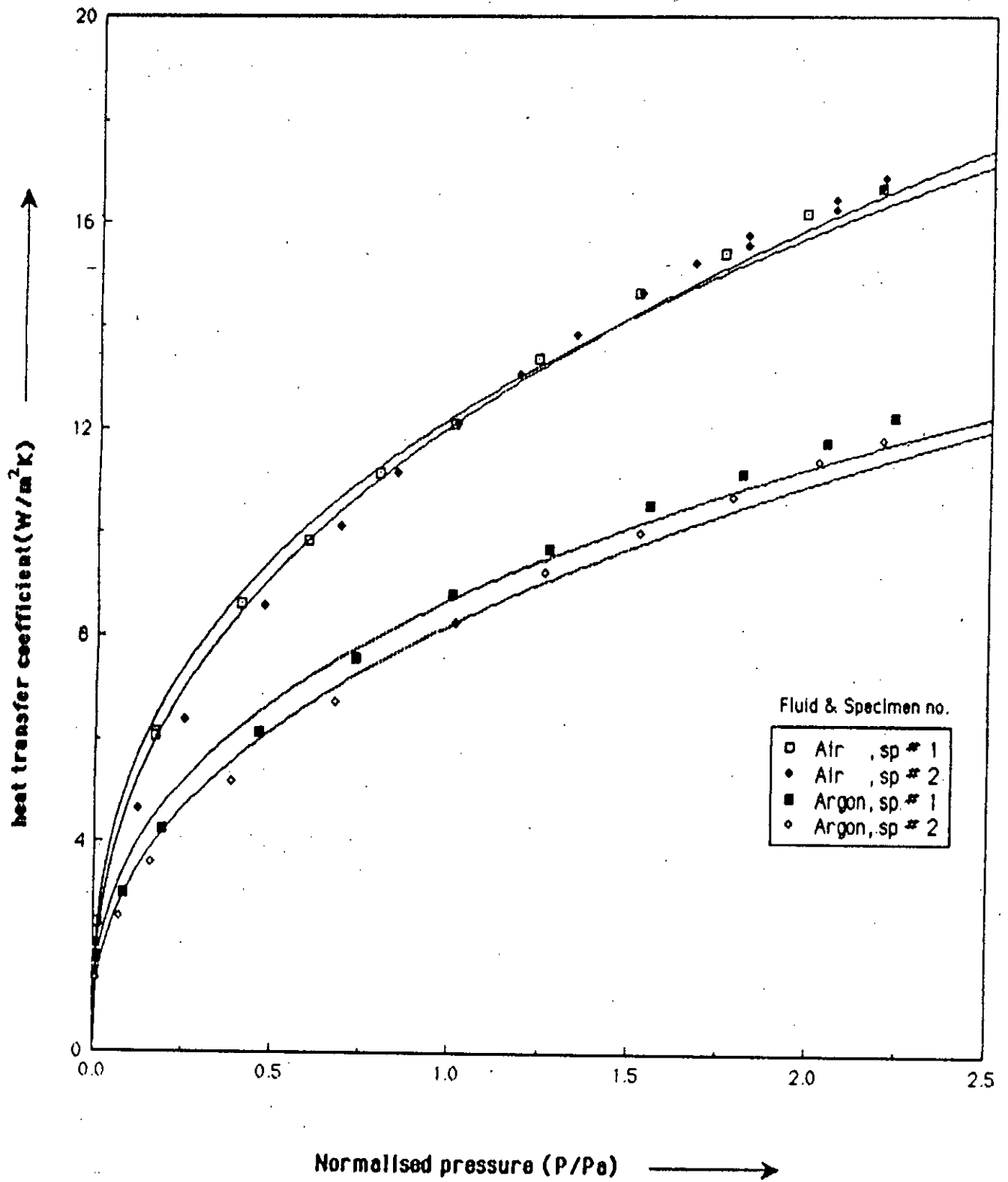


Fig-4. Comparison of heat transfer coefficients obtained from the two specimens in both air and argon for 60 degree inclination of the cylinder with horizontal.

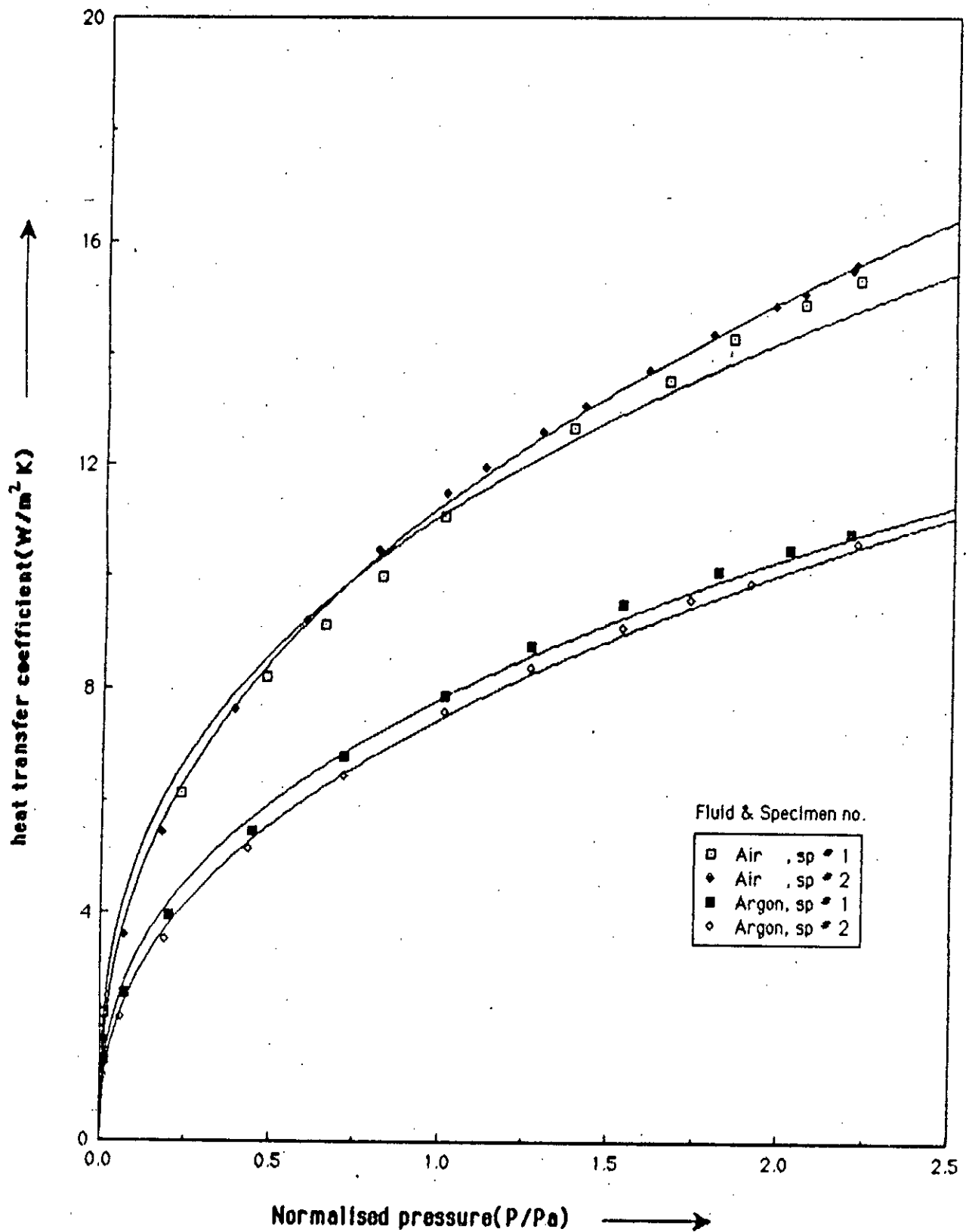


Fig-5. Comparison of heat transfer coefficient obtained from the two specimens in both air and argon for vertical position of the cylinder.

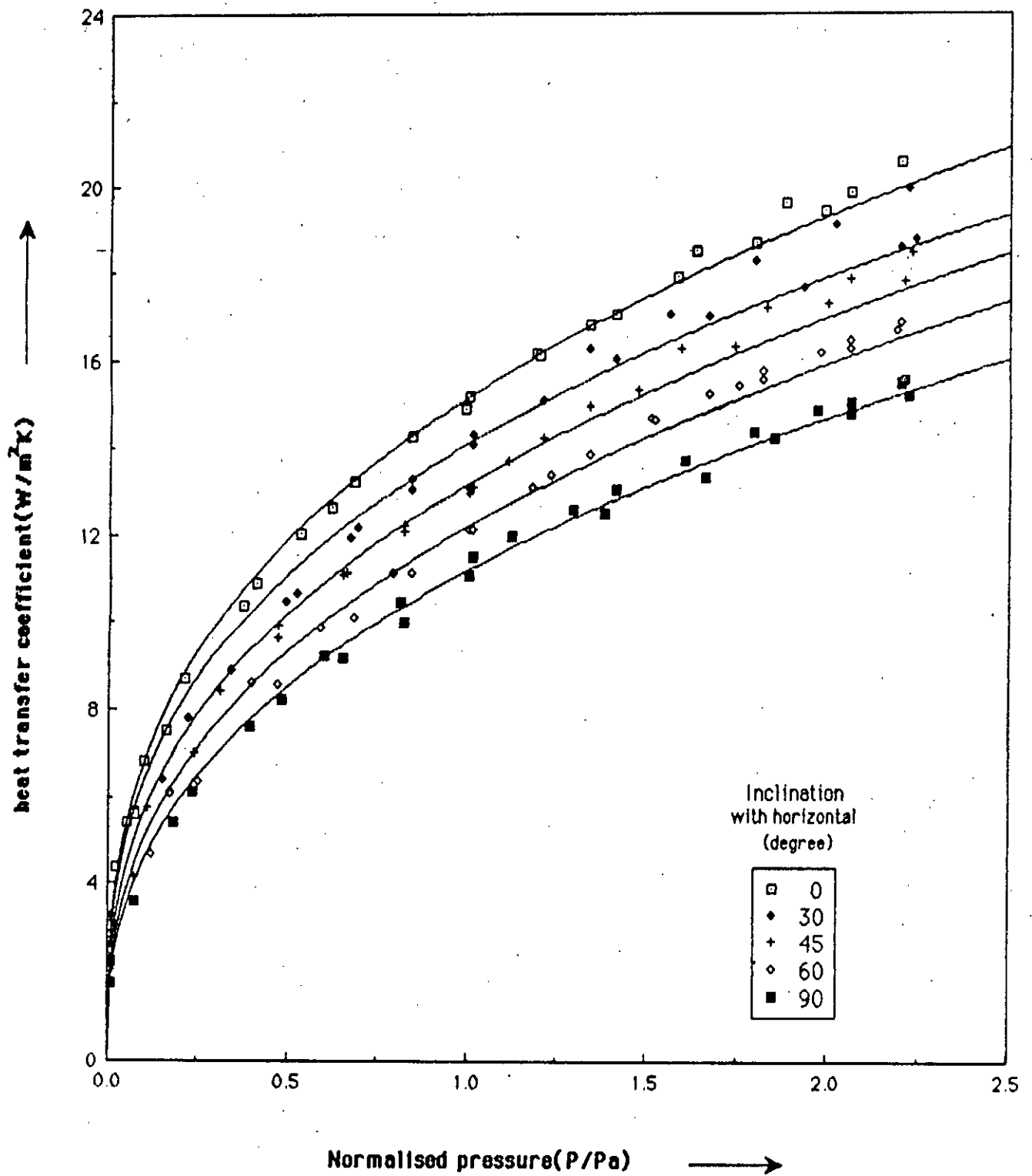


Fig-6. Plot of observed heat transfer coefficient for different inclinations of the cylinder in air against normalised pressure.

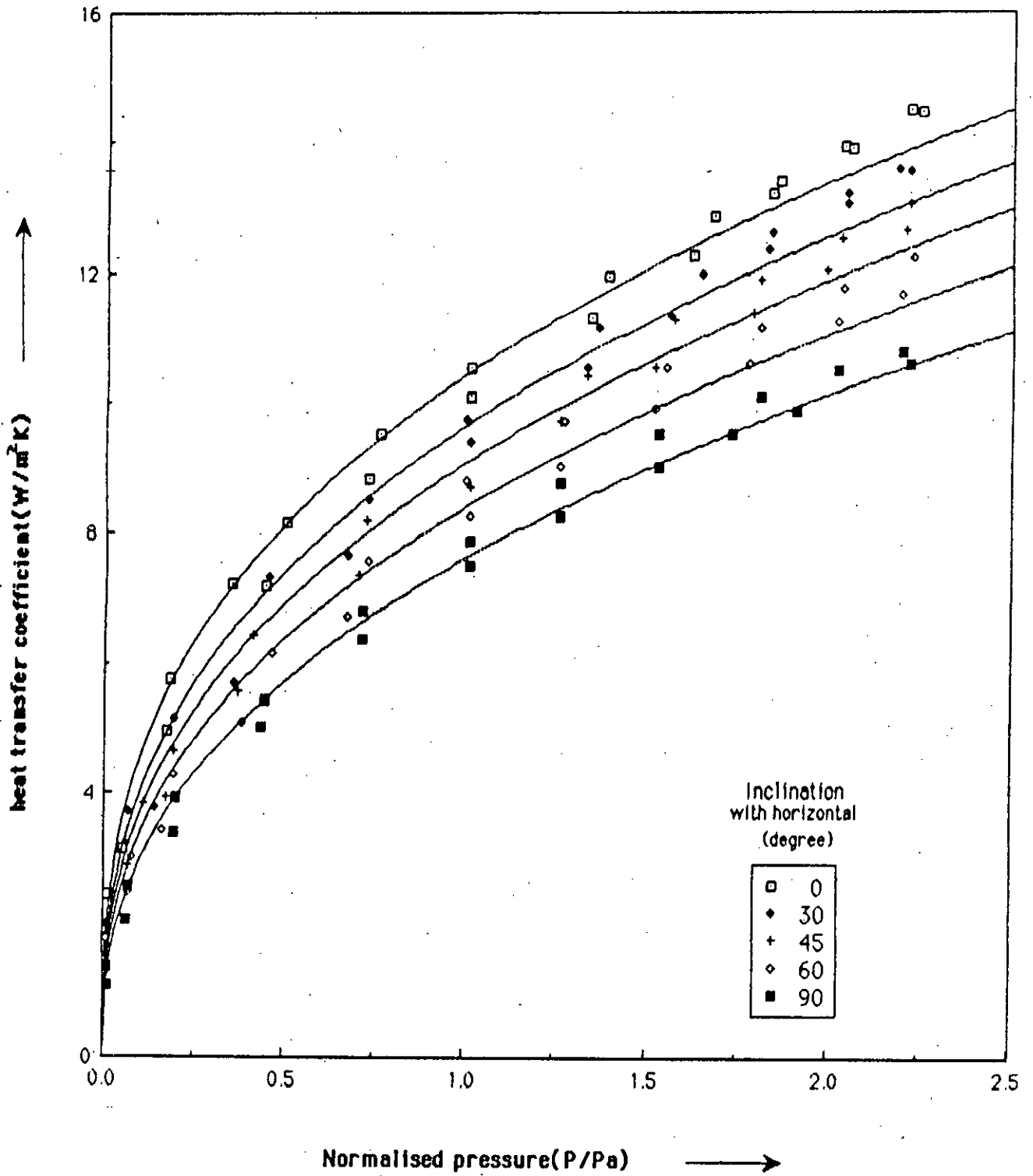


Fig-7. Plot of observed heat transfer coefficient for different inclinations of the cylinder in argon against normalised pressure.

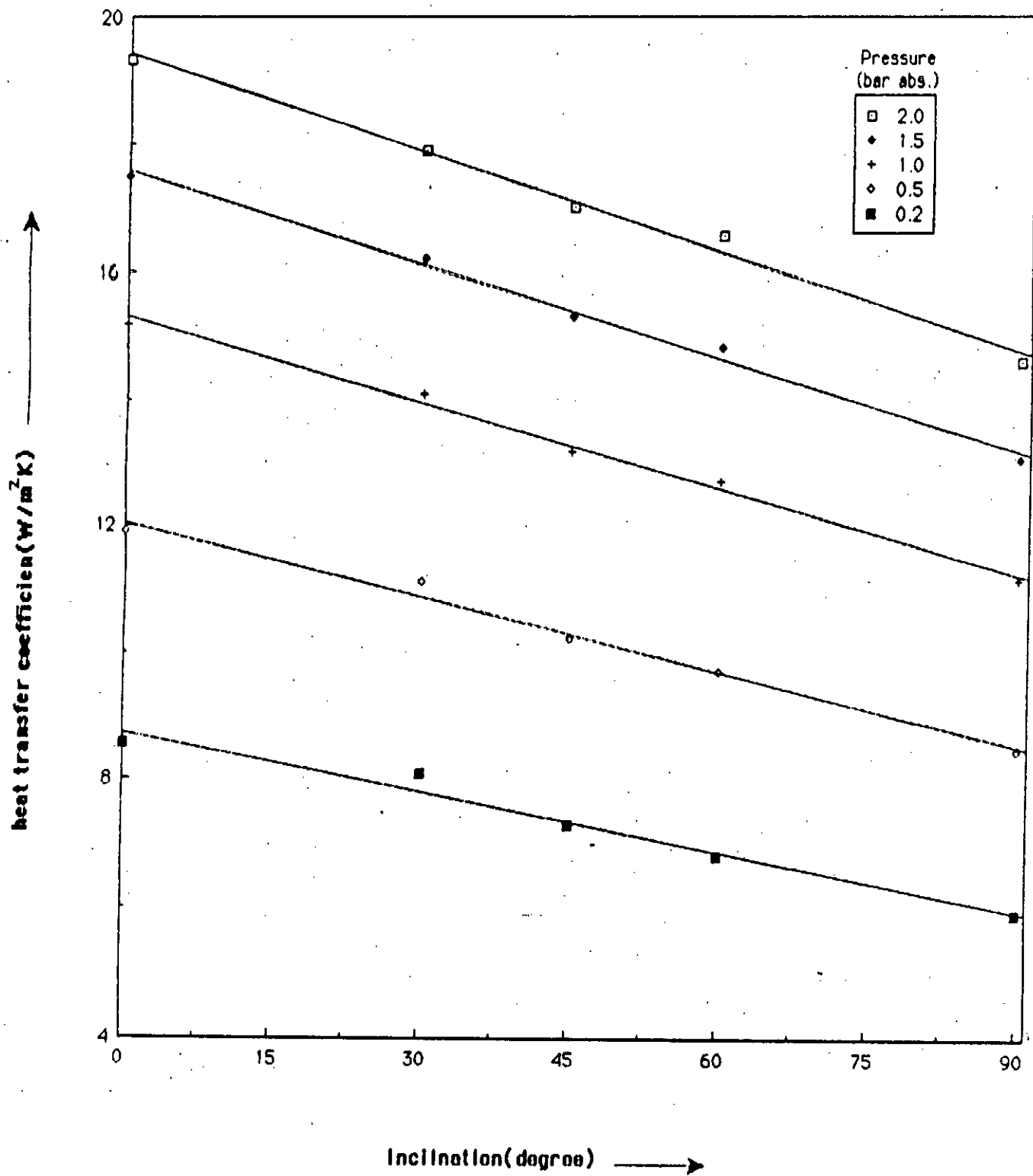


Fig-8. Plot of observed heat transfer coefficient versus inclination of the cylinder in air.

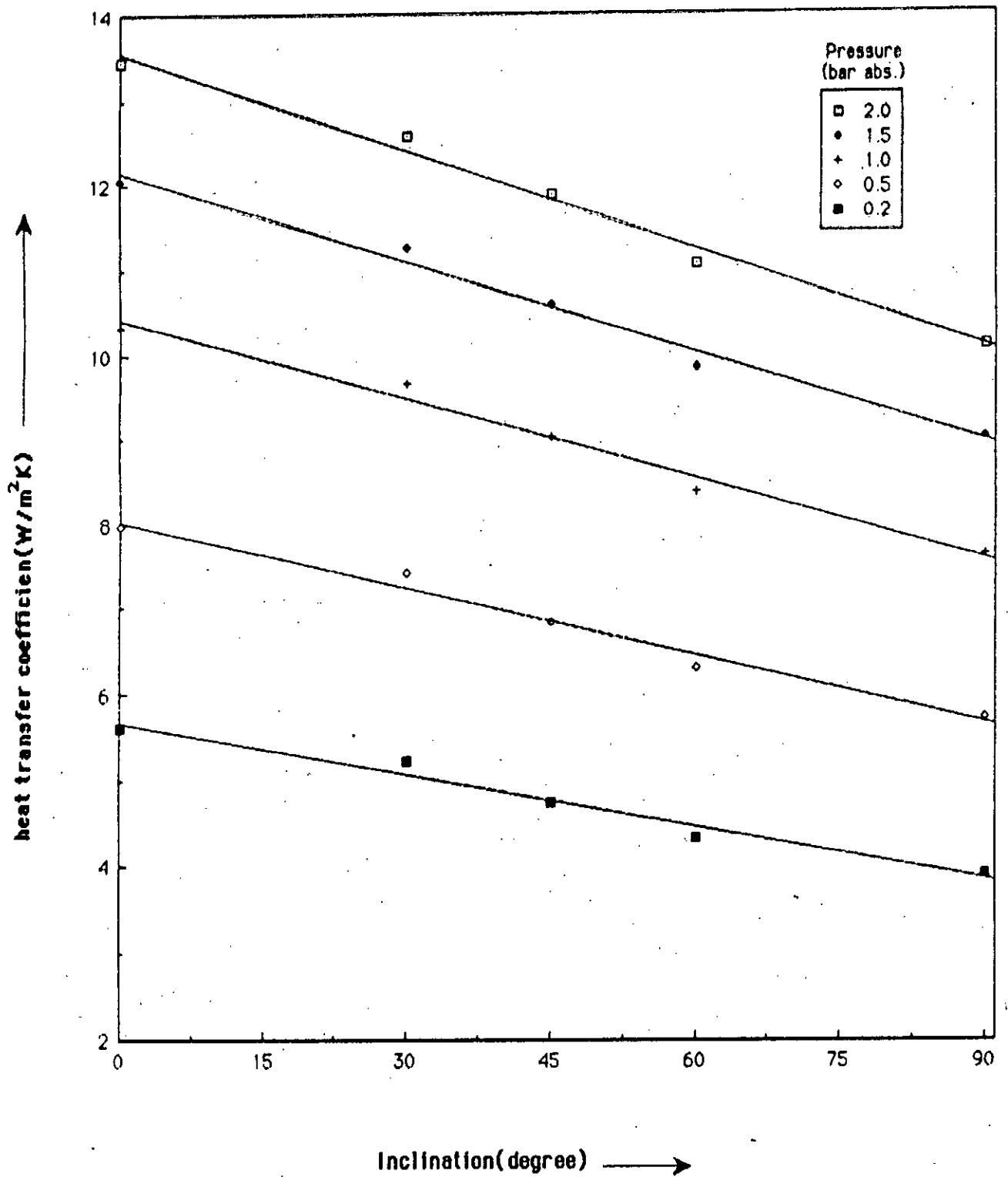


Fig-9. Plot of observed heat transfer coefficient versus inclination of the cylinder for argon.

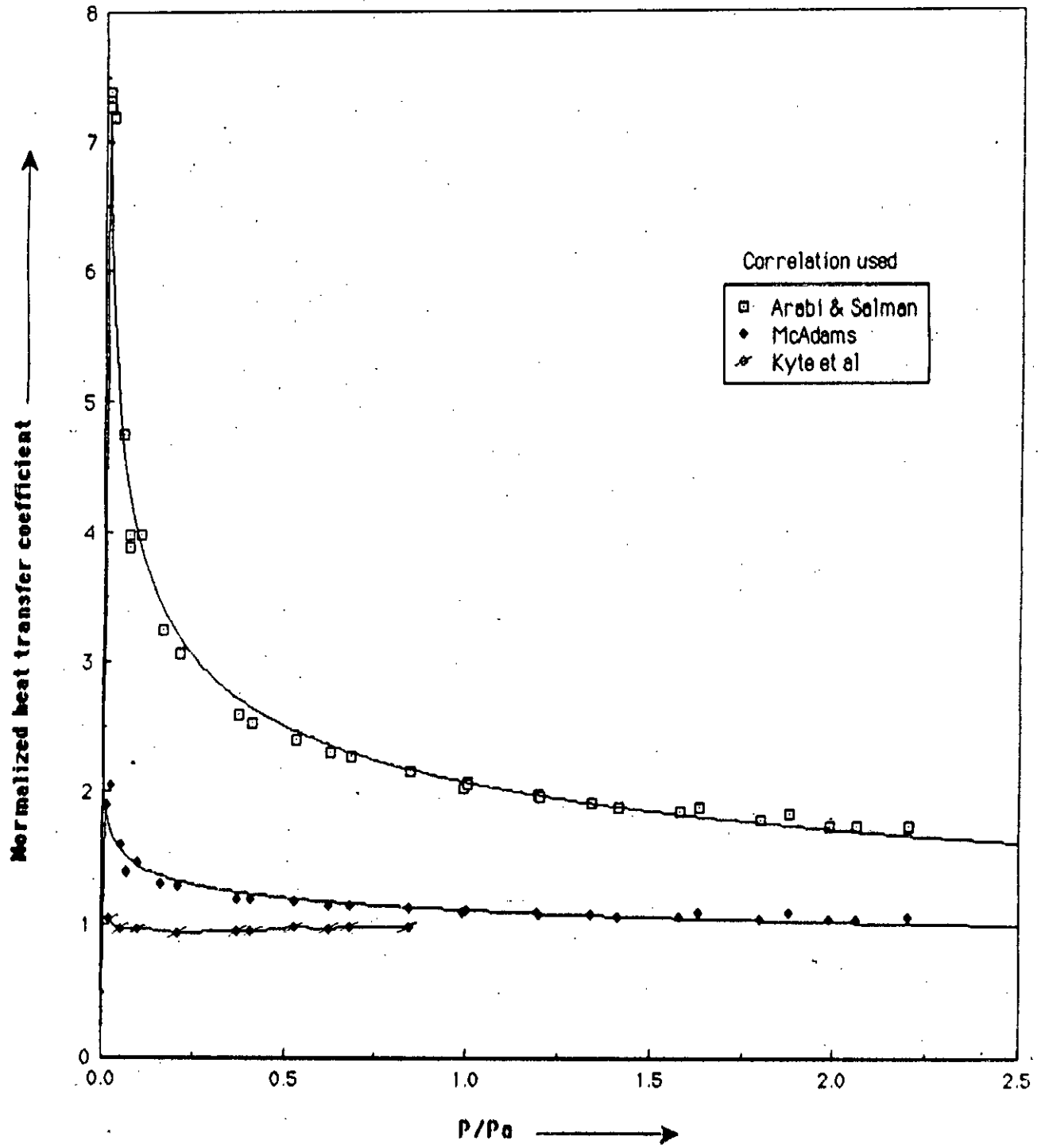


Fig-10. Comparison of the normalized heat transfer coefficient against normalised pressure for horizontal cylinders in air using different correlations.

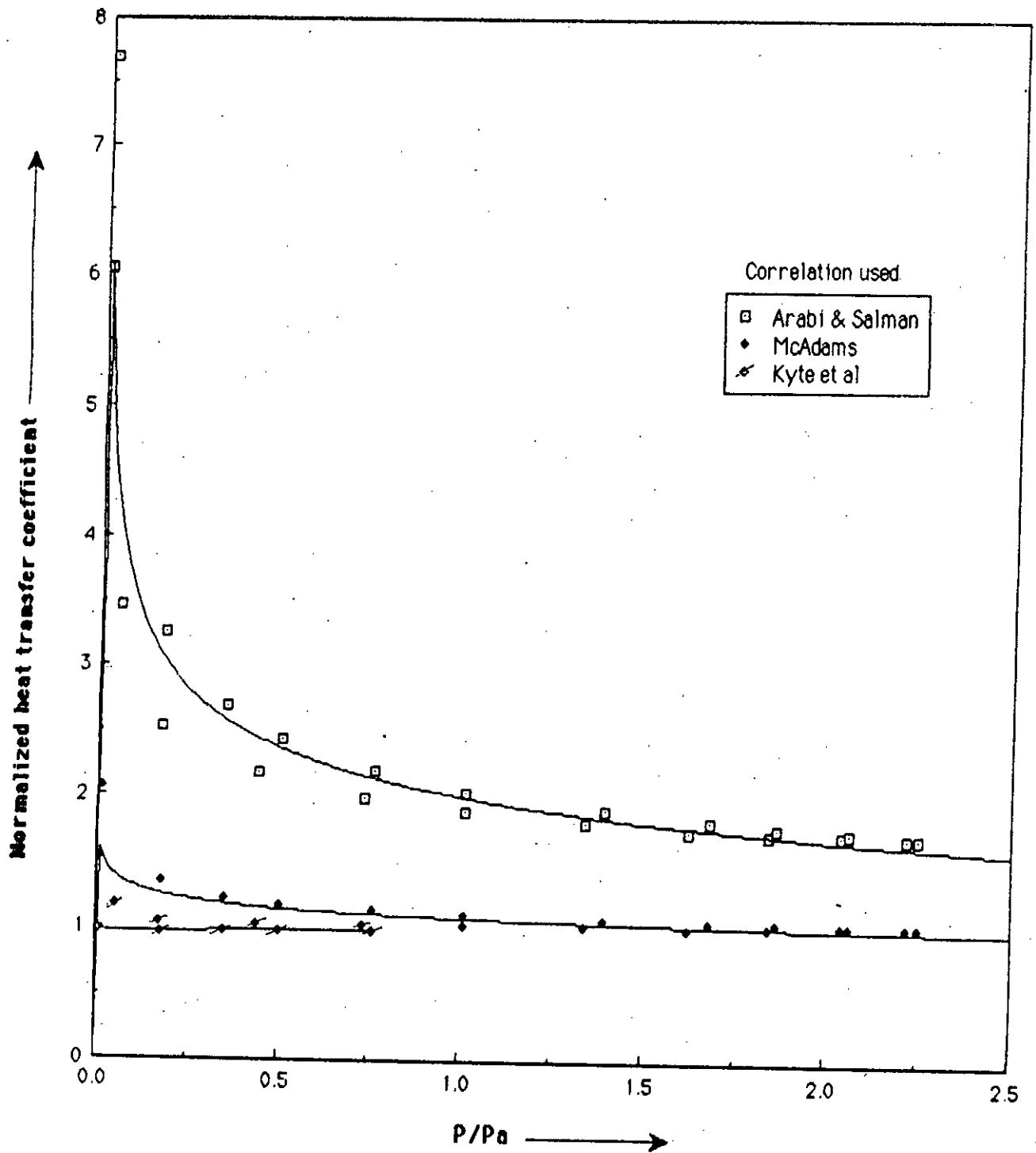


Fig-11. Comparison of the normalized heat transfer coefficient against normalised pressure for horizontal cylinders in argon using different correlations.

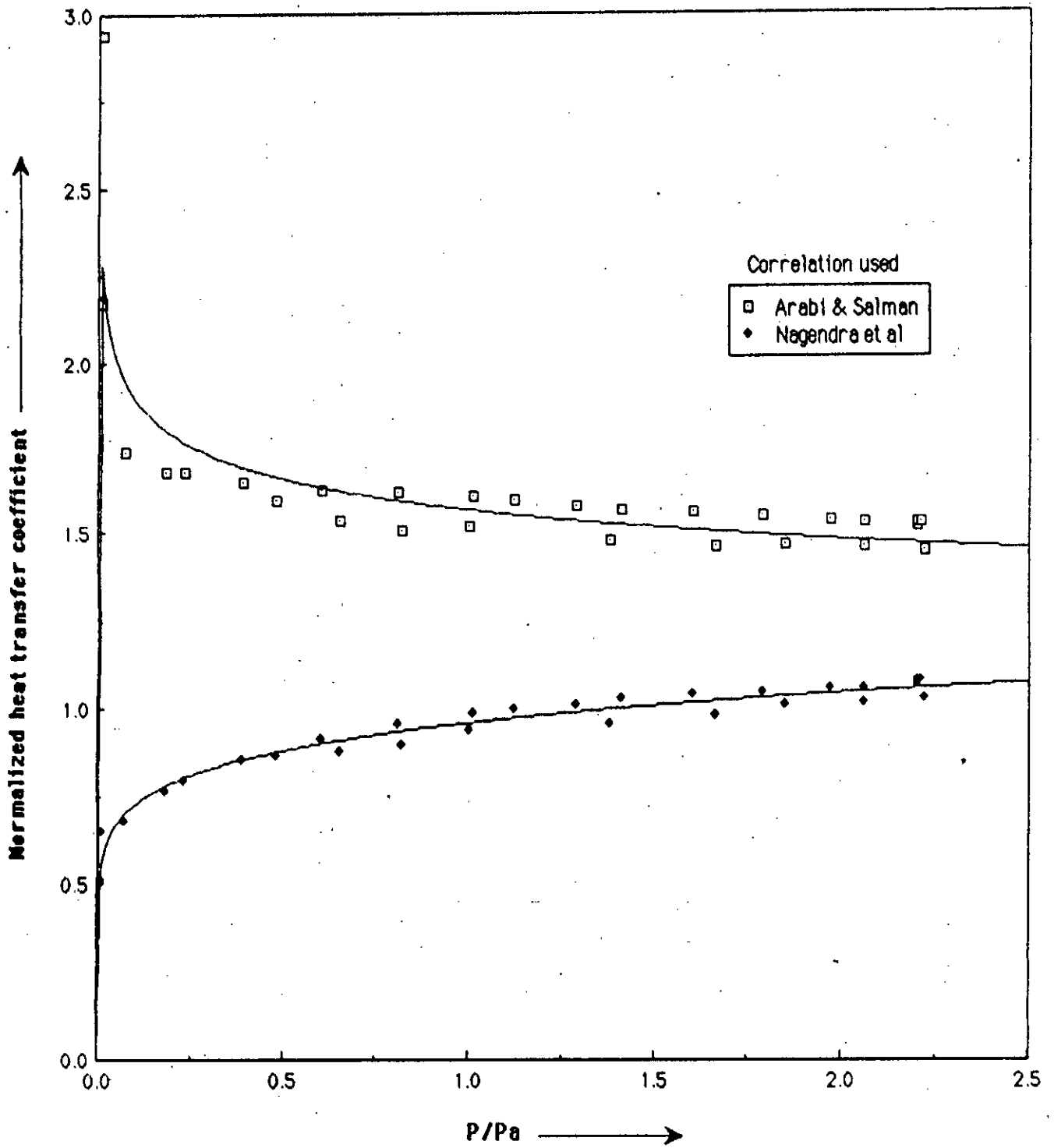


Fig- 12. Comparison of normalized heat transfer coefficient using the correlations of Arabi & Salman and Nagendra et al against normalized pressure for vertical cylinders in air.

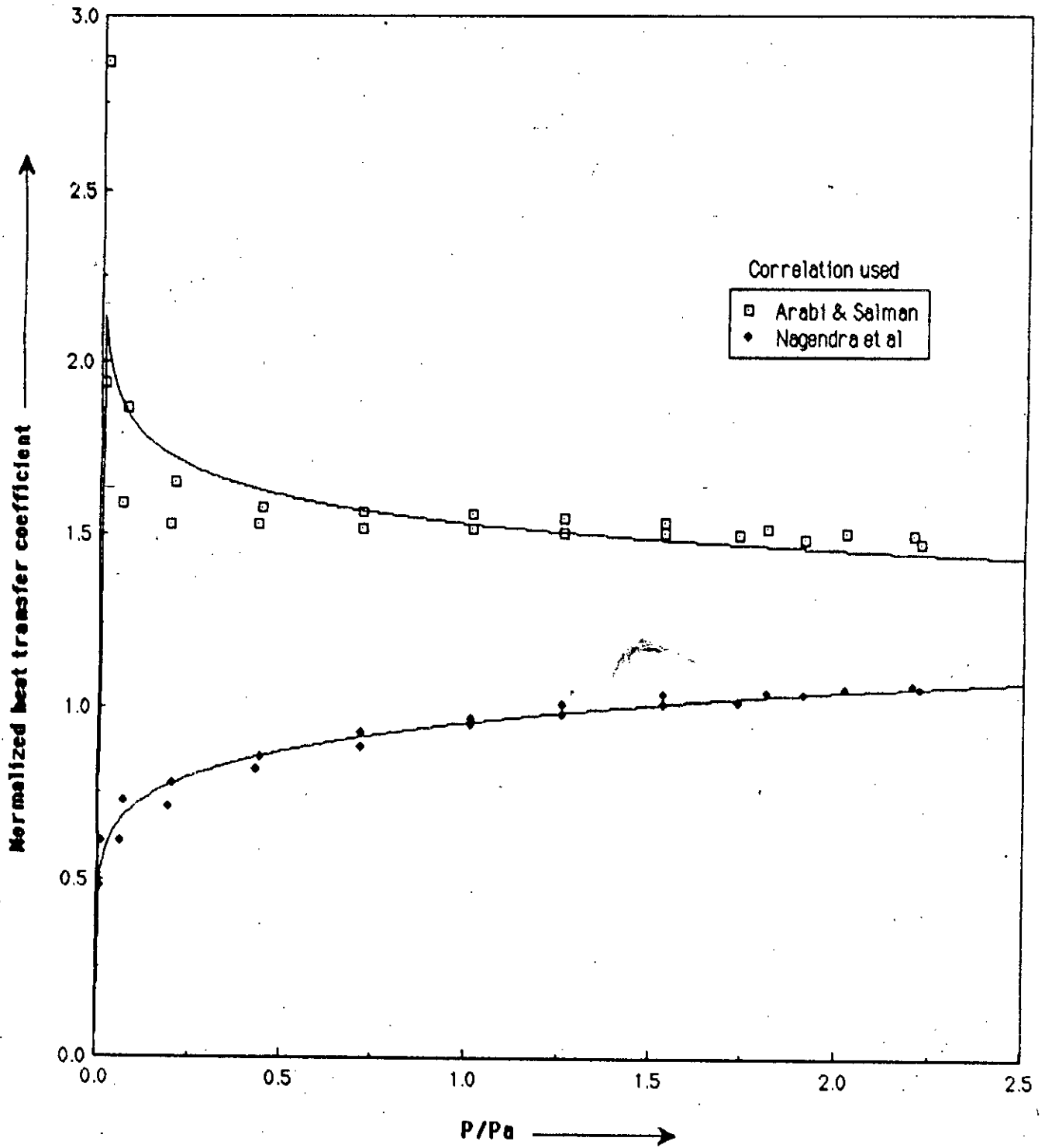


Fig- 13. Comparison of normalized heat transfer coefficient using the correlations of Arabi & Salman and Nagendra et al against normalized pressure for vertical cylinders in argon.

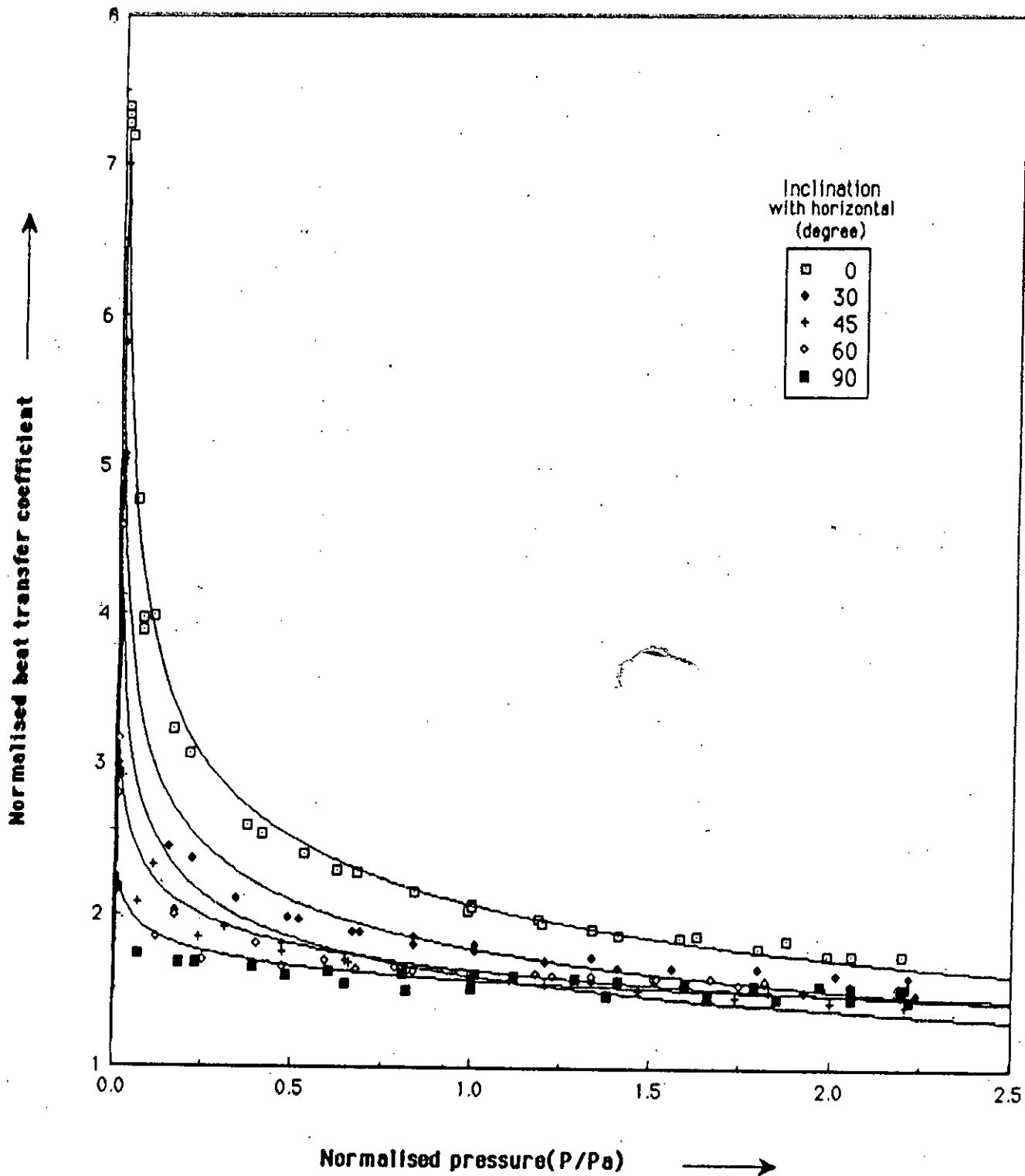


Fig-14. Plot of normalised heat transfer coefficient against normalised pressure for different inclinations in air using correlation of Arabi and Salman.

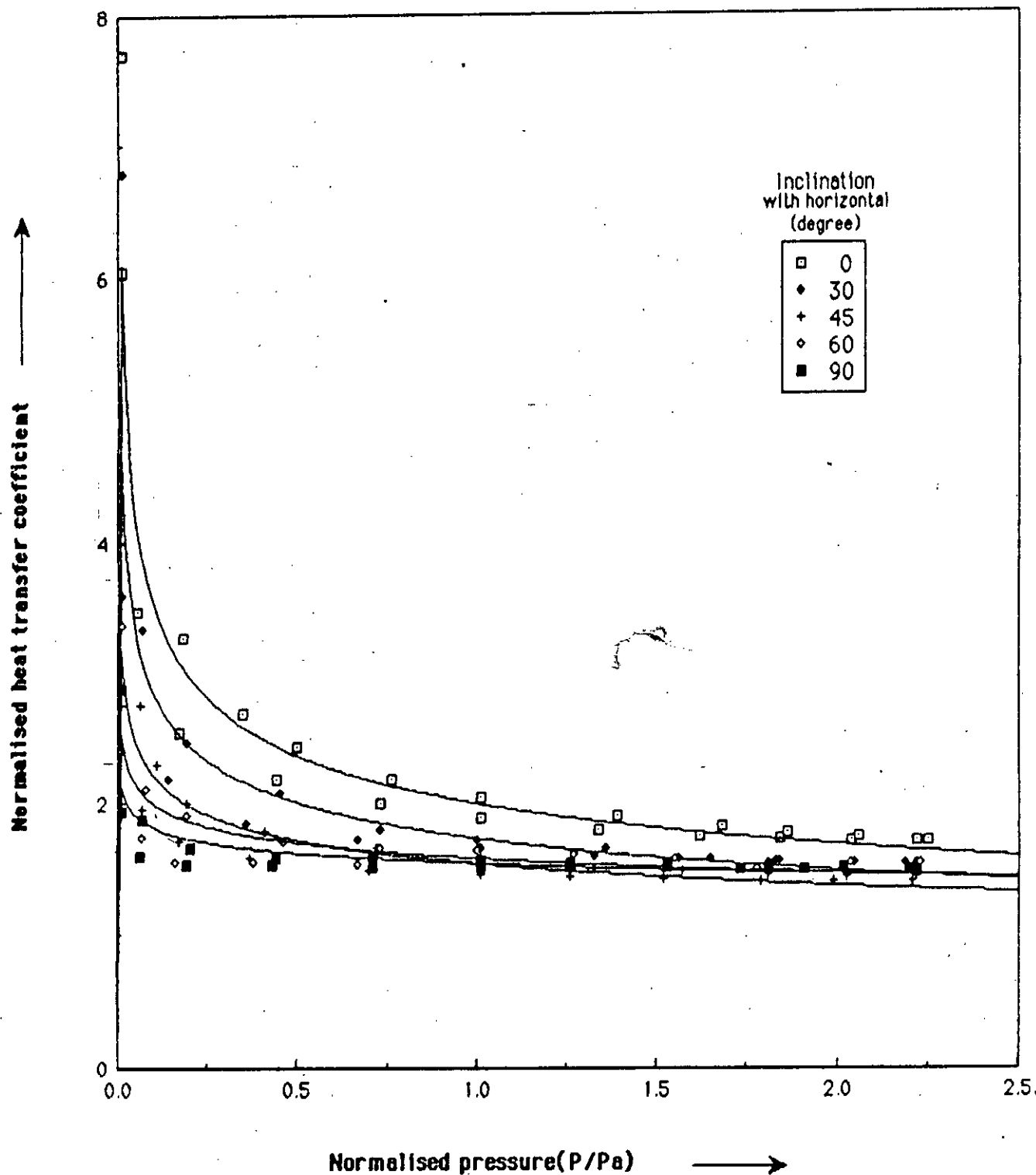


Fig-15. Plot of normalised heat transfer coefficient against normalised pressure for different inclinations in argon using correlation of Arabi and Salman.

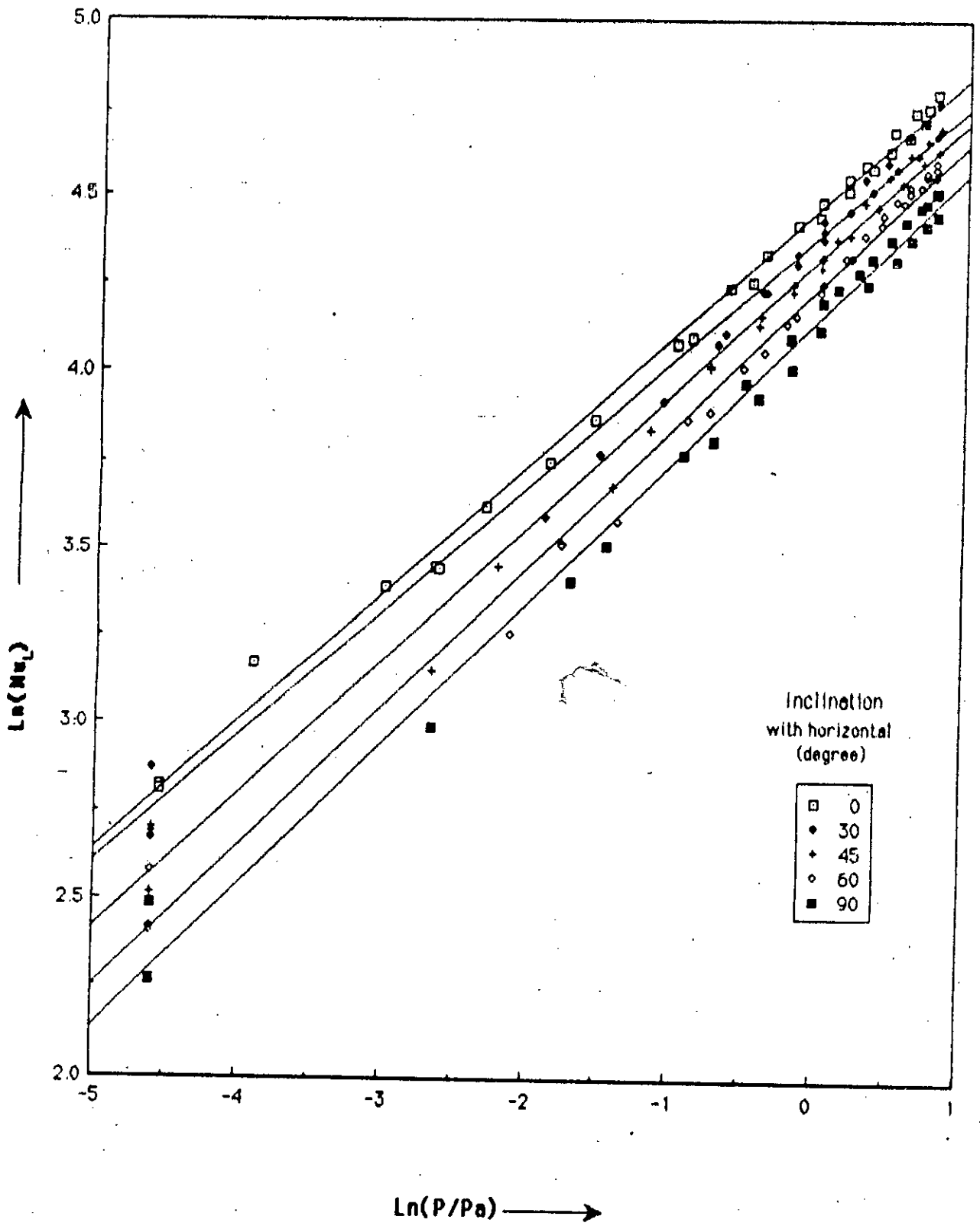


Fig-16. Log-Log plot of observed Nusselt no. versus normalised pressure for air.

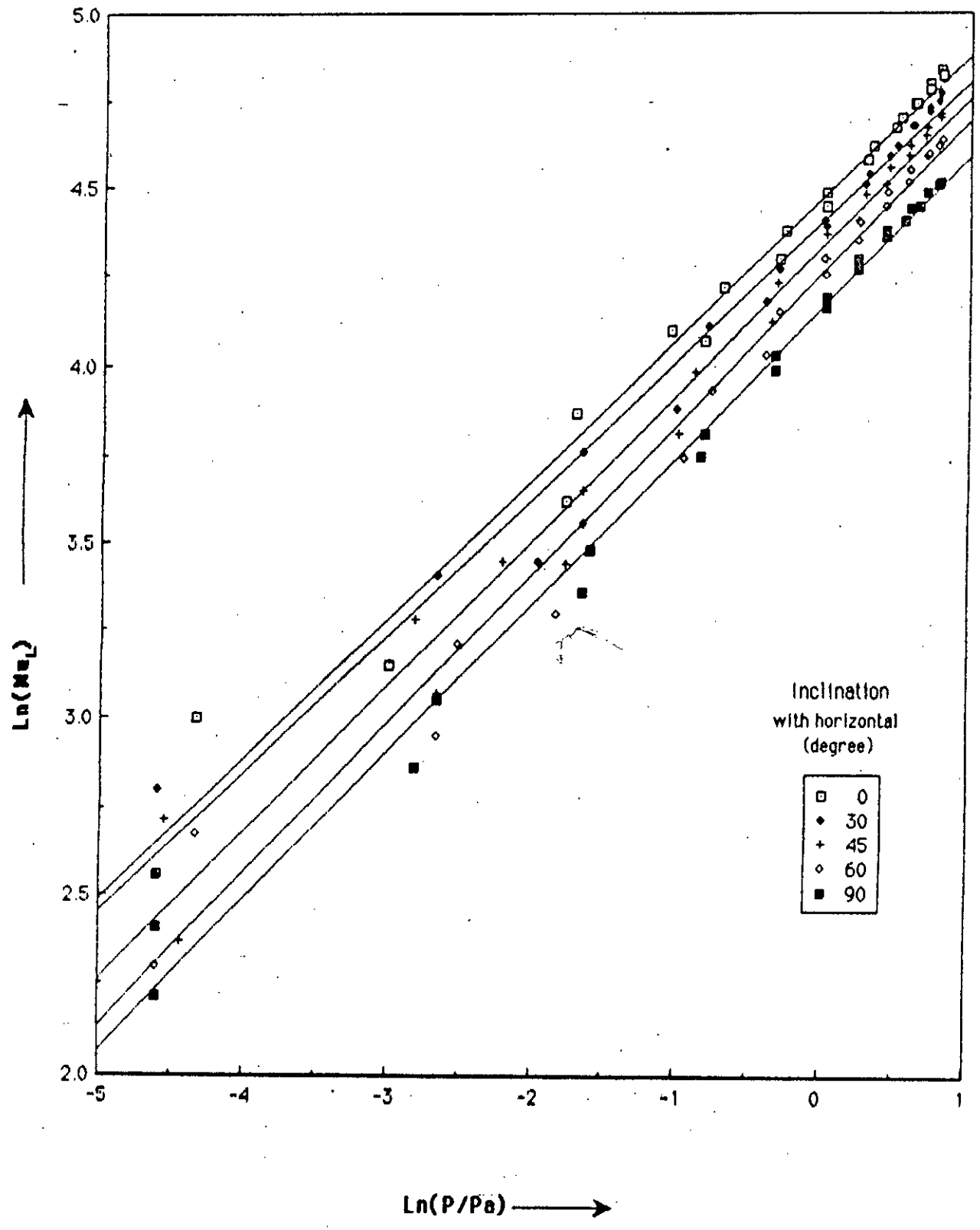


Fig-17. Log-Log plot of observed Nusselt no. versus normalised pressure for argon.

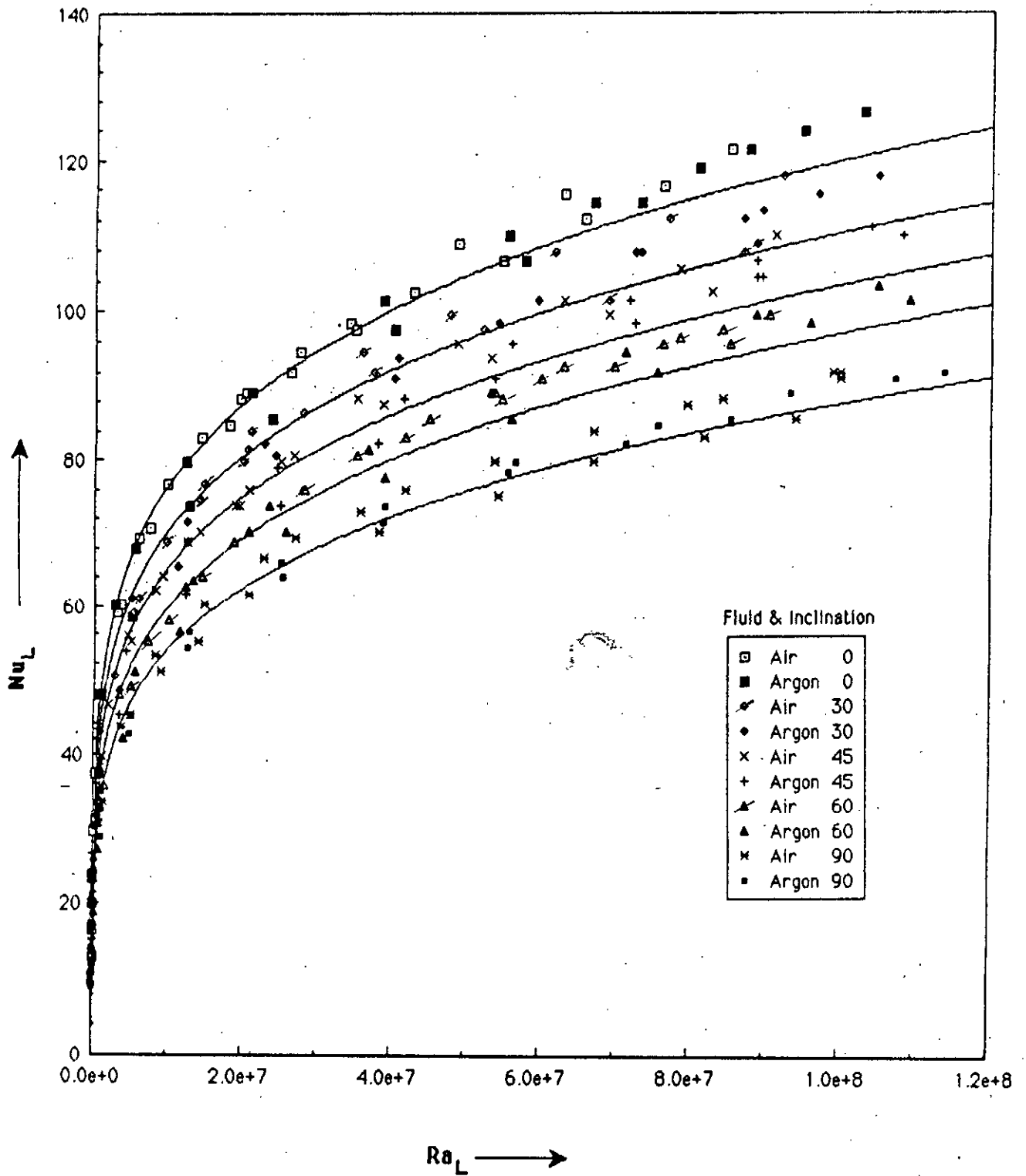


Fig-18. Plot of observed Nusselt no. for both air and argon.

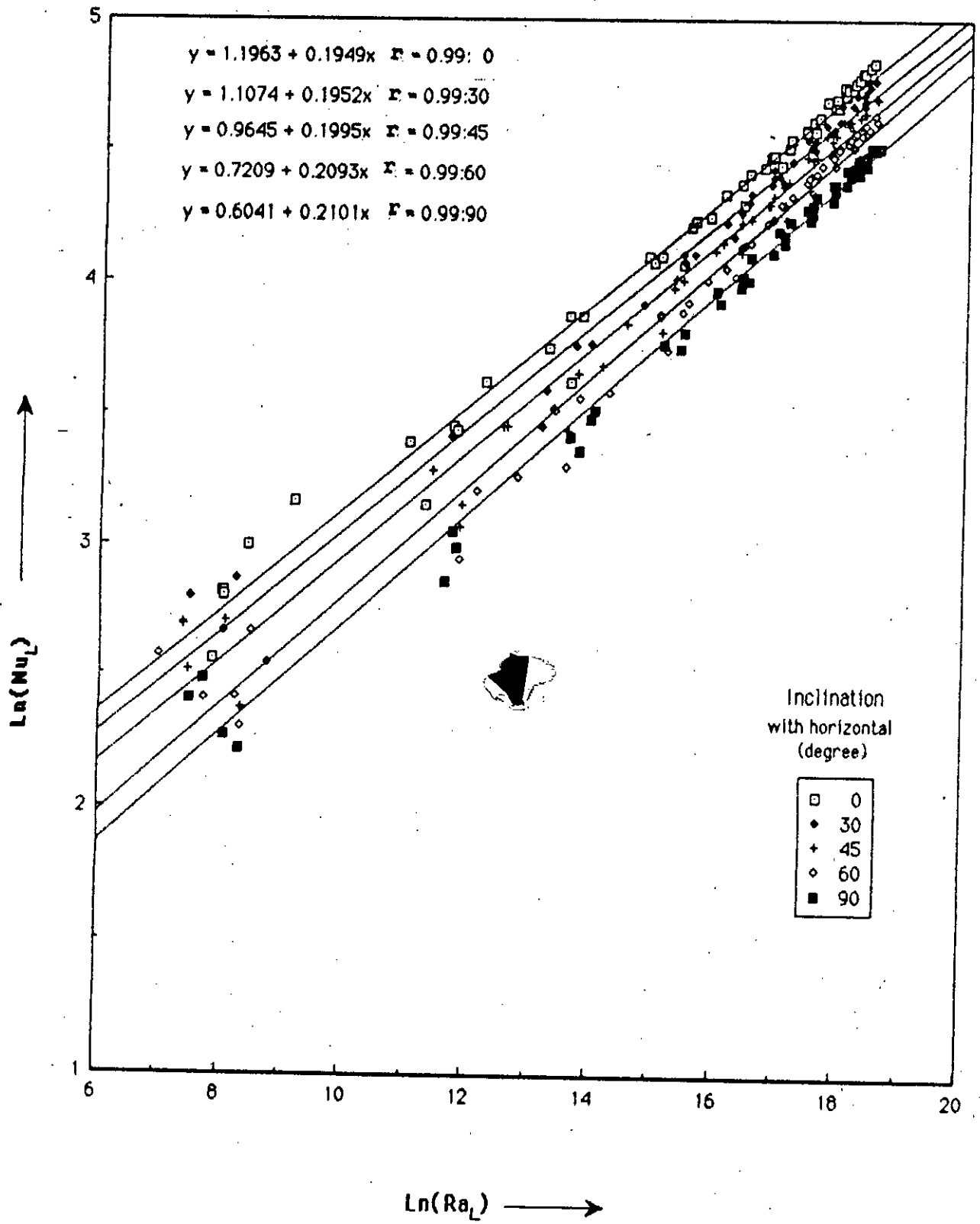


Fig-19. Log-Log plot of observed Nusselt no. versus Rayleigh no. for both air and argon.

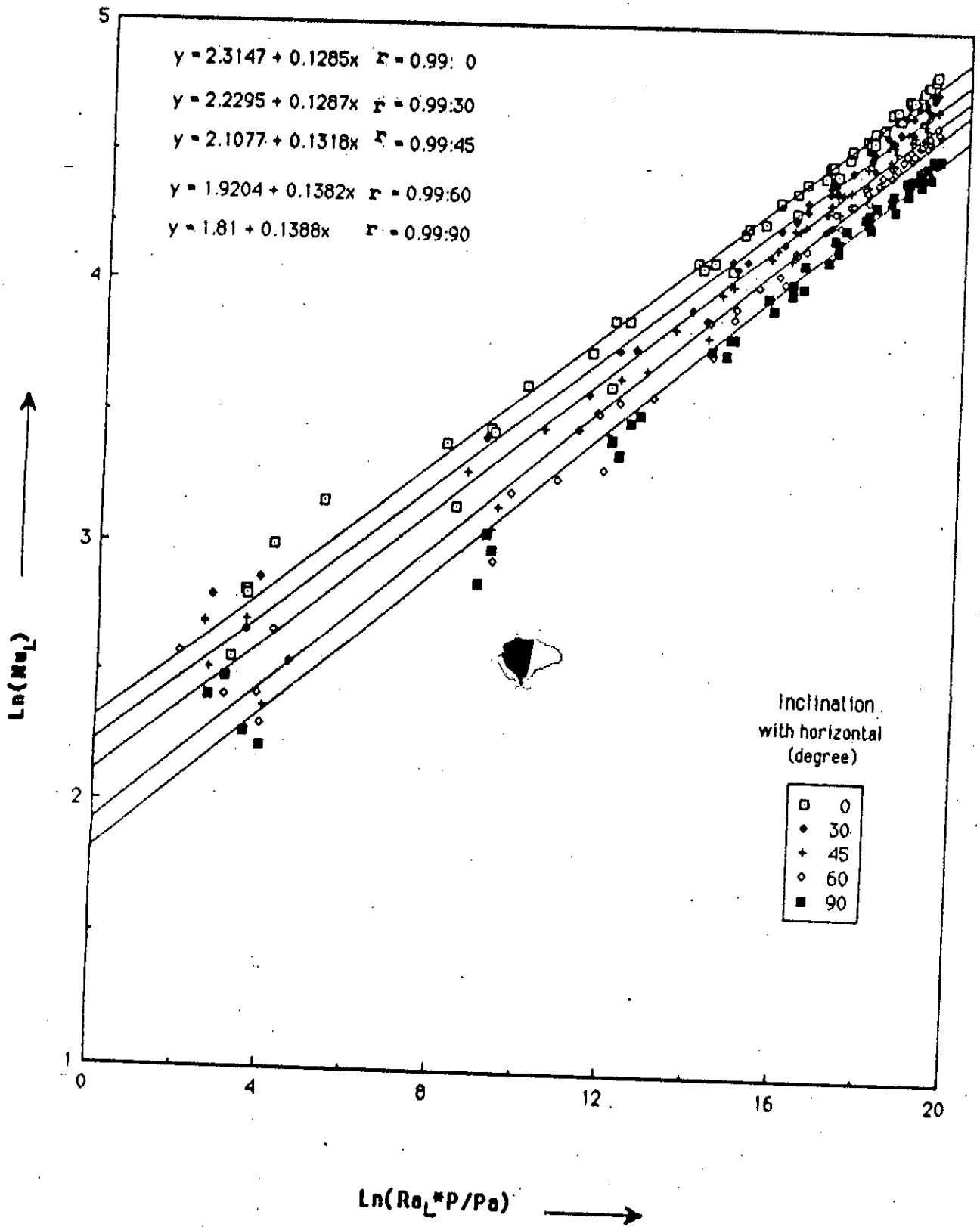
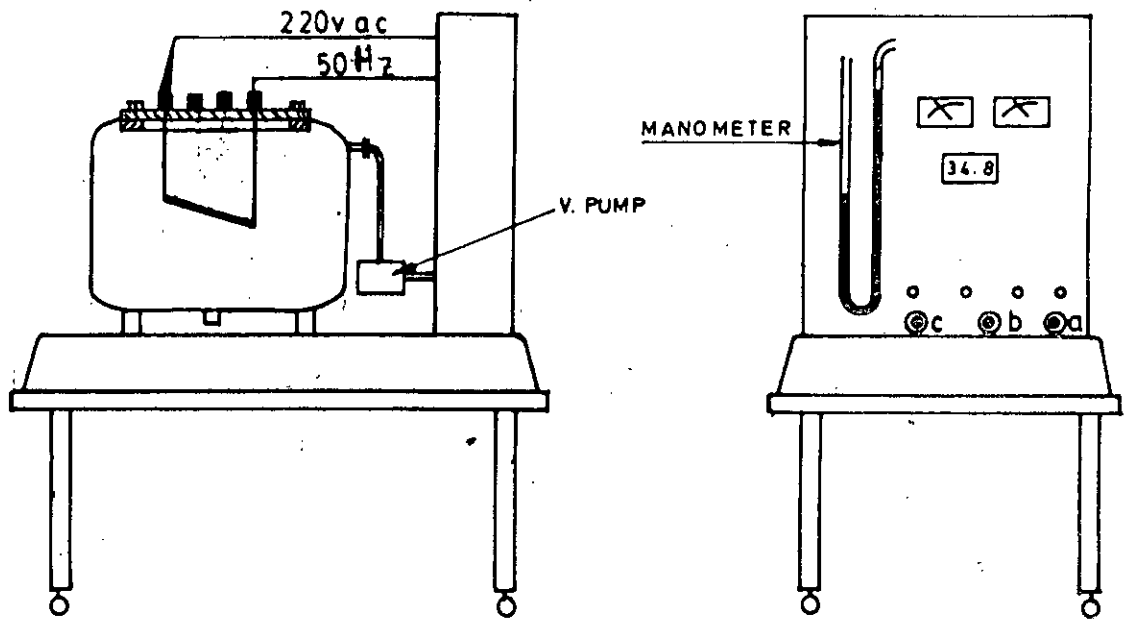
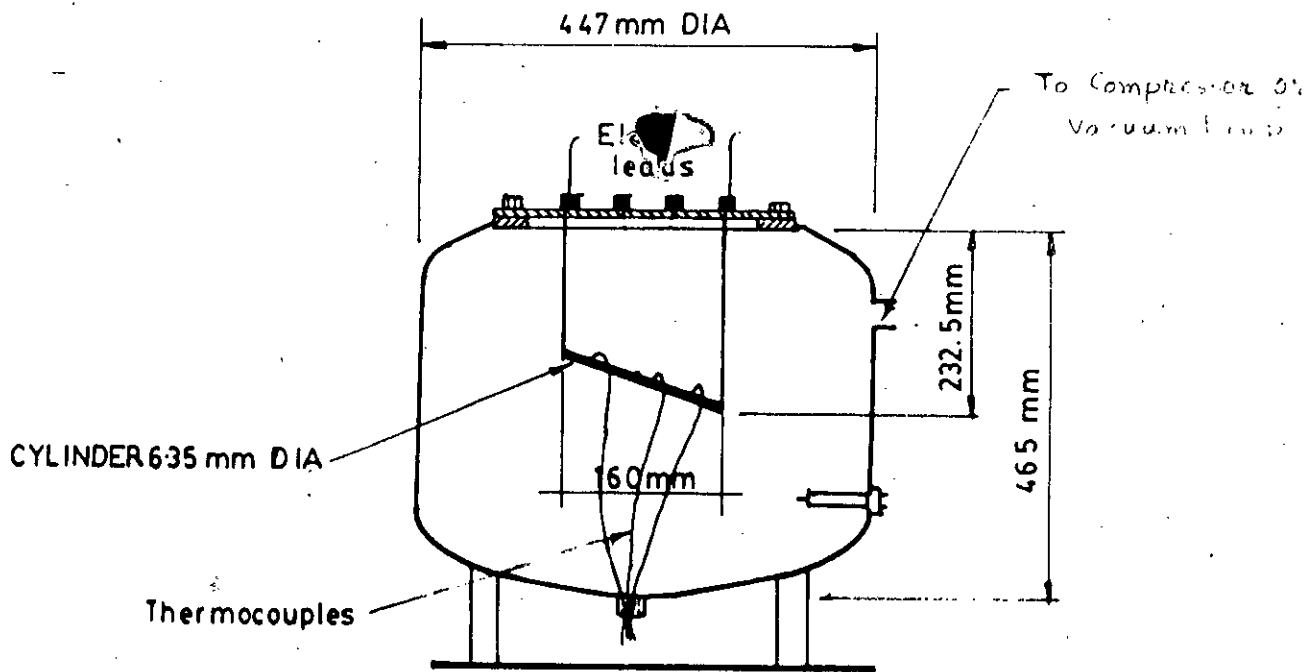


Fig-20. Combined plot of observed Nusselt no. against Product of Rayleigh no. and normalised pressure for both air and argon.



INSTRUMENT



VESSEL

FIG. 21

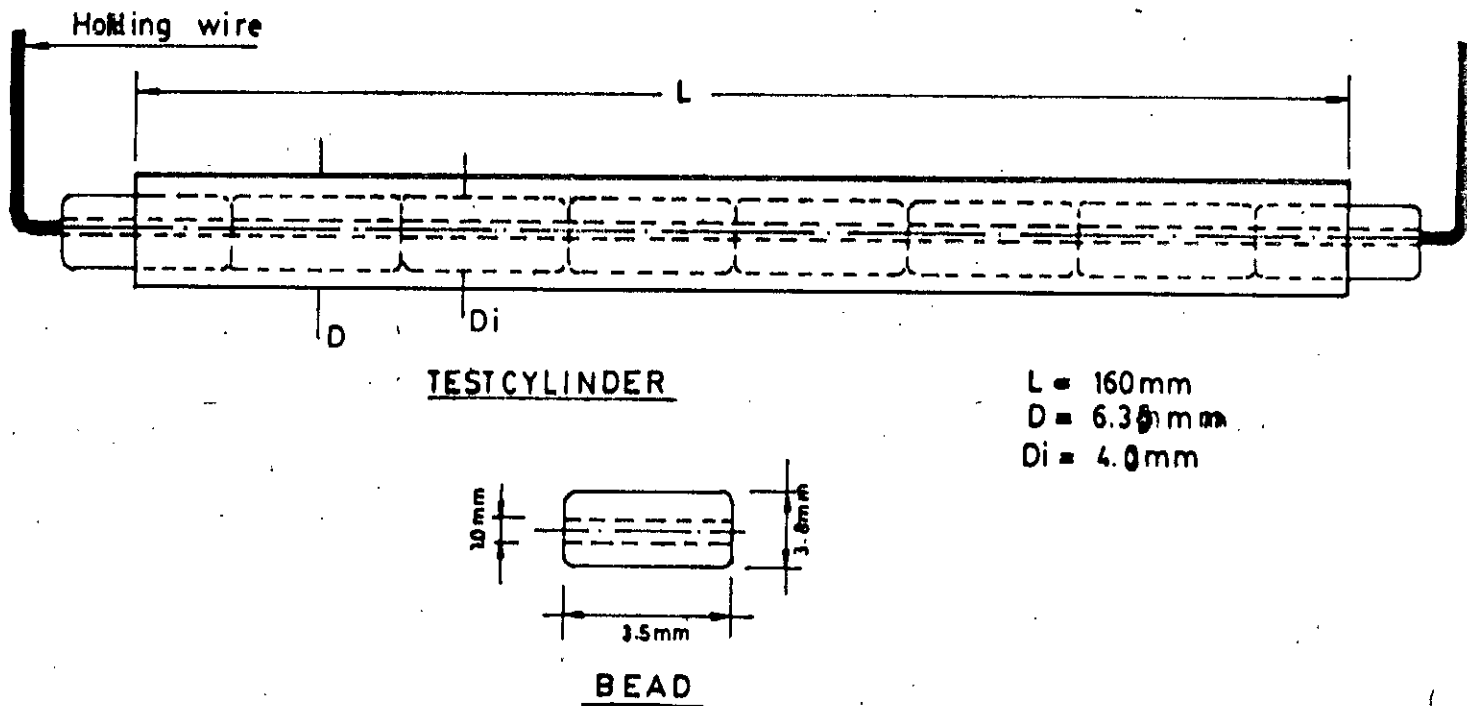


FIG. 22 TEST SPECIMEN

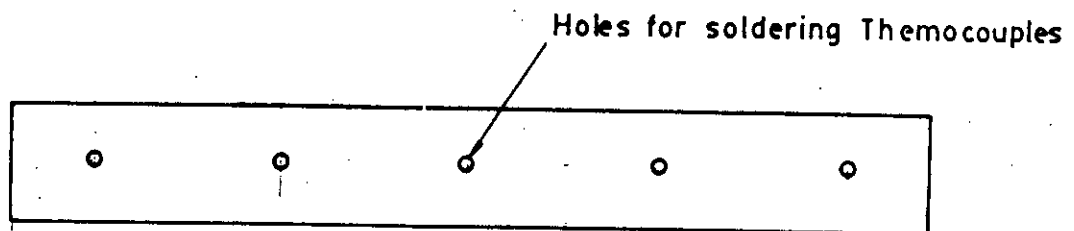


FIG. 23 CYLINDER WITH HOLES FOR THERMOCOUPLES

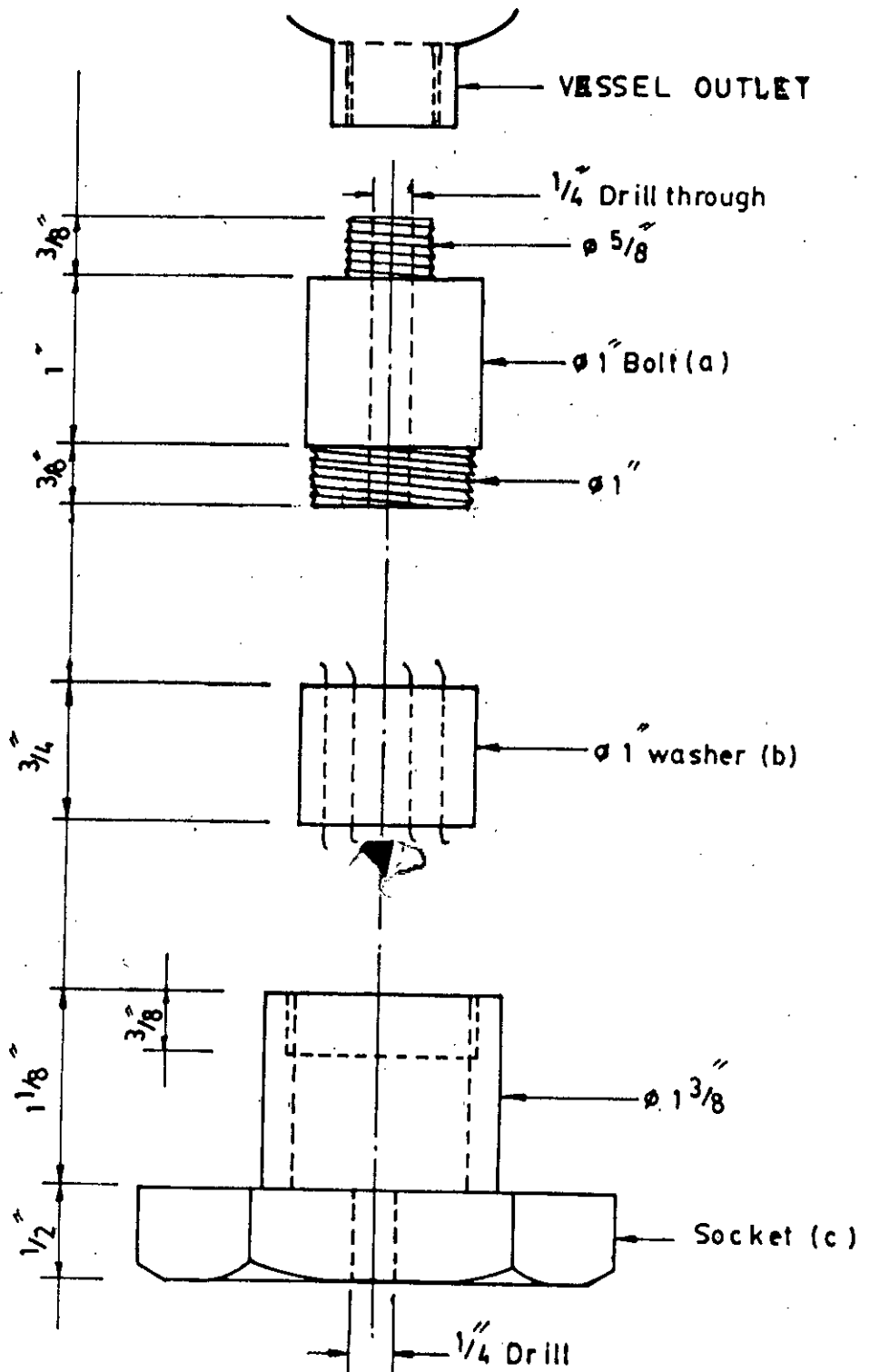


Fig. 24 BOLT, WASHER AND SOCKET

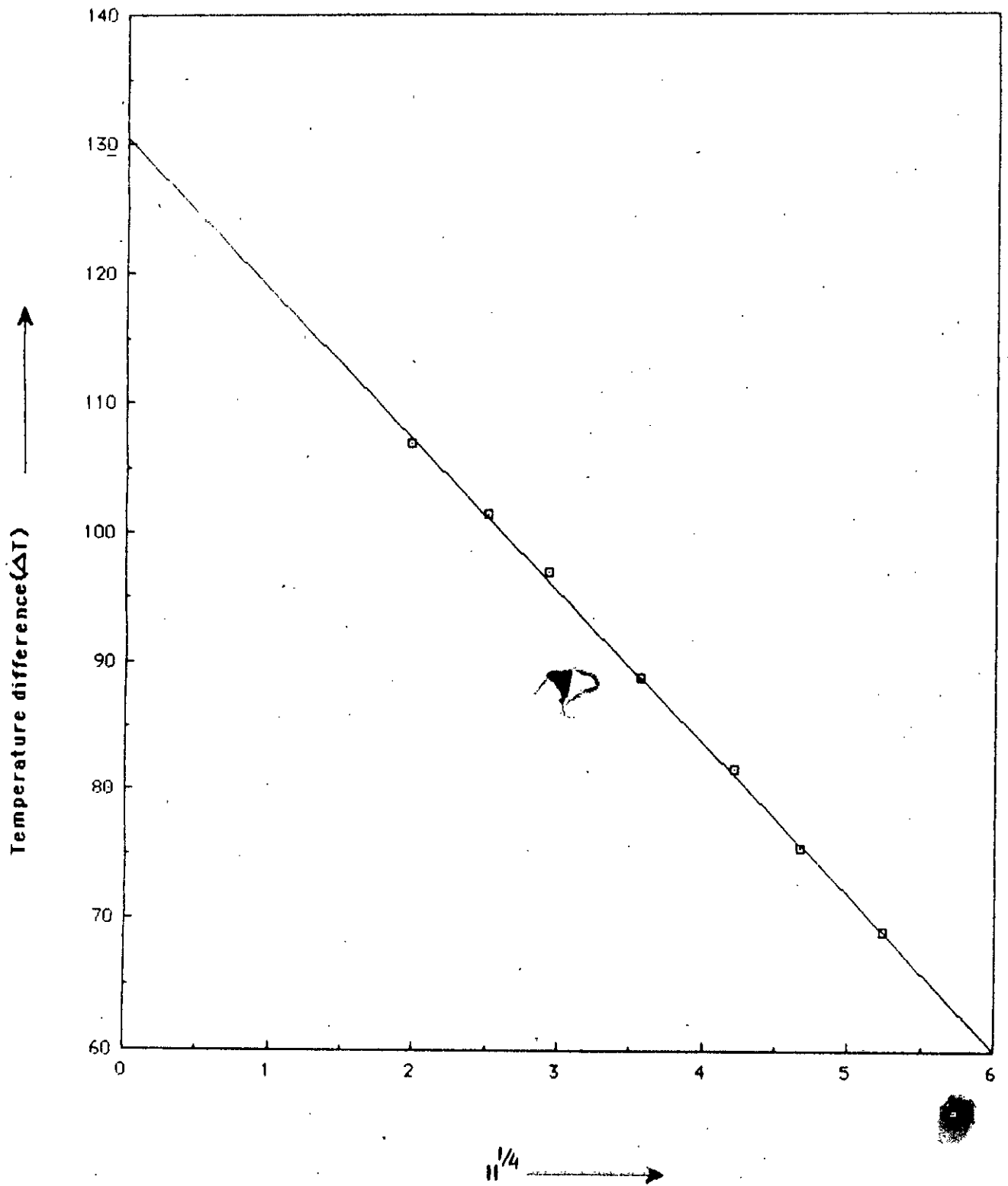


Fig. B-1 : Temperature difference (ΔT) versus $H^{1/4}$ curve for Specimen 1.

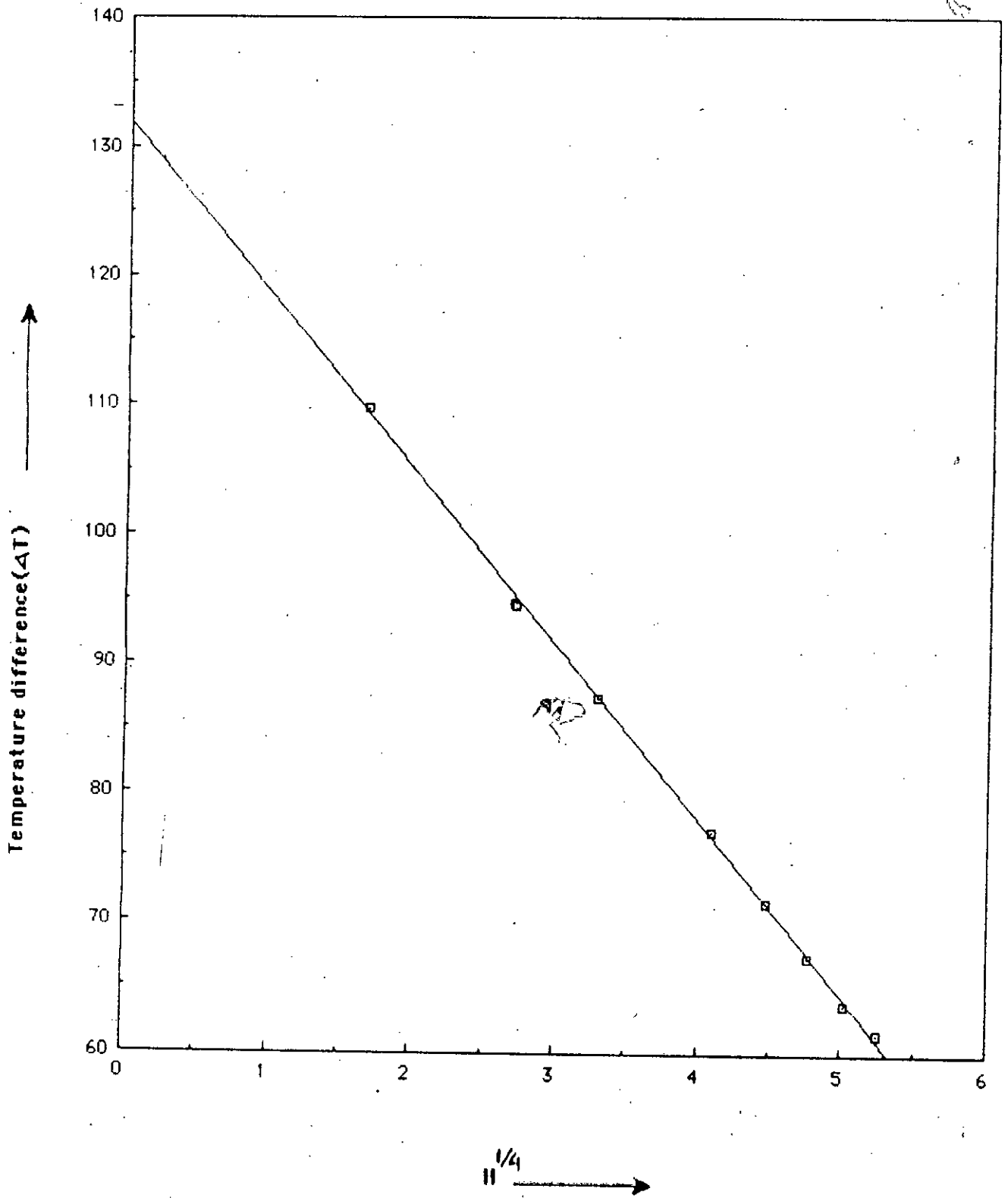


Fig. B-2 : Temperature difference (ΔT) versus $H^{1/4}$ curve for Specimen 2

